A SECOND-ORDER EPSILON METHOD FOR CONSTRAINED TRAJECTORY OPTIMIZATION

Marle David Hewett

NAVAL POSTGRADUATE SCHOOL
Monterey, California

THESIS

A SECOND-ORDER EPSILON METHOD FOR
CONSTRAINED TRAJECTORY OPTIMIZATION

by

Marle David Hewett

Thesis Advisor: D. E. Kirk

June 1974

Approved for public release; distribution unlimited.

A Second-Order Epsilon Method for
Constrained Trajectory Optimization

by

Marle David Hewett
Commander, United States Navy
B.A.E., Rensselaer Polytechnic Institute, 1959
M.S., Naval Postgraduate School, 1971

Submitted in partial fulfillment of the
requirements for the degree of

DOCTOR OF PHILOSOPHY

from the

NAVAL POSTGRADUATE SCHOOL
June 1974

ABSTRACT

A second-order epsilon method is developed for trajectory optimization problems. The method is applied to several aircraft and missile performance and air combat maneuvering problems. Heavy emphasis is placed on the realistic modeling of the flight vehicle's motion and maneuvering limitations.

The proposed optimization technique, which is an extension of Balakrishnan's epsilon method, uses either the full second-order Newton-Raphson method or the "modified" Newton-Raphson method to minimize the epsilon functional. The full Newton-Raphson method exhibits terminal convergence characteristics superior to the "modified" method, whereas the "modified" method is generally superior in the initial stages of a problem. An algorithm is developed which uses both techniques in a complementary way.

A new penalty functional which has desirable theoretical properties and exhibits excellent computational behavior is introduced to treat state and control inequality constraints.

TABLE OF CONTENTS

ACKNOWLEDGMENT

To my advisor, Professor Donald E. Kirk, I wish to offer my deep appreciation for the invaluable aid rendered in my research. To the members of my Doctoral Committee, I express my gratitude for the assistance so freely given in this effort. I give special thanks to Professors Frank D. Faulkner and Ronald A. Hess for their time and effort with the mathematical proofs and models.

Finally, I dedicate this work, whatever its worth, to the memory of my father, Merton E. Hewett. Realizing the restrictions imposed by his own limited schooling, he constantly urged his son to pursue every educational opportunity. Without his lifelong influence, this summit would not have been attained.

I. INTRODUCTION

The objective of the research reported on herein is to develop a method of solving realistic problems in aircraft and missile performance optimization. Optimization problems of this type have been the subject of considerable research [Refs. 1, 2, 3, 4, 5, 6, and 7]. The mathematical models used in these references are the products of many simplifications and assumptions. Typically, the degree of simplification used to render these problems solvable by some optimization technique is such that the solutions obtained are of limited practical value. This is particularly true in the modeling of aircraft maneuvering limitations, such as aerodynamic stall, maximum structural load factor, and placard Mach number, which require the use of multiple state and control inequality constraints. Since these limitations play an extremely important role in maneuvering flight and air combat, they must be modeled as accurately as possible. It is, therefore, imperative that the optimization technique used to solve the problems posed herein be capable of handling state and control inequality constraints with relative ease.

Balakrishnan's epsilon method is an attractive optimization technique because of the natural manner in which state and control inequality constraints are introduced. The epsilon method is a penalty method in which terms are added

[illegible]

to the performance measure to penalize deviations from the state equations written as equality constraints. Likewise, state and control inequality constraints may be treated by the addition of appropriate penalty terms to the performance measure. The resulting augmented performance measure is minimized by an appropriate algorithm for solving unconstrained optimization problems.

The optimization technique used most successfully in the literature with the epsilon method is a "modified" Newton-Raphson technique, hereafter referred to as the MNR technique. In this method certain second-order terms present in the full Newton-Raphson formulation are neglected. It is argued [Ref. 8] that since computer storage and time requirements to compute these terms are large, and since satisfactory results can be obtained over a large class of problems without the terms, their inclusion is not justified. For these reasons the full Newton-Raphson formulation, hereafter referred to as the FNR technique, has not been previously utilized with the epsilon method.

Difficulties were experienced by the author, however, in applying the MNR technique to problems of the type formulated in this dissertation. The MNR technique was not effective in problems with state equations and multiple inequality constraints resulting from a realistic modeling of the flight vehicle's motion and maneuvering limitations.

For this reason the FNR method was investigated and found to be feasible in terms of computational storage and

time requirements. The FNR method exhibits terminal convergence characteristics superior to the MNR method although the MNR method is generally superior in starting a problem. Problems not solvable by the MNR method alone were solved by an algorithm which uses both methods in a complementary way. The power of the FNR technique close to the minimum can also be used to advantage to obtain a family of optimal trajectories for different end conditions. The optimal trajectory for one set of end conditions is used as a first guess for the optimal trajectory for a neighboring set of end conditions.

Several simplified problems in aircraft performance optimization were attempted initially to gain experience with the epsilon method. In these problems inequality constraints were treated by using interior penalty functionals of the type recommended by Fiacco, McCormick, and Jones [Refs. 9 and 10]. Computational results were unsatisfactory. Difficulties were experienced in keeping the constrained state or control completely admissible; a requirement for the success of an algorithm with this type of penalty functional. To alleviate this difficulty a new penalty functional for inequality constraints is introduced which exhibits excellent computational behavior. The proposed functional has performed well in computation with up to eight inequality constraints represented in a single problem.

The thesis is divided into eight sections. In Section II the epsilon method is presented. The FNR and MNR techniques are derived and discussed. The effectiveness of the FNR method as opposed to the MNR method is demonstrated by a scalar example. Finally, the computational experience gained with both methods in solving realistic performance problems is presented. In Section III the method of treating state and control inequality constraints is presented. The author's experience with interior penalty methods is related and a new penalty functional is proposed. Computational experience with the new penalty functional is related and, finally, several desirable theoretical properties of the new penalty functional are presented. In Section IV the algorithm developed for minimizing the epsilon functional by either the MNR or FNR methods is presented. In Sections V, VI, and VII three aircraft and missile performance optimization problems are solved. These problems are pertinent and realistic in their operational applicability. The three-degree-of-freedom models are the same as those used in basic aircraft performance analysis. Finally, the summary and conclusions are presented in Section VIII.

II. THE EPSILON METHOD

This section describes the epsilon method and reviews the significant contributions of other investigators. The full Newton-Raphson (FNR) equations for minimizing the augmented performance measure are derived and compared to the modified Newton-Raphson (MNR) equations published elsewhere [Refs. 8, 11, and 12].

A. DESCRIPTION OF THE EPSILON METHOD

1. Statement of the Problem

A dynamic system characterized by the nonlinear state equations

$$\dot{\underset{\sim}{x}}(t) = \underset{\sim}{f}[\underset{\sim}{x}(t),\underset{\sim}{u}(t),t] \tag{2.1}$$

is to be controlled to minimize the performance measure

$$J(\underset{\sim}{x},\underset{\sim}{u}) = h[\underset{\sim}{x}(T),T] + \int_{t_o}^{T} g[\underset{\sim}{x}(t),\underset{\sim}{u}(t),t]dt \tag{2.2}$$

where $\underset{\sim}{x}(t)$ is an n x 1 state vector and $\underset{\sim}{u}(t)$ is an ℓ x 1 control vector. State and control inequality constraints are omitted for the present. In Section III the inclusion of these constraints is discussed in detail.

2. The Augmented Performance Measure

In the epsilon method as proposed by Balakrishnan [Refs. 13 and 14], the performance measure (2.2) is augmented

by a penalty functional which involves a weighted integral of the Euclidean norm of the state equations written as equality constraints. The augmented performance measure is

$$J_a(\underset{\sim}{x},\underset{\sim}{u},\varepsilon) = J(\underset{\sim}{x},\underset{\sim}{u}) + \frac{1}{\varepsilon}\int_{t_0}^{T} ||\dot{\underset{\sim}{x}} - \underset{\sim}{f}(\underset{\sim}{x},\underset{\sim}{u},t)||^2 dt \tag{2.3}$$

$$= J(\underset{\sim}{x},\underset{\sim}{u}) + \frac{1}{\varepsilon} J_s(\underset{\sim}{x},\underset{\sim}{u}). \tag{2.4}$$

The weighting factor ε is a positive quantity.

3. Behavior as $\varepsilon \to 0$

As ε is reduced, the penalty term J_s is more heavily weighted, thereby placing greater emphasis on satisfying the state equations. Balakrishnan [Refs. 13 and 14] and Taylor [Ref. 11] have shown that under appropriate assumptions as $\varepsilon \to 0$, the epsilon method yields the necessary conditions of optimality obtained by applying Pontryagin's minimum principle [Refs. 15 and 16]:

$$\dot{\underset{\sim}{x}}^*(t) = \frac{\partial H}{\partial \underset{\sim}{p}}[\underset{\sim}{x}^*(t),\underset{\sim}{u}^*(t),t], \tag{2.5}$$

$$\dot{\underset{\sim}{p}}^*(t) = -\frac{\partial H}{\partial \underset{\sim}{x}}[\underset{\sim}{x}^*(t),\underset{\sim}{u}^*(t),t], \tag{2.6}$$

and

$$H[\underset{\sim}{x}^*(t),\underset{\sim}{u}^*(t),\underset{\sim}{p}^*(t),t] \leq H[\underset{\sim}{x}^*(t),\underset{\sim}{u}(t),\underset{\sim}{p}^*(t),t] \tag{2.7}$$

where H is the Hamiltonian function defined as

$$\mathcal{H}[\underset{\sim}{x}(t),\underset{\sim}{u}(t),\underset{\sim}{p}(t),t] \triangleq g[\underset{\sim}{x}(t),\underset{\sim}{u}(t),t] + \underset{\sim}{p}^T(t)\underset{\sim}{f}[\underset{\sim}{x}(t),\underset{\sim}{u}(t),t], \tag{2.8}$$

$\underset{\sim}{p}(t)$ is the costate or adjoint vector, $\underset{\sim}{u}^*(t)$ is an extremal control vector, and $\underset{\sim}{x}^*(t)$ is an extremal trajectory. The assumptions made are that the minimization problem has a unique solution with $\underset{\sim}{x}(t)$ absolutely continuous for each ε, and that $\underset{\sim}{f}$ and g are continuously differentiable in $\underset{\sim}{x}$ and $\underset{\sim}{u}$ [Ref. 11]. Thus, under appropriate assumptions, it can be shown that as $\varepsilon \to 0$, the epsilon method yields the results of Pontryagin's minimum principle. That is, if the optimal control $\underset{\sim}{u}^*(t,\varepsilon)$ of equation (2.3) exists for each ε, that solution will approach the optimal control $\underset{\sim}{u}^*(t)$ of equation (2.2) as $\varepsilon \to 0$.

4. State Equation Integration

It should be noted that the epsilon method is a non-dynamic method in that the state equations are not integrated during the minimization process. Once the augmented performance measure has been minimized a check on the degree of satisfaction of the state equations can be obtained by integrating the state equations with the optimal control.

B. MINIMIZING THE AUGMENTED PERFORMANCE MEASURE

1. Sequence of Unconstrained Problems

Once the augmented performance measure (2.3) is formulated, any unconstrained optimization algorithm can

be applied to it. A sequence of unconstrained problems referred to as sub-problems is solved. In each sub-problem ε is held constant and a minimization is performed until some stopping criterion is satisfied. At this point ε is decreased and a new sub-problem is commenced using the optimum trajectory found in the previous sub-problem as a first guess. In this manner a sequence of sub-problems is solved until, if convergence occurs, some overall stopping criterion is satisfied.

2. Unknowns and Time Discretization

The states and controls can be approximated by any orthogonal expansions. The coefficients in these expansions, along with all free end conditions, become the parameters or unknowns in the optimization. A functional expansion of the form (2.9) is convenient because it is continuous and the period can be selected so that the value of the expansion is zero at the end points. Since the problems solved involve time-invariant systems, t_o is selected as zero and the states and controls are written as

$$\underset{\sim}{y}(t) = \begin{bmatrix} \underset{\sim}{x}(t) \\ \hline \underset{\sim}{u}(t) \end{bmatrix} = \underset{\sim}{y}(0) + \frac{\underset{\sim}{y}(T) - \underset{\sim}{y}(0)}{T}\, t + \underset{\sim}{D} \begin{bmatrix} \sin \frac{\pi t}{T} \\ \sin \frac{2\pi t}{T} \\ \vdots \\ \sin \frac{M\pi t}{T} \end{bmatrix} \qquad (2.9)$$

where M is the number of harmonics used and

$$\underset{\sim}{D} = \begin{bmatrix} \underset{\sim}{D}_{\underset{\sim}{x}} \\ --- \\ \underset{\sim}{D}_{\underset{\sim}{u}} \end{bmatrix} \tag{2.10}$$

is an $(n + \ell) \times M$ matrix of coefficients. The derivative of the expansion of the state vector given in equation (2.9) with respect to time is required and is given by

$$\dot{\underset{\sim}{x}}(t) = \frac{\underset{\sim}{x}(T) - \underset{\sim}{x}(0)}{T} + \underset{\sim}{D}_{\underset{\sim}{x}} \begin{bmatrix} \frac{\pi}{T} \cos \frac{\pi t}{T} \\ \frac{2\pi}{T} \cos \frac{2\pi t}{T} \\ \cdot \\ \cdot \\ \cdot \\ \frac{M\pi}{T} \cos \frac{M\pi t}{T} \end{bmatrix} \tag{2.11}$$

The objective is to find the $\underset{\sim}{D}$ matrix along with the values of the free end conditions which minimize equation (2.3) for a given ε. In order to perform this minimization, the time interval T is divided into $(K - 1)$ sub-intervals each of duration Δt so that there are K discrete time points. The augmented performance measure given by Equation (2.3) is written as

$$\begin{aligned} J_a(\underset{\sim}{x},\underset{\sim}{u},\varepsilon) = \frac{1}{\varepsilon}\Big[& \int_0^T [\dot{x}_1(t)-f_1(\underset{\sim}{x},\underset{\sim}{u})]^2 dt + \int_0^T [\dot{x}_2(t)-f_2(\underset{\sim}{x},\underset{\sim}{u})]^2 dt \\ & + \ldots + \int_0^T [\dot{x}_n(t)-f_n(\underset{\sim}{x},\underset{\sim}{u})]^2 dt\Big] \qquad (2.12) \\ & + \int_0^T g[\underset{\sim}{x},\underset{\sim}{u}]dt + h[\underset{\sim}{x}(T),T]. \end{aligned}$$

Suppressing the arguments for clarity, equation (2.12) is expanded to yield

$$
\begin{aligned}
J_a = \frac{1}{\varepsilon}\Bigg[& \int_0^{\Delta t} (\dot{x}_1 - f_1)^2 dt + \int_{\Delta t}^{2\Delta t} (\dot{x}_1 - f_1)^2 dt + \cdots + \int_{(K-1)\Delta t}^{K\Delta t} (\dot{x}_1 - f_1)^2 dt \\
& + \int_0^{\Delta t} (\dot{x}_2 - f_2)^2 dt + \int_{\Delta t}^{2\Delta t} (\dot{x}_2 - f_2)^2 dt + \cdots + \int_{(K-1)\Delta t}^{K\Delta t} (\dot{x}_2 - f_2)^2 dt \\
& + \cdots \qquad\qquad (2.13) \\
& + \int_0^{\Delta t} (\dot{x}_n - f_n)^2 dt + \int_{\Delta t}^{2\Delta t} (\dot{x}_n - f_n)^2 dt + \cdots + \int_{(K-1)\Delta t}^{K\Delta t} (\dot{x}_n - f_n)^2 dt \Bigg] \\
& + \int_0^{\Delta t} g\Delta t + \int_{\Delta t}^{2\Delta t} g\Delta t + \cdots + \int_{(K-1)\Delta t}^{K\Delta t} g\Delta t + h[\underset{\sim}{x}(T),T]
\end{aligned}
$$

which can be approximated by

$$
\begin{aligned}
J_a \approx & \left\{\dot{x}_1(0) - f_1[\underset{\sim}{x}(0),\underset{\sim}{u}(0)]\right\}^2 \frac{\Delta t}{\varepsilon} + \left\{\dot{x}_1(\Delta t) - f_1[\underset{\sim}{x}(\Delta t),\underset{\sim}{u}(\Delta t)]\right\}^2 \frac{\Delta t}{\varepsilon} \\
& + \cdots + \left\{\dot{x}_1([K-1]\Delta t) - f_1[\underset{\sim}{x}([K-1]\Delta t),\underset{\sim}{u}((K-1)\Delta t)]\right\}^2 \frac{\Delta t}{\varepsilon} + \\
& \left\{\dot{x}_2(0) - f_2[\underset{\sim}{x}(0),\underset{\sim}{u}(0)]\right\}^2 \frac{\Delta t}{\varepsilon} + \left\{\dot{x}_2(\Delta t) - f_2[\underset{\sim}{x}(\Delta t),\underset{\sim}{u}(\Delta t)]\right\}^2 \frac{\Delta t}{\varepsilon} \\
& + \cdots + \left\{\dot{x}_2((K-1)\Delta t) - f_2[\underset{\sim}{x}((K-1)\Delta t),\underset{\sim}{u}((K-1)\Delta t)]\right\}^2 \frac{\Delta t}{\varepsilon} + \cdots + \qquad (2.14) \\
& \left\{\dot{x}_n(0) - f_n[\underset{\sim}{x}(0),\underset{\sim}{u}(0)]\right\}^2 \frac{\Delta t}{\varepsilon} + \left\{\dot{x}_n(\Delta t) - f_n[\underset{\sim}{x}(\Delta t),\underset{\sim}{u}(\Delta t)]\right\}^2 \frac{\Delta t}{\varepsilon} \\
& + \cdots + \left\{\dot{x}_n((K-1)\Delta t) - f_n[\underset{\sim}{x}((K-1)\Delta t),\underset{\sim}{u}((K-1)\Delta t)]\right\}^2 \frac{\Delta t}{\varepsilon} + \\
& \left\{g[\underset{\sim}{x}(0),\underset{\sim}{u}(0)]\right\}\Delta t + \left\{g[\underset{\sim}{x}(\Delta t),\underset{\sim}{u}(\Delta t)]\right\}\Delta t + \cdots + \\
& \left\{g[\underset{\sim}{x}((K-1)\Delta t),\underset{\sim}{u}((K-1)\Delta t)]\right\}\Delta t + h[\underset{\sim}{x}(T),T] \quad .
\end{aligned}
$$

Hence, the augmented performance measure can be written as

$$J_a = w_1^{\,2} + w_2^{\,2} + \ldots + w_Q^{\,2} \tag{2.15}$$

$$= \underset{\sim}{w}^T \underset{\sim}{w} \tag{2.16}$$

where $\underset{\sim}{w}$ is a Q x 1 column vector. The first K elements of $\underset{\sim}{w}$ are

$$w_k = \left\{\dot{x}_1[(k-1)\Delta t] - f_1[\underset{\sim}{x}((k-1)\Delta t)_1 \underset{\sim}{u}((k-1)\Delta t)]\right\}\left[\frac{\Delta t}{\varepsilon}\right]^{\frac{1}{2}}, \quad k = 1,2,\ldots,K, \tag{2.17}$$

etc. The form of equation (2.16) is convenient for computer programming the epsilon method and for the derivation of the minimization techniques that follow. In minimum time problems where the performance measure is given by

$$J = \int_0^T dt. \tag{2.18}$$

one element of $\underset{\sim}{w}$ of the form

$$w_Q = [(K-1)\Delta t]^{\frac{1}{2}} \tag{2.19}$$

is used to represent equation (2.18). In these type problems the number of time points K is held constant during the minimization in order to keep the dimensions of all vectors and matrices constant and the time interval Δt is minimized.

The values of the states and controls required in equation (2.14) are obtained by evaluating equations (2.9) and (2.11) at each time point $t = (k - 1)\Delta t$ where $k = 1,2, \ldots,K$. Written in discrete form equation (2.9) is

$$\underset{\sim}{y}[(k-1)\Delta t] = \underset{\sim}{y}(0) + \frac{\underset{\sim}{y}[(K-1)\Delta t]-\underset{\sim}{y}(0)}{K-1}(k-1) + \underset{\sim}{D} \begin{bmatrix} \sin \frac{\pi(k-1)}{K-1} \\ \sin \frac{2\pi(k-1)}{K-1} \\ \cdot \\ \cdot \\ \cdot \\ \sin \frac{M\pi(k-1)}{K-1} \end{bmatrix} \tag{2.20}$$

and equation (2.11) is

$$\dot{\underset{\sim}{x}}[(k-1)\Delta t] = \frac{\underset{\sim}{x}[(K-1)\Delta t]-\underset{\sim}{x}(0)}{(K-1)\Delta t} + \underset{\sim}{D}_x \begin{bmatrix} \frac{\pi}{(K-1)\Delta t} \cos \frac{\pi(k-1)}{K-1} \\ \frac{2\pi}{(K-1)\Delta t} \cos \frac{2\pi(k-1)}{K-1} \\ \cdot \\ \cdot \\ \cdot \\ \frac{M\pi}{(K-1)\Delta t} \cos \frac{M\pi(k-1)}{K-1} \end{bmatrix} \tag{2.21}$$

A vector of unknowns $\underset{\sim}{c}$ is formed and is given by

$$\underset{\sim}{c}^T = (d_{1,1}, d_{1,2}, \ldots, d_{1,M}, d_{2,1}, d_{2,2}, \ldots, d_{2,M}, \ldots,$$
$$d_{n+\ell,1}, d_{n+\ell,2}, \ldots, d_{n+\ell,M}, z_1, z_2, \ldots, z_P, \Delta t) \tag{2.22}$$

where $d_{i,j}$ is the element in the i^{th} row and j^{th} column of $\underset{\sim}{D}$ and $z_1, z_2, \ldots, z_P$ represent P free end conditions some of which occur at t = 0, and others at t = T. Some of the z_p's correspond to states and others to controls. The last element, Δt, is present only if time is to be minimized. The $\underset{\sim}{c}$ vector consists of L elements where

$$L = (n+\ell) \times M + P \tag{2.23}$$

for all problems except minimum time problems and

$$L = (n+\ell) \times M + P + 1 \tag{2.24}$$

for minimum-time problems.

With the states and controls given by equation (2.20) and the augmented performance measure given by equation (2.16), the problem has been transformed into a parameter optimization problem with the unknowns given by $\underset{\sim}{c}$ (2.22).

3. Minimization Techniques

The methods which have received attention in the literature for finding $\underset{\sim}{c}^*$ which minimizes the augmented performance measure given in equation (2.3) are the gradient method and a "modified" Newton-Raphson method (MNR).

The gradient method has been investigated by J. Taylor [Refs. 11 and 12] and L. Taylor [Ref. 8] with unsatisfactory results. These investigators report that

[illegible]

[illegible]

[illegible]

[illegible]

[illegible]

in non-linear problems the gradient method frequently obtains false minima and requires considerable computation time compared to other methods.

An MNR method in which certain second-order terms present in the full Newton-Raphson (FNR) method are neglected has enjoyed greater success and requires less computation time than the gradient method [Refs. 8, 11, and 12]. However, in Ref. 8 difficulties are reported with the MNR method in non-linear problems. J_a often begins an oscillation after two or three iterations and does not settle to a minimum. In the problems solved herein the same oscillations have been observed when the MNR algorithm has been used. Convergence to the minimum, when it does occur, is typically very slow. Typical performance of the MNR method is shown in Figure 1.

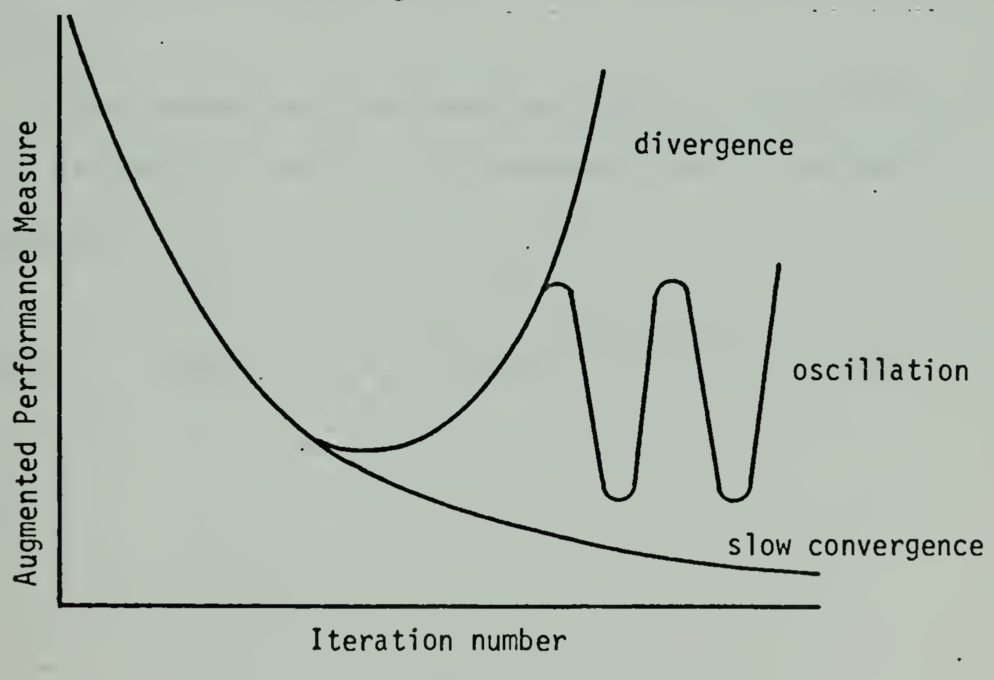

Figure 1

Augmented performance measure vs. iteration number-MNR method

The FNR method has not been used by other investigators with the epsilon method because of the increased computer time for each iteration, the additional storage space required, and a significantly increased analytic workload involved in deriving second partial derivatives. Because of the poor performance of the MNR method on problems of the type solved herein, the FNR method has been investigated in detail in this work. With careful programming the computer time for each iteration and storage space required for the FNR method has been reduced to an extent which makes the method computationally feasible.

4. <u>The Full and Modified Newton-Raphson Equations</u>

The FNR equations for finding $\underset{\sim}{c}^*$ are derived here in a manner which permits the MNR equations derived in the literature [Refs. 8 and 11] to be obtained by neglecting a term.

The augmented performance measure is expanded in a Taylor series including up to second-order terms and is written as

$$J_a(\underset{\sim}{c}+\Delta\underset{\sim}{c}) \simeq J_a(\underset{\sim}{c}) + (\nabla_{\underset{\sim}{c}} J_a)_{\underset{\sim}{c}}^T \Delta\underset{\sim}{c} + \tfrac{1}{2}(\Delta\underset{\sim}{c})^T(\nabla_{\underset{\sim}{c}}^2 J_a)_{\underset{\sim}{c}}(\Delta\underset{\sim}{c}) \qquad (2.25)$$

where

$$\nabla_{\underset{\sim}{c}} J_a = \begin{bmatrix} \dfrac{\partial J_a}{\partial c_1} \\ \dfrac{\partial J_a}{\partial c_2} \\ \vdots \\ \dfrac{\partial J_a}{\partial c_L} \end{bmatrix} \tag{2.26}$$

and

$$\nabla_{\underset{\sim}{c}}^{2} J_a = \begin{bmatrix} \dfrac{\partial^2 J_a}{\partial c_1^{2}} & \dfrac{\partial^2 J_a}{\partial c_1 \partial c_2} & \cdots & \dfrac{\partial^2 J_a}{\partial c_1 \partial c_L} \\ \dfrac{\partial^2 J_a}{\partial c_2 \partial c_1} & \dfrac{\partial^2 J_a}{\partial c_2^{2}} & \cdots & \dfrac{\partial^2 J_a}{\partial c_2 \partial c_L} \\ \vdots & \vdots & & \vdots \\ \dfrac{\partial^2 J_a}{\partial c_L \partial c_1} & \dfrac{\partial^2 J_a}{\partial c_L \partial c_2} & \cdots & \dfrac{\partial^2 J_a}{\partial c_L^{2}} \end{bmatrix} . \tag{2.27}$$

Solving for the increment of J_a, we have

$$\Delta J_a \overset{\Delta}{=} J_a(\underset{\sim}{c}+\Delta\underset{\sim}{c}) - J_a(\underset{\sim}{c}) \tag{2.28}$$

$$\approx (\nabla_{\underset{\sim}{c}} J_a)_{\underset{\sim}{c}}^{T} \Delta\underset{\sim}{c} + \tfrac{1}{2}(\Delta\underset{\sim}{c})^{T}(\nabla_{\underset{\sim}{c}}^{2} J_a)_{\underset{\sim}{c}}(\Delta\underset{\sim}{c}). \tag{2.29}$$

Applying the necessary condition for a minimum, we have

$$\frac{\partial(\Delta J_a)}{\partial(\Delta \underset{\sim}{c})} = (\nabla_{\underset{\sim}{c}} J_a)_{\underset{\sim}{c}} + (\nabla_{\underset{\sim}{c}}^2 J_a)_{\underset{\sim}{c}} \, \Delta \underset{\sim}{c} = \underset{\sim}{0} \tag{2.30}$$

which when solved for $\Delta \underset{\sim}{c}$ yields

$$\Delta \underset{\sim}{c} = -(\nabla_{\underset{\sim}{c}}^2 J_a)_{\underset{\sim}{c}}^{-1} \, (\nabla_{\underset{\sim}{c}} J_a)_{\underset{\sim}{c}}. \tag{2.31}$$

If the augmented performance measure is written as

$$J_a \overset{\Delta}{=} \underset{\sim}{w}^T \underset{\sim}{w} \tag{2.14}$$

where $\underset{\sim}{w}$ is a Q-dimensional column vector, then

$$\begin{aligned} \nabla_{\underset{\sim}{c}} J_a &= \nabla_{\underset{\sim}{c}} (\underset{\sim}{w}^T \underset{\sim}{w}) \\ &= 2(\nabla_{\underset{\sim}{c}} \underset{\sim}{w})^T \underset{\sim}{w} \end{aligned} \tag{2.32}$$

and

$$\begin{aligned} \nabla_{\underset{\sim}{c}}^2 J_a &= 2\nabla_{\underset{\sim}{c}} [(\nabla_{\underset{\sim}{c}} \underset{\sim}{w})^T \underset{\sim}{w}] \\ &= 2\left[(\nabla_{\underset{\sim}{c}} \underset{\sim}{w})^T (\nabla_{\underset{\sim}{c}} \underset{\sim}{w}) + (\nabla_{\underset{\sim}{c}}^2 \underset{\sim}{w})^T \underset{\sim}{w}\right]. \end{aligned} \tag{2.33}$$

The matrix $\nabla_{\underset{\sim}{c}} \underset{\sim}{w}$ is given by

$$
\nabla_{\underset{\sim}{c}} \underset{\sim}{w} \overset{\Delta}{=} \begin{bmatrix} \dfrac{\partial w_1}{\partial c_1} & \dfrac{\partial w_2}{\partial c_2} & \cdots & \dfrac{\partial w_1}{\partial c_L} \\ \dfrac{\partial w_2}{\partial c_1} & \dfrac{\partial w_2}{\partial c_2} & \cdots & \dfrac{\partial w_2}{\partial c_L} \\ \vdots & \vdots & & \vdots \\ \dfrac{\partial w_Q}{\partial c_1} & \dfrac{\partial w_Q}{\partial c_2} & \cdots & \dfrac{\partial w_Q}{\partial c_L} \end{bmatrix} \tag{2.34}
$$

$\nabla_{\underset{\sim}{c}}^{2} \underset{\sim}{w}$ is a three-dimensional array composed of L matrices each of dimension Q x L which has as its ijk th element $\dfrac{\partial^2 w_i}{\partial c_k \partial c_j}$; that is

$$
\nabla_{\underset{\sim}{c}}^{2} \underset{\sim}{w} = \begin{bmatrix} \dfrac{\partial^2 w_1}{\partial c_1^2} & \dfrac{\partial^2 w_1}{\partial c_1 \partial c_2} & \cdots & \dfrac{\partial^2 w_1}{\partial c_1 \partial c_L} \\ \dfrac{\partial^2 w_2}{\partial c_1^2} & \dfrac{\partial^2 w_2}{\partial c_1 \partial c_2} & \cdots & \dfrac{\partial^2 w_2}{\partial c_1 \partial c_L} \\ \vdots & \vdots & & \vdots \\ \dfrac{\partial^2 w_Q}{\partial c_1^2} & \dfrac{\partial^2 w_Q}{\partial c_1 \partial c_2} & \cdots & \dfrac{\partial^2 w_Q}{\partial c_1 \partial c_L} \end{bmatrix}, \begin{bmatrix} & & & \dfrac{\partial^2 w_1}{\partial c_2 \partial c_L} \\ & & & \dfrac{\partial^2 w_2}{\partial c_2 \partial c_L} \\ & & & \vdots \\ \dfrac{\partial^2 w_Q}{\partial c_2 \partial c_1} & \dfrac{\partial^2 w_Q}{\partial c_2^2} & \cdots & \dfrac{\partial^2 w_Q}{\partial c_2 \partial c_L} \end{bmatrix}, \begin{bmatrix} & & & \cdot \\ & & & \cdot \\ & & & \vdots \\ \cdot & \cdot & \cdots & \cdot \end{bmatrix}, \begin{bmatrix} & & & \dfrac{\partial^2 w_1}{\partial c_L^2} \\ & & & \dfrac{\partial^2 w_2}{\partial c_L^2} \\ & & & \cdot \\ \dfrac{\partial^2 w_Q}{\partial c_L \partial c_1} & \dfrac{\partial^2 w_Q}{\partial c_L \partial c_2} & \cdots & \dfrac{\partial^2 w_Q}{\partial c_L^2} \end{bmatrix} \tag{2.35}
$$

Substituting equations (2.32) and (2.33) into equation (2.31), we have

$$\Delta\underset{\sim}{c} = -\left[(\nabla_{\underset{\sim}{c}}\underset{\sim}{w})_{\underset{\sim}{c}}^{T}(\nabla_{\underset{\sim}{c}}\underset{\sim}{w})_{\underset{\sim}{c}} + (\nabla_{\underset{\sim}{c}}^{2}\underset{\sim}{w})_{\underset{\sim}{c}}^{T}\underset{\sim}{w}_{\underset{\sim}{c}}\right]^{-1}(\nabla_{\underset{\sim}{c}}\underset{\sim}{w})_{\underset{\sim}{c}}^{T}\,\underset{\sim}{w}_{\underset{\sim}{c}} \quad . \qquad (2.36)$$

This is the full Newton-Raphson equation. The modified Newton-Raphson equation can be obtained by neglecting the second term in the inverse in equation (2.36), which yields

$$\Delta\underset{\sim}{c} = -\left[(\nabla_{\underset{\sim}{c}}\underset{\sim}{w})_{\underset{\sim}{c}}^{T}(\nabla_{\underset{\sim}{c}}\underset{\sim}{w})_{\underset{\sim}{c}}\right]^{-1}(\nabla_{\underset{\sim}{c}}\underset{\sim}{w})_{\underset{\sim}{c}}^{T}\,\underset{\sim}{w}_{\underset{\sim}{c}} \qquad (2.37)$$

Several comments concerning equations (2.36) and (2.37) are in order:

a. the term $\nabla_{\underset{\sim}{c}}\underset{\sim}{w}$ given by equation (2.34) is a Q x L matrix;
b. the term $(\nabla_{\underset{\sim}{c}}\underset{\sim}{w})^{T}(\nabla_{\underset{\sim}{c}}\underset{\sim}{w})$ is a symmetric L x L matrix;
c. the term $(\nabla_{\underset{\sim}{c}}\underset{\sim}{w})^{T}\underset{\sim}{w}$ is an L x 1 vector;
d. the term $\nabla_{\underset{\sim}{c}}^{2}\underset{\sim}{w}$ given by equation (2.35) is a Q x L x L three-dimensional array;
e. the term $(\nabla_{\underset{\sim}{c}}^{2}\underset{\sim}{w})^{T}\underset{\sim}{w}$ is a symmetric L x L matrix;
f. $(\nabla_{\underset{\sim}{c}}^{2}\underset{\sim}{w})^{T}$ is defined as the three-dimensional array obtained by transposing each individual Q x L matrix given in equation (2.35);
g. the result of the operation $(\nabla_{\underset{\sim}{c}}^{2}\underset{\sim}{w})^{T}\underset{\sim}{w}$ is defined as an L x L matrix in which the i^{th} column is the product $\left[\frac{\partial}{\partial c_i}(\nabla_{\underset{\sim}{c}}\underset{\sim}{w})\right]^{T}\underset{\sim}{w}$.

5. A Scalar Illustration of the MNR and FNR Methods

The potential importance of the second-order term neglected in the MNR equations can be illustrated with a simple scalar problem in function minimization. The Newton-Raphson equation to minimize a function f(x) takes the well known form

$$\Delta x = - \frac{f'(x)}{f''(x)} \quad . \tag{2.38}$$

If

$$f(x) = w^2(x) \tag{2.39}$$

which is the form of equation (2.16) with $\underset{\sim}{w}$ taken as a scalar, then

$$f'(x) = 2w(x) \frac{dw}{dx}(x) \tag{2.40}$$

and

$$f''(x) = 2 \left[\frac{dw}{dx}(x)\right]^2 + 2w(x) \frac{d^2w}{dx^2}(x) \quad . \tag{2.41}$$

The FNR equation (2.36) is

$$\Delta x = \frac{-w(x) \frac{dw}{dx}(x)}{\left[\frac{dw}{dx}(x)\right]^2 + w(x) \frac{d^2w}{dx^2}(x)} \tag{2.42}$$

whereas the MNR equation (2.37) is

$$\Delta x = \frac{-w(x)\ \frac{dw}{dx}(x)}{\left[\frac{dw}{dx}(x)\right]^2} \tag{2.43}$$

$$= -\frac{w(x)}{\frac{dw}{dx}(x)}\ . \tag{2.44}$$

Applying equations (2.42) and (2.44) to the function

$$f(x) = (x-1)^4 + 1 \tag{2.45}$$

in which

$$w(x) = [(x-1)^4 + 1]^{\frac{1}{2}}\ , \tag{2.46}$$

we obtain

$$\Delta x = -\frac{1}{3}(x-1) \tag{2.47}$$

for the FNR algorithm and

$$\Delta x = -\frac{(x-1)^4 + 1}{2(x-1)^3} \tag{2.48}$$

for the MNR algorithm. Tables 1 and 2 show the first few iterations by both methods from an initial guess of $x(0) = 3$.

MNR Equation (2.48)			
Iteration	x	Δx	f(x)
1	3.000	-1.062	17.000
2	1.937	-1.076	1.772
3	0.862	190.070	1.000
4	190.932	145.121	1.329×10^9

Table 1

FNR Equation (2.47)			
Iteration	x	Δx	f(x)
1	3.000	-0.667	17.000
2	2.333	-0.444	4.160
3	1.889	-0.296	1.625
4	1.593	-0.197	1.124
5	1.395	-0.132	1.024
6	1.263	-0.088	1.005
7	1.175	-0.058	1.001
8	1.117	-0.039	1.000
9	1.078	-0.026	1.000

Table 2

Clearly the MNR equation causes x to diverge after an initial period of convergence while the FNR equation causes x to approach the minimum.

6. Computation Experience With the FNR and MNR Methods

The performance of the MNR method in the preceding scalar example is typical of the performance observed by the author in large problems. However, the FNR equation is also

not uniformly effective when used exclusively in large problems. Fortunately, the areas of effectiveness of the two methods are complementary.

In order to discuss the effectiveness of the two methods it is convenient to define two areas in the minimization process. Initial behavior refers to the behavior of J_a during the first two or three iterations in a sub-problem. Terminal behavior refers to the behavior of J_a after the first two or three iterations within the same sub-problem. The following behavior has been observed.

a. Initial behavior: The MNR equation outperforms the FNR equation in this area. The ability of the FNR equation to minimize J_a is very sensitive to the starting value of the unknowns ($\underset{\sim}{c}$). With the values of $\underset{\sim}{c}$ far removed from the optimum, the FNR equation generally causes J_a to increase rapidly and diverge from the minimum. The MNR equation on the other hand is relatively insensitive to the starting $\underset{\sim}{c}$ and can usually be counted on to move J_a toward the minimum for at least one or two iterations.

b. Terminal behavior: As the minimum is approached, the MNR equation produces the behavior shown in Figure 1. The FNR equation, however, generally becomes extremely effective in rapidly finding the minimum.

7. <u>A Combination FNR-MNR Minimization Method</u>

The obvious approach suggested by the previous observations is to devise an algorithm which minimizes by the MNR equation initially in a given sub-problem and switches to

[illegible]

the FNR equation at some appropriate point in the iteration process. Such an algorithm is presented in Section IV.

III. AN INEQUALITY CONSTRAINT PENALTY FUNCTIONAL

In this section a new penalty functional is introduced for state and control inequality constraints of the form

$$x_{i_L} \leq x_i(t) \leq x_{i_M} \quad , \quad i=1,2,\ldots,I_s \leq n \ , \quad t \,\varepsilon\, [t_o,T] \ , \quad (3.1)$$

$$u_{j_L} \leq u_j(t) \leq u_{j_M} \quad , \quad j=1,2,\ldots,I_c \leq \ell \ , \quad t \,\varepsilon\, [t_o,T] \ . \quad (3.2)$$

All state and control inequality constraints encountered in the problems solved herein are of this type. The difficulties encountered with existing penalty methods which led to the use of a new functional are related. The new penalty functional has performed well in computation and is used exclusively in the solution of the problems presented. Additionally, several desirable theoretical properties of the proposed penalty functional are presented.

A. INTERIOR PENALTY METHODS

1. Past Research

In Ref. 10 Jones and McCormick present a number of theoretical results concerning interior penalty functionals of the Fiacco-McCormick type [Ref. 9] in conjunction with the epsilon method. If, for example, a state or control, denoted by y(t) for generality, is constrained by

$$y(t) \leq Y \quad , \qquad t \,\varepsilon\, [t_o,T] \ , \qquad (3.3)$$

a Fiacco-McCormick penalty functional [Ref. 9] of the form

$$\int_{t_o}^{T} \frac{r}{1 - y(t)}\, dt \tag{3.4}$$

is added to the augmented performance measure. The behavior of the integrand of expression (3.4) for a fixed time $t \in [t_o, T]$ as the positive weighting factor r approaches 0 is shown in Figure 2.

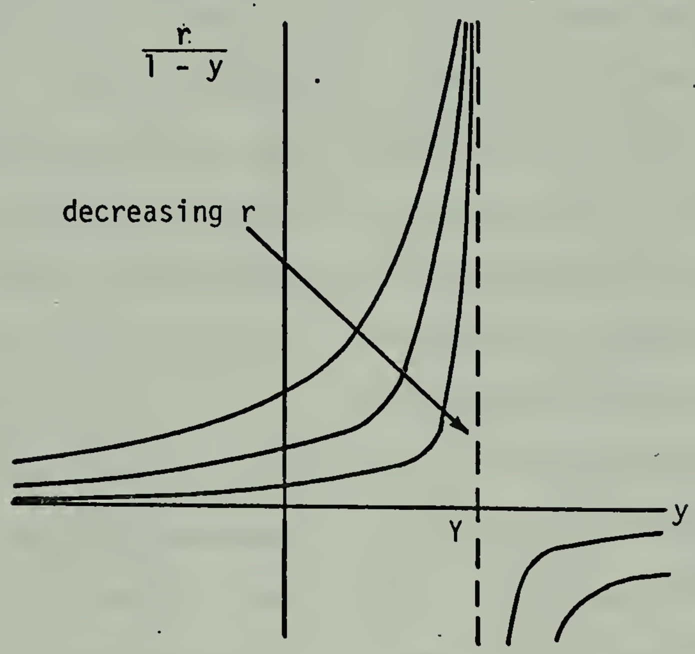

Figure 2

Fiacco-McCormick penalty function vs. constrained variable for a fixed time

If penalty functionals of this type are added to the performance measure, it can be shown [Ref. 10] that as r approaches 0 and ε approaches 0, the epsilon method yields Pontryagin's minimum principle. The development parallels and augments Balakrishnan's work [Refs. 13 and 14] without inequality constraints. No computational results, however, are presented.

2. Computational Experience

A simple problem involving one state variable and one constrained control was attempted using the epsilon method and a penalty functional of the form given by equation (3.4). The optimal control was on the constraint boundary. The algorithm was unable to solve the problem by either the FNR or MNR method from a variety of starting points. Once the control penetrated the constraint boundary for a finite time interval, the algorithm failed on the next iteration. The value of r required to keep the control admissible for all $t \in [t_o,T]$ throughout the iteration process was large, resulting in the augmented performance measure being dominated by the Fiacco-McCormick penalty term. As a result, the optimal solution $[\underset{\sim}{u}^*(t,\varepsilon,r)]$ to the augmented problem could not be made to approach the optimal solution $[\underset{\sim}{u}^*(t)]$.

B. A NEW PENALTY FUNCTIONAL: COMPUTATIONAL PROPERTIES

1. The Form of the New Penalty Functional

Consider a control or state y(t) which is subject to a constraint of the form

$$y(t) \in [y_L, y_M] \quad , \quad t \in [t_o, T] \quad . \tag{3.5}$$

A penalty functional of the form

$$J_p(y,r,K_p) = r \int_{t_o}^{T} \left[\frac{2y(t) - y_M - y_L}{y_M - y_L} \right]^{2K_p} dt \tag{3.6}$$

where K_p is a positive integer is added to the augmented performance measure. The effect of K_p can be seen from Figure 3 which shows the integrand of equation (3.6) as a function of y(t) for a fixed time $t \in [t_o, T]$.

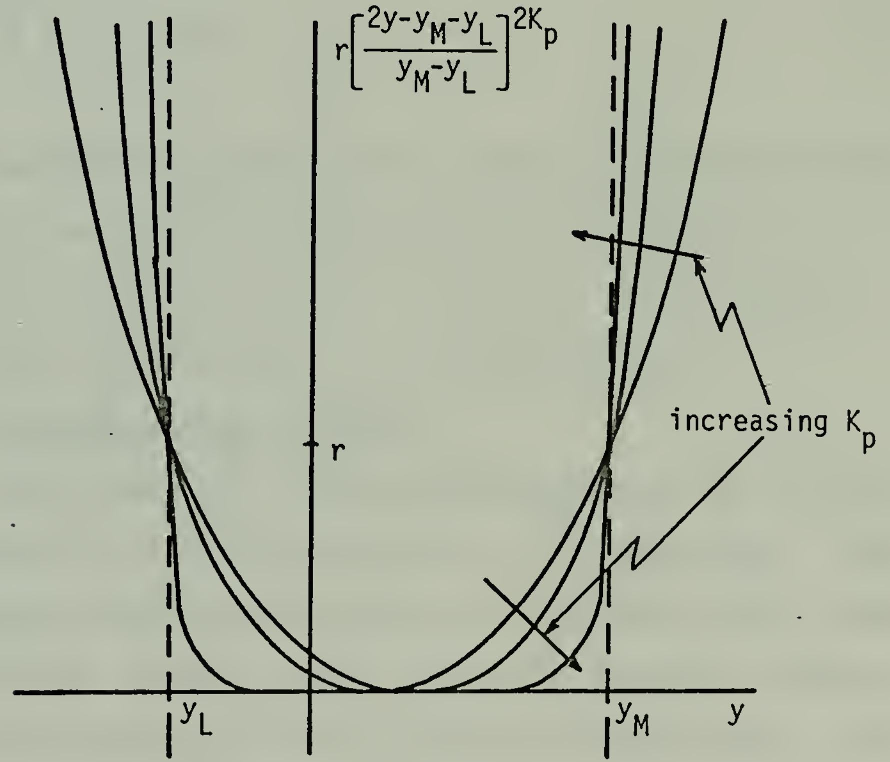

Figure 3

New penalty function vs. constrained variable for a fixed time

A functional of the form given by equation (3.6) is added to the augmented performance measure for each inequality constraint of the form given by equations (3.1) and (3.2). For I_c control constraints and I_s state constraints of this form the total augmented performance measure for the epsilon method written for time invariant problems with $t_o = 0$ is

$$J_a = J + \int_0^T \frac{1}{\varepsilon} \, ||\dot{\underset{\sim}{x}} - \underset{\sim}{f}(\underset{\sim}{x},\underset{\sim}{u})||^2 \, dt$$

$$+ r\int_0^T \left\{ \sum_{j=1}^{I_c} \left[\frac{2u_j(t)-u_{j_M}-u_{j_L}}{u_{j_M} - u_{j_L}}\right]^{2K_p} + \sum_{i=1}^{I_s} \left[\frac{2x_i(t)-x_{i_M}-x_{i_L}}{x_{i_M} - x_{i_L}}\right]^{2K_p} \right\} dt \qquad (3.7)$$

$$= J + \frac{1}{\varepsilon} J_s + r J_p \qquad (3.8)$$

The "two-sided" feature of the penalty functional makes it especially suited to constraints of the form given by equations (3.1) and (3.2). In effect, two inequality constraints are included in one penalty term.

2. Computational Strategy

The power K_p is increased gradually in numerical computation in the same manner as ε is decreased. Thus, increasingly refined boundaries to the admissible region are provided. Both ε and K_p are held constant within a sub-problem and are altered between sub-problems. The weighting factor r, which is required to provide an overall weighting among J, J_s, and J_p, is held constant throughout the entire problem.

Computational results with this penalty functional have been excellent. Up to eight inequality constraints have been treated successfully in one problem.

C. THEORETICAL PROPERTIES OF THE NEW PENALTY FUNCTIONAL

1. Introduction

Three desirable properties of the new penalty functional are presented here. These properties and their importance are discussed followed by a proof of each property.

a. Penalty functionals of the form of equation (3.6) are convex on R^n where $\underset{\sim}{c}_y \in R^n$ is defined by

$$\underset{\sim}{c}_y^T \triangleq [a_1, a_2, \ldots, a_M, y(t_o), y(T)] \tag{3.9}$$

and

$$y(t) = y(t_o) + \frac{y(T)-y(t_o)}{T-t_o}(t-t_o) + \sum_{m=1}^{M} a_m \sin\frac{m\pi(t-t_o)}{T-t_o} \tag{3.10}$$

It is desirable that the augmented performance measure be convex in the unknowns of the minimization to insure that a global minimum is attained. If it can be shown that the inequality constraint penalty functionals (3.6) are convex, then the addition of any number of these functionals does not destroy a convexity condition which exists without these terms, because the sum of convex functionals is also convex. Indeed, the addition of terms of the type given in equation (3.6) may create a convexity condition where one does not exist without the terms.

[illegible]

b. If for a fixed $\underset{\sim}{c}_y$ given by equation (3.9), the expansion (3.10) of a constrained state or control is inadmissible by a finite amount $\varepsilon_p(\varepsilon_p > 0)$ at $t_* \varepsilon (t_o, T)$, its associated penalty functional (3.6) is unbounded as $K_p \to \infty$. This means that as $K_p \to \infty$, the contribution of a penalty term (3.6) to the augmented performance measure for an inadmissible state or control becomes very large. Therefore, if J_a is being minimized under the condition of ever increasing K_p, the constrained states or controls must at least approach admissibility.

c. If for a fixed $\underset{\sim}{c}_y$ given by equation (3.9), the expansion (3.10) of a constrained state or control lies completely within the admissible region, its associated penalty functional (3.6) has limit zero as $K_p \to \infty$. The significance of this result is that penalty terms of the form given by equation (3.6) will add less and less to the augmented performance measure as K_p is increased for states and controls that are completely admissible.

2. Convexity

Property a discussed above is shown here. The theorem to be proved follows.

Theorem 1. If a constrained state or control y(t) is bounded for $t \; \varepsilon \; [t_o, T]$ and is given by

$$y(t) = y(t_o) + \frac{y(T)-y(t_o)}{T-t_o}(t-t_o) + \sum_{m=1}^{M} a_m \sin \frac{m\pi(t-t_o)}{T-t_o} \qquad (3.10)$$

where $\underset{\sim}{c}_y \; \varepsilon \; R^n$ is defined by

$$\underset{\sim}{c}_y^T \triangleq [a_1, a_2, \ldots, a_M, y(t_o), y(T)] \neq \underset{\sim}{0} , \qquad (3.9)$$

then the penalty functional

$$J_p(y,K_p) = r \int_{t_o}^{T} \left[\frac{2y(t)-y_M-y_L}{y_M-y_L}\right]^{2K_p} dt \qquad (3.6)$$

is convex on R^n. The constants y_M and y_L define the admissible region for $y(t)$ and r is a constant.

Proof. Consider the case of $K_p = 1$. Equation (3.6) becomes

$$J_p(y,K_p) = \frac{r}{(y_M-y_L)^2} \int_{t_o}^{T} [2y(t)-(y_M+y_L)]^2 \, dt. \qquad (3.11)$$

Let

$$d \triangleq \frac{y_M + y_L}{2} \qquad (3.12)$$

and

$$r_o \triangleq \frac{4r}{(y_M-y_L)^2} . \qquad (3.13)$$

Substituting equations (3.12) and (3.13) into equation (3.11), we obtain

[illegible]

[illegible]

[illegible]

[illegible]

[illegible]

[illegible]

[illegible]

[illegible]

$$J_p = r_o \int_{t_o}^{T} [y(t) - d]^2 \, dt \tag{3.14}$$

$$= r_o \int_{t_o}^{T} [y^2(t) - 2y(t)d + d^2] \, dt \, . \tag{3.15}$$

Substituting the expansion (3.10) into equation (3.15), we obtain

$$J_p = r_o \int_{t_o}^{T} \left\{ \left[y(t_o) + \frac{y(T)-y(t_o)}{T-t_o} (t-t_o) + \sum_{m=1}^{M} a_m \sin \frac{m\pi(t-t_o)}{T-t_o} \right]^2 \right. \tag{3.16}$$

$$\left. -2\left[y(t_o) + \frac{y(T)-y(t_o)}{T-t_o} (t-t_o) + \sum_{m=1}^{M} a_m \sin \frac{m\pi(t-t_o)}{T-t_o} \right] d + d^2 \right\} dt.$$

Equation (3.16) may be written as a quadratic functional of the form

$$J_p = r_o \int_{t_o}^{T} \left[\frac{1}{2} \langle \underset{\sim}{c}_y, \underset{\sim}{Q}_1(t) \underset{\sim}{c}_y \rangle + \langle \underset{\sim}{c}_y, \underset{\sim}{\alpha}(t) \rangle + \beta \right] dt \tag{3.17}$$

where $\underset{\sim}{\alpha}(t) \in R^n$ is

$$\underset{\sim}{\alpha}(t)^T = -2d \left[\sin \frac{\pi(t-t_o)}{T-t_o} , \frac{\sin 2\pi(t-t_o)}{T-t_o} , \ldots , \frac{\sin M\pi(t-t_o)}{T-t_o} , (1-\frac{t-t_o}{T-t_o}), \frac{t-t_o}{T-t_o} \right] . \tag{3.18}$$

$\underset{\sim}{Q}_1(t)$ is the outer product given by

$$\underset{\sim}{Q}_1(t) = \frac{\underset{\sim}{\alpha}(t)\underset{\sim}{\alpha}(t)^T}{4d^2} \tag{3.19}$$

and

$$\beta = d^2 \quad . \tag{3.20}$$

At an arbitrary fixed time $t_* \varepsilon [t_o, T]$, the integrand of equation (3.14) is

$$[y(t_*) - d]^2 = \frac{1}{2} \langle \underset{\sim}{c}_y, \underset{\sim}{Q}_1(t_*) \underset{\sim}{c}_y \rangle + \langle \underset{\sim}{c}_y, \underset{\sim}{\alpha}(t_*) \rangle + \beta \quad . \tag{3.21}$$

The first term on the right side of equation (3.21) is

$$\frac{1}{2} \langle \underset{\sim}{c}_y, Q_1(t_*) \underset{\sim}{c}_y \rangle = \left[y(t_o) + \frac{y(T)-y(t_o)}{T-t_o} (t_*-t_o) + \sum_{m=1}^{M} a_m \sin\frac{m\pi(t_*-t_o)}{T-t_o} \right]^2 \quad . \tag{3.22}$$

Since the terms in the finite expansion of $y(t_*)$ given in equation (3.10) are linearly independent and analytic, $y(t_*)$ is different from zero almost everywhere and

$$y^2(t_*) \geq 0 \quad , \quad t_* \ \varepsilon \ [t_o, T], \quad \underset{\sim}{c}_y \neq \underset{\sim}{0}. \tag{3.23}$$

Thus,

$$\tfrac{1}{2} \langle \underset{\sim}{c}_y, \underset{\sim}{Q}_1(t_*) \underset{\sim}{c}_y \rangle \geq 0, \quad t_* \ \varepsilon \ [t_o, T], \quad \underset{\sim}{c}_y \neq \underset{\sim}{0}, \tag{3.24}$$

and $\underset{\sim}{Q}_1(t_*)$ is, therefore, positive semi-definite, at least, and positive definite almost everywhere for any $\underset{\sim}{c}_y \neq \underset{\sim}{0}$. Applying Theorem 4.5 of Reference 17 (p. 27)[1], the function given in equation (3.21) is convex on R^n at $t = t_*$.

Next, consider the case where K_p is any positive integer. In Appendix E the following theorem is proved: if $f(\underset{\sim}{x})$ is convex on R^n where $\underset{\sim}{x} \in R^n$ and $f(\underset{\sim}{x}) \geq 0$, then $f^K(\underset{\sim}{x})$ is convex on R^n where K is any positive integer. Since

$$[y(t_*) - d]^2 \geq 0, \tag{3.25}$$

is convex, it follows immediately that

$$[y(t_*) - d]^{2K_p} \tag{3.26}$$

is convex on R^n at a fixed time $t_* \in [t_o, T]$. Since y(t) is bounded by assumption for $t \in [t_o, T]$, it follows that for

---

[1]Let f be a twice continuously differentiable real-valued function on an open convex set c in R^n. Then f is convex on c if and only if its Hessian matrix

$$Q_x = (q_{ij}(x)), \quad q_{ij}(x) = \frac{\partial^2 f}{\partial \xi_i \partial \xi_j}(\xi_1, \ldots, \xi_n)$$

is positive semi-definite for every $x \in c$. A quadratic function

$$f(x) = \tfrac{1}{2}\langle x, Qx\rangle + \langle x, a\rangle + \alpha$$

where Q is a symmetric n x n matrix, is convex on R^n if and only if Q is positive semi-definite.

any finite positive integer K_p, the expression (3.26) is bounded for $t_* \epsilon [t_o,T]$. By Theorem 4, (p. 536) of Reference 18[1]

$$\int_{t_o}^{T} [y(t) - d]^{2K_p} \, dt \tag{3.27}$$

is convex on R^n. Hence equation (3.6) is convex on R^n for all finite positive integer values of K_p.

3. Behavior of the New Penalty Functional for an Inadmissible Constrained State or Control

Property b is shown below.

Theorem 2. Assume y(t) is bounded and given by equation (3.10) for $t \epsilon [t_o,T]$ where $\underset{\sim}{c}_y \neq \underset{\sim}{0}$, as defined by equation (3.9). If for a given y(t)

$$y(t_*) \geq y_M + \epsilon_p \tag{3.28}$$

or

$$y(t_*) \leq y_L - \epsilon_p \tag{3.29}$$

---

[1]Let

$$I_f(x) = \int_T f(t,x(t)) \, dt.$$

Let T be of finite measure. Let f(t,x) be a finite convex function of x for each t and a bounded measurable function of t for each x. Then I_f is a well-defined finite convex function on $L_n^\infty(T)$ which is everywhere continuous with respect to the uniform norm.

[illegible]

at some time $t_* \varepsilon (t_o,T)$, where $\varepsilon_p > 0$, then

$$\underset{K_p \to \infty}{\text{Limit}}\ J_p(y,K_p) = \infty \tag{3.30}$$

where

$$J_p(y,K_p) = r \int_{t_o}^{T} \left[\frac{2y(t)-y_M-y_L}{y_M-y_L}\right]^{2K_p} dt. \tag{3.6}$$

In order to prove this theorem the following lemma is required.

Lemma 1. Assume $y(t)$ is bounded by

$$-\infty < M_1 \leq y(t) \leq M_2 < \infty \tag{3.31}$$

and is given by equation (3.10) for $t \varepsilon [t_o,T]$ where $\underset{\sim}{c}_y \neq \underset{\sim}{0}$ as defined by equation (3.9). Then, if

$$y(t_*) \geq y_M + \varepsilon_p \tag{3.28}$$

at some time $t_* \varepsilon (t_o,T)$ for any $\varepsilon_p > 0$, there exists a $\delta > 0$ such that

$$y(t) \geq y_M + \frac{\varepsilon_p}{2} \tag{3.32}$$

for the finite time interval

$$t_* - \delta \leq t \leq t_* + \delta. \tag{3.33}$$

Similarly, if

$$y(t_*) \leq y_L - \varepsilon_p \tag{3.29}$$

at some time $t_* \in (t_o,T)$ for any $\varepsilon_p > 0$, there exists a $\delta > 0$ such that

$$y(t) \leq y_L - \frac{\varepsilon_p}{2} \tag{3.34}$$

for the finite time interval

$$t_* - \delta \leq t \leq t_* + \delta. \tag{3.33}$$

<u>Proof of the lemma</u>. First, it is necessary to show that the coefficients in equation (3.10) are bounded; that is

$$|a_m| \leq M_3, \quad m = 1,2,\ldots,M \tag{3.35}$$

where $M_3 > 0$. To this end consider

$$\int_{t_o}^{T} [y(t)]^2 dt = \int_{t_o}^{T} \left[y(t_o) + \frac{y(T)-y(t_o)}{T-t_o}(t-t_o) + \sum_{m=1}^{M} a_m \sin\frac{m\pi(t-t_o)}{T-t_o} \right]^2 dt \tag{3.36}$$

$$= \langle \underset{\sim}{c}_y, \underset{\sim}{Q}_2 \underset{\sim}{c}_y \rangle \tag{3.37}$$

where $\underset{\sim}{c}_y$ is given by the definition (3.9). $\underset{\sim}{Q}_2$ is a symmetric matrix given by

$$\underset{\sim}{Q}_2 = \begin{bmatrix} \frac{T-t_o}{2} & 0 & \cdots & 0 & \frac{2(T-t_o)}{\pi} & \frac{2(T-t_o)}{\pi} \\ 0 & \frac{T-t_o}{2} & \cdots & 0 & \frac{2(T-t_o)}{2\pi} & -\frac{2(T-t_o)}{2\pi} \\ \vdots & \vdots & & \vdots & \vdots & \vdots \\ 0 & 0 & \cdots & \frac{T-t_o}{2} & \frac{2(T-t_o)}{M\pi} & \pm\frac{2(T-t_o)}{M\pi} \\ \frac{2(T-t_o)}{\pi} & \frac{2(T-t_o)}{2\pi} & \cdots & \frac{2(T-t_o)}{M\pi} & \frac{T-t_o}{3} & \frac{T-t_o}{3} \\ \frac{2(T-t_o)}{\pi} & -\frac{2(T-t_o)}{2\pi} & \cdots & \pm\frac{2(T-t_o)}{M\pi} & \frac{T-t_o}{3} & \frac{T-t_o}{3} \end{bmatrix} \tag{3.38}$$

where the terms with $\pm$ are positive if M is odd and negative if M is even. Since y(t) is bounded by assumption and the expansion (3.10) is the sum of M + 2 linearly independent terms, we have

$$0 < \int_{t_o}^{T} [y(t)]^2 dt \leq M_4 \tag{3.39}$$

where $M_4 > 0$. Using equation (3.37) and inequality (3.39), we obtain

$$0 < \langle \underset{\sim}{c}_y, \underset{\sim}{Q}_2 \underset{\sim}{c}_y \rangle \leq M_4. \tag{3.40}$$

$\underset{\sim}{Q}_2$ is, therefore, positive definite. Using Theorem 2.5 of Reference 15 (p. 52)[1], we have

$$\langle \underset{\sim}{c}_y, \underset{\sim}{Q}_2 \underset{\sim}{c}_y \rangle \geq \underline{\lambda} \, ||\underset{\sim}{c}_y||^2 \tag{3.41}$$

where $\underline{\lambda} > 0$ is the smallest eigenvalue of $\underset{\sim}{Q}_2$ and $||\underset{\sim}{c}_y|| = \sqrt{\langle \underset{\sim}{c}_y, \underset{\sim}{c}_y \rangle}$. Therefore, using the inequality (3.40), we obtain

$$||\underset{\sim}{c}_y||^2 \leq \frac{M_4}{\underline{\lambda}} \, . \tag{3.42}$$

Since a_m, $m = 1,2,\ldots,M$ is a subset of $\underset{\sim}{c}_y$, it follows that

$$|a_m| \leq M_3, \quad m=1,2,\ldots,M \tag{3.35}$$

where $M_3 > 0$.

Now consider the derivative of equation (3.10) which is

$$\dot{y}(t) = \frac{y(T)-y(t_o)}{T-t_o} + \sum_{m=1}^{M} a_m \frac{m\pi}{T-t_o} \cos \frac{m\pi(t-t_o)}{T-t_o} \, . \tag{3.43}$$

---

[1]Let $Q = (q_{ij})$ be a symmetric n x n matrix. Then Q is positive definite if and only if there is a $k > 0$ such that

$$\langle \underset{\sim}{v}, \underset{\sim}{Q}\underset{\sim}{v} \rangle \geq k||\underset{\sim}{v}||^2$$

for all v in R^n, where $||v|| = \sqrt{\langle \underset{\sim}{v}, \underset{\sim}{v} \rangle}$ is the Euclidean norm of $\tilde{v}$.

Taking the absolute value of both sides of equation (3.43) and applying inequality laws, we obtain

$$|\dot{y}(t)| \leq \left|\frac{y(T)-y(t_o)}{T-t_o}\right| + \left|\sum_{m=1}^{M} a_m \frac{m\pi}{T-t_o} \cos \frac{m\pi(t-t_o)}{T-t_o}\right| \qquad (3.44)$$

which further simplifies to

$$|\dot{y}(t)| \leq \left|\frac{y(T)-y(t_o)}{T-t_o}\right| + \sum_{m=1}^{M} |a_m| \frac{m\pi}{T-t_o} . \qquad (3.45)$$

Applying the inequality (3.35), we obtain

$$|\dot{y}(t)| \leq \left|\frac{y(T)-y(t_o)}{T-t_o}\right| + \frac{M_3\pi}{T-t_o} \sum_{m=1}^{M} m \qquad (3.46)$$

$$\leq M_5 \qquad (3.47)$$

for all $t \in (t_o,T)$ where $M_5 > 0$. The first part of the lemma as expressed by the inequality (3.32) will now be shown. Let

$$\delta \triangleq \frac{\varepsilon_p/2}{M_5} \qquad (3.48)$$

as shown in Figure 4. Consider

$$y(t) = y(t_*) + \int_{t_*}^{t} \dot{y}(\tau)\, d\tau . \qquad (3.49)$$

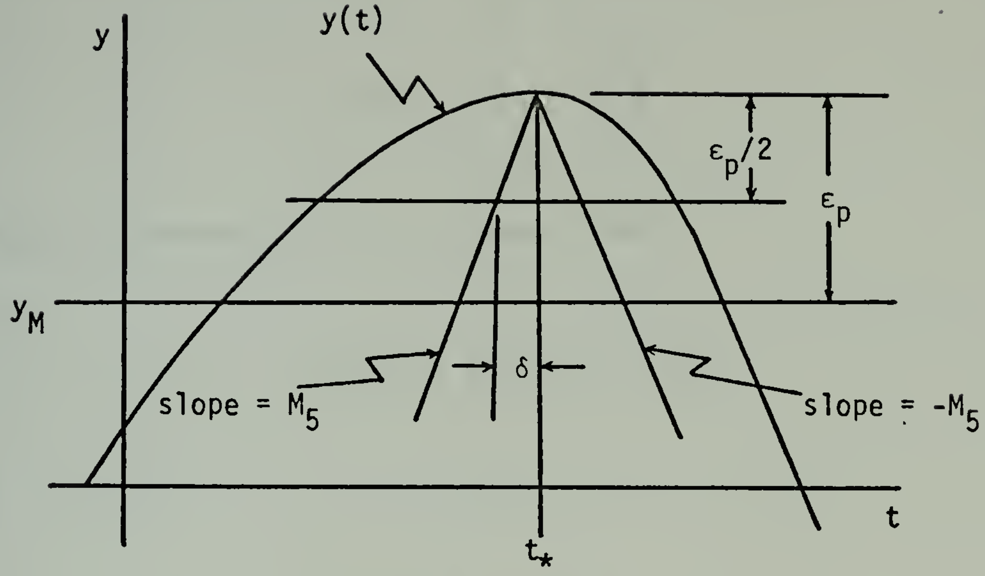

Figure 4
Constrained Variable vs. time

Applying inequality (3.47), we have

$$y(t) \geq y(t_*) - M_5 \, |t_* - t| \, . \tag{3.50}$$

Consider t in the interval $t_* - \delta \leq t \leq t_* + \delta$. In this interval δ satisfies

$$\delta \geq |t_* - t| \, . \tag{3.51}$$

Applying inequality (3.50), we have

$$y(t) \geq y(t_*) - M_5 \, \delta \, . \tag{3.52}$$

Using the definition (3.48), we obtain

$$y(t) \geq y(t_*) - \frac{\varepsilon_p}{2} . \tag{3.53}$$

Applying inequality (3.28), we obtain

$$y(t) \geq y_M + \varepsilon_p - \frac{\varepsilon_p}{2} \tag{3.54}$$

or

$$y(t) \geq y_M + \frac{\varepsilon_p}{2} , \tag{3.32}$$

thus proving the first portion of Lemma 1. The second portion of the lemma as given by inequality (3.34) can be proved in a similar manner. It is possible at this point to return to the proof of Theorem 2.

Proof of Theorem 2. If inequality (3.28) applies, then by Lemma 1 inequality (3.32) is true. Considering the integrand of equation (3.6), since $y_M > y_L$, it follows that

$$\left[\frac{2y(t)-y_M-y_L}{y_M-y_L}\right]^{2K_p} \geq \left[\frac{2(y_M+\frac{\varepsilon_p}{2})-y_M-y_L}{y_M-y_L}\right]^{2K_p} \tag{3.55}$$

for $t_* - \delta \leq t \leq t_* + \delta$. Further simplification yields

$$\left[\frac{2y(t)-y_M-y_L}{y_M-y_L}\right]^{2K_p} \geq \left[\frac{\varepsilon_p+y_M-y_L}{y_M-y_L}\right]^{2K_p} , \tag{3.56}$$

$$\geq \left[1 + \frac{\varepsilon_p}{y_M-y_L}\right]^{2K_p} . \tag{3.57}$$

Since the integrand of equation (3.6) is nonnegative for $t \varepsilon (t_o,T)$ and $r > 0$, it follows that

$$J_p(y,K_p) = r\int_{t_o}^{T} \left[\frac{2y(t)-y_M-y_L}{y_M-y_L}\right]^{2K_p} dt \tag{3.6}$$

$$\geq r \int_{t_*-\delta}^{t_*+\delta} \left[\frac{2y(t)-y_M-y_L}{y_M-y_L}\right]^{2K_p} dt . \tag{3.58}$$

Applying inequality (3.57), we have

$$J_p(y,K_p) \geq r \int_{t_*-\delta}^{t_*+\delta} \left[1 + \frac{\varepsilon_p}{y_M-y_L}\right]^{2K_p} dt . \tag{3.59}$$

The integration of inequality (3.59) yields

$$J_p(y,K_p) \geq r \left[1 + \frac{\varepsilon_p}{y_M-y_L}\right]^{2K_p} 2\delta . \tag{3.60}$$

Since $y_M > y_L$ and $\varepsilon_p > 0$, it follows that

$$\underset{K_p\to\infty}{\text{Limit}} \left[1 + \frac{\varepsilon_p}{y_M-y_L}\right]^{2K_p} = \infty , \tag{3.61}$$

and in view of inequality (3.60)

$$\underset{K_p \to \infty}{\text{Limit}}\ J_p(y,K_p) = \infty \quad . \tag{3.62}$$

If inequality (3.29) applies, then by Lemma 1, inequality (3.34) is true. Since $y_M > y_L$, it follows that

$$\left[\frac{2y(t)-y_M-y_L}{y_M-y_L}\right] \leq \left[\frac{2(y_L-\frac{\varepsilon_p}{2})-y_M-y_L}{y_M-y_L}\right] \tag{3.63}$$

for $t_* - \delta \leq t \leq t_* + \delta$. Simplifying, we obtain

$$\left[\frac{2y(t)-y_M-y_L}{y_M-y_L}\right] \leq -\left[1 + \frac{\varepsilon_p}{y_M-y_L}\right] \quad . \tag{3.64}$$

Squaring both sides of inequality (3.64), we have

$$\left[\frac{2y(t)-y_M-y_L}{y_M-y_L}\right]^2 \geq \left[1 + \frac{\varepsilon_p}{y_M-y_L}\right]^2 . \tag{3.65}$$

Raising inequality (3.65) to the K_p th power, we obtain

$$\left[\frac{2y(t)-y_M-y_L}{y_M-y_L}\right]^{2K_p} \geq \left[1 + \frac{\varepsilon_p}{y_M-y_L}\right]^{2K_p} \tag{3.57}$$

which is identical to inequality (3.57). The remainder of the proof follows inequality (3.57) to equation (3.62) exactly. The theorem is proved for the open interval $t \varepsilon (t_o,T)$. The extension of the theorem to cover the closed interval $t \varepsilon [t_o,T]$ is not difficult.

4. Behavior of the New Penalty Functional for an Admissible Constrained State or Control

Property c above is shown below.

Theorem 3. Assume $y(t)$ is given by equation (3.10) for $t \in [t_o, T]$. If for a given $y(t)$

$$y_L + \varepsilon_q \leq y(t) \leq y_M - \varepsilon_q \tag{3.66}$$

for all $t \in [t_o, T]$ where $\varepsilon_q > 0$, then

$$\lim_{K_p \to \infty} J_p(y, K_p) = 0 \quad . \tag{3.67}$$

Proof. From inequality (3.66) it can be seen that

$$y_L + \varepsilon_q \leq y_M - \varepsilon_q \quad . \tag{3.68}$$

Since $y_M > y_L$, inequality (3.68) may be rarranged to the form

$$1 - \frac{2\varepsilon_q}{y_M - y_L} \geq 0 \quad . \tag{3.69}$$

The inequality (3.69) will become useful shortly.

Starting with inequality (3.66), multiplying through by 2, and subtracting y_M and y_L, we obtain

$$2(y_L+\varepsilon_q)-y_M-y_L \leq 2y(t)-y_M-y_L \leq 2(y_M-\varepsilon_q)-y_M-y_L \quad . \tag{3.70}$$

Dividing through by the positive quantity $y_M - y_L$, we obtain

$$\frac{2(y_L+\varepsilon_q)-y_M-y_L}{y_M-y_L} \leq \frac{2y(t)-y_M-y_L}{y_M-y_L} \leq \frac{2(y_M-\varepsilon_q)-y_M-y_L}{y_M-y_L} . \tag{3.71}$$

This inequality can be reduced to

$$- \; 1 - \frac{2\varepsilon_q}{y_M-y_L} \leq \left[\frac{2y(t)-y_M-y_L}{y_M-y_L}\right] \leq 1 - \frac{2\varepsilon_q}{y_M-y_L} . \tag{3.72}$$

In view of inequality (3.69), inequality (3.72) may be rewritten as

$$\left|\left[\frac{2y(t)-y_M-y_L}{y_M-y_L}\right]\right| \leq 1 - \frac{2\varepsilon_q}{y_M-y_L} . \tag{3.73}$$

Raising inequality (3.73) to the $2K_p$ power, we have

$$\left|\left[\frac{2y(t)-y_M-y_L}{y_M-y_L}\right]\right|^{2K_p} \leq \left[1 - \frac{2\varepsilon_q}{y_M-y_L}\right]^{2K_p} . \tag{3.74}$$

Observing that

$$\left|\left[\frac{2y(t)-y_M-y_L}{y_M-y_L}\right]\right|^{2K_p} = \left[\frac{2y(t)-y_M-y_L}{y_M-y_L}\right]^{2K_p} , \tag{3.75}$$

we have from inequality (3.74)

$$\left[\frac{2y(t)-y_M-y_L}{y_M-y_L}\right]^{2K_p} \leq \left[1 - \frac{2\varepsilon_q}{y_M-y_L}\right]^{2K_p} . \tag{3.76}$$

for all $t \in [t_o,T]$. In view of inequality (3.76), it is easily seen that

[illegible]

$$\int_{t_o}^{T}\left[\frac{2y(t)-y_M-y_L}{y_M-y_L}\right]^{2K_p} dt \leq \int_{t_o}^{T}\left[1-\frac{2\varepsilon_q}{y_M-y_L}\right]^{2K_p} dt \quad .(3.77)$$

Performing the integration, we have

$$\int_{t_o}^{T}\left[\frac{2y(t)-y_M-y_L}{y_M-y_L}\right]^{2K_p} dt \leq \left[1-\frac{2\varepsilon_q}{y_M-y_L}\right]^{2K_p} (T-t_o) \quad .(3.78)$$

In view of inequality (3.69), and the fact that $y_M > y_L$, it follows that

$$\underset{K_p \to \infty}{\text{Limit}} \left[1-\frac{2\varepsilon_q}{y_M-y_L}\right]^{2K_p} = 0 \ . \qquad (3.79)$$

Observing inequality (3.78), we obtain

$$\underset{K_p \to \infty}{\text{Limit}} \int_{t_o}^{T}\left[\frac{2y(t)-y_M-y_L}{y_M-y_L}\right]^{2K_p} dt = 0 \ . \qquad (3.80)$$

The theorem is proved.

IV. THE ALGORITHM

This section describes the algorithm used for minimizing the augmented performance measure.

A. GENERAL MINIMIZATION STRATEGY

1. Sequence of Unconstrained Sub-problems

A sequence of unconstrained sub-problems is solved by the algorithm. In each sub-problem the algorithm minimizes the augmented performance measure for given values of the weighting factors (ε and r) and the inequality constraint penalty term power (K_p). After an appropriate stopping criterion is satisfied, ε is reduced, K_p is increased, and a new sub-problem is commenced using the optimal solution to the last sub-problem as a first guess. This procedure is repeated until enough sub-problems are completed to meet a second stopping criterion.

The algorithm is programmed to do one sub-problem on each computer run. The results are stored on an external storage device between computer runs and are retrieved at the commencement of the next run (new sub-problem).

2. Minimization Strategy

The algorithm minimizes by either the FNR or MNR method. The user must decide which method to use on each iteration. This is a matter of experimentation, especially for the first two or three sub-problems. An effective procedure is to run the sub-problem once using the MNR equation

throughout and once using the FNR equation throughout. From these results an effective minimization strategy can generally be deduced for the sub-problem. Occasionally further experimentation is required. This experimentation points out the advantages of using separate computer runs for each sub-problem. Once a sub-problem is completed and the results stored, the computation does not have to be redone each time an experimental run is made in the next sub-problem.

B. COMMENCING THE PROBLEM

1. Initial Decisions

Three interrelated decisions must be made to begin a problem. First, the number of time points K must be chosen. Second, the number of coefficients M for each state and control expansion must be chosen. The same number of coefficients is used for all expansions in a given problem in this dissertation, but this is not a requirement. From a theoretical standpoint it is desirable to use a large number of coefficients and time points to insure that an adequate approximation of the optimal control and state trajectory is obtained, but practically, computer time and storage requirements limit the number of each. The computational penalty for using a large number of coefficients is the more severe of the two as the number of equations in (2.36) and (2.37) which must be solved is equal to the total number of coefficients plus the number of free end conditions. The solution of equation (2.36) or (2.37) represents a considerable portion of the overall computer time.

[illegible]

The third decision involves the initial values of ε, r, and K_p. The weighting factor r for the inequality constraint penalty terms is held constant throughout the entire problem. A satisfactory value used in all problems in this dissertation for all inequality constraint penalty terms is r = 100. An initial value of K_p which has worked well in all problems is $K_p = 4$. Larger values of K_p generally cause computer overflow in the first sub-problem. With these values chosen there exists a region of ε's for which the first sub-problem will respond to an appropriate minimization strategy. This acceptable range of starting ε's is different for each problem but is in the range

$$10^{-5} \leq \varepsilon \leq 10^{-3}$$

for all problems solved herein. Numerical experimentation is the only method available to determine an acceptable starting ε. There is no theoretical requirement to use the same value of ε for each state equation equality constraint term in the augmented performance measure or the same K_p in each inequality constraint term, but the use of different ε's and K_p's has never been required.

2. <u>Initial Guess for the Unknowns</u>

Once the above three initial decisions are made, an initial guess for the vector of unknowns $\underset{\sim}{c}$ is required. The vector $\underset{\sim}{c}$ includes all coefficients and free end conditions.

All coefficients are set equal to zero initially unless there is good reason to make a different choice.

C. ITERATION

1. Required Vectors and Matrices

The states and controls are calculated at each time increment by evaluating the functional expansions. The $\underset{\sim}{w}$ vector defined in (2.15) is calculated using these states and controls. Next, the gradient matrix (2.34), the augmented performance measure (2.16), the symmetric matrix $(\nabla_{\underset{\sim}{c}}\underset{\sim}{w})_{\underset{\sim}{c}}^{T}(\nabla_{\underset{\sim}{c}}\underset{\sim}{w})_{\underset{\sim}{c}}$, and the vector $(\nabla_{\underset{\sim}{c}}\underset{\sim}{w})_{\underset{\sim}{c}}^{T}\underset{\sim}{w}_{\underset{\sim}{c}}$ are calculated.

At this point the algorithm begins the iteration process with either the MNR or the FNR method depending on the value of a flag set by the user (the method selected is based on the iteration number being performed). If the MNR method is to be used, equation (2.37) is formed. If the FNR method is called for, the three-dimensional array (2.35) is calculated and the symmetric matrix $(\nabla_{\underset{\sim}{c}}^{2}\underset{\sim}{w})_{\underset{\sim}{c}}^{T}\underset{\sim}{w}_{\underset{\sim}{c}}$ is formed. It is prohibitive to store the entire three-dimensional array, but a feasible alternative is to multiply each matrix in this array by $\underset{\sim}{w}$ as the matrix is calculated and store the resulting column vector. Once a matrix in the three-dimensional array is multiplied by $\underset{\sim}{w}$, it is no longer required by the algorithm. The next matrix in the array is calculated and stored in the same storage locations used by the first matrix. Only the symmetric matrix $(\nabla_{\underset{\sim}{c}}^{2}\underset{\sim}{w})_{\underset{\sim}{c}}^{T}\underset{\sim}{w}_{\underset{\sim}{c}}$ need be stored. The total increase in storage

requirements of the FNR method over the MNR method using this computation technique is less than 10 percent in the problems solved herein. It is also imperative in terms of computation time to take full advantage of the symmetry of the matrix $(\nabla_{\underset{\sim}{c}}{}^2 \underset{\sim}{w})_{\underset{\sim}{c}}{}^T \underset{\sim}{w}_{\underset{\sim}{c}}$. Due to this symmetry it is necessary to calculate only one column of the first matrix in the array, two columns of the second matrix, and n columns of the n^{th} matrix. By taking advantage of the symmetry the average time for each FNR iteration is approximately twice the time for each MNR iteration.

2. Solving the Linear System

At this point equation (2.36) or (2.37) is formed and must be solved for $\Delta\underset{\sim}{c}$. This is a linear system of the form

$$\underset{\sim}{A}\ \underset{\sim}{x} = \underset{\sim}{b} \tag{4.1}$$

and is solved in the algorithm by one of three methods available to the user. They are:

a. Gauss elimination with improvement by residuals using total pivoting,

b. Gauss elimination with improvment by residuals using main diagonal pivoting and a computation technique which capitalizes on the symmetry of $\underset{\sim}{A}$, and

c. Gauss-Seidel iteration.

In the problems solved herein the number of unknowns varied from 37 to 74. In spite of the large number of

unknowns involved, the elimination methods required less computation time to solve the linear system than the Gauss-Seidel iteration method. It was observed for the problems solved that total pivoting was not required in the elimination method. Method b, therefore, was the most economical and effective method for solving the linear system and was used in all problems. Method c is retained in the event that the algorithm is used to solve problems with a larger number of unknowns.

In each solution of equation (4.1) one improvement is made using residuals. That is, after equation (4.1) is solved,

$$\underset{\sim}{A}\,\underset{\sim}{x} - \underset{\sim}{b} = \underset{\sim}{r} \tag{4.2}$$

is formed. The system

$$\underset{\sim}{A}\,\underset{\sim}{y} = \underset{\sim}{r} \tag{4.3}$$

is solved and the resulting $\underset{\sim}{y}$ is subtracted from $\underset{\sim}{x}$ to form the final solution to equation (4.1).

3. <u>Interpolation</u>

Tabular functions of two independent variables are used extensively in the problems to represent aircraft and missile parameters accurately. Parabolic interpolation is used to obtain the functional values in these tables and the required first and second partial derivatives. The

derivation of the necessary difference equations for parabolic interpolation in two independent variables is presented in Appendix C.

Excerpts from the tabular data used in the problems is presented in Appendix B along with graphical representations of the data. The data represents typical supersonic aircraft and missile performance parameters and has been obtained from several sources. Considerable effort was expended to smooth the data before the tables were constructed since finite difference methods were used not only for functional values but also for first and second partial derivatives.

4. Stopping Criteria

Once the linear system is solved, a new $\underset{\sim}{c}$ vector is calculated from

$$\underset{\sim}{c}^{i+1} = \underset{\sim}{c}^{i} + \Delta\underset{\sim}{c}^{i} . \tag{4.4}$$

At this point a stopping criterion is tested. If

$$|J_a{}^{i} - J_a{}^{i+1}| \leq \mathrm{STOP1} , \tag{4.5}$$

the sub-problem is finished. Otherwise the iteration process is continued. At the completion of the sub-problem the results are stored off line. The computer run is complete.

To begin a new sub-problem a new computer run is initiated, recalling the results stored from the last

sub-problem. Epsilon is decreased, K_p is increased, and the minimization strategy is altered by the user as required. Typically, ε is divided by a factor of between two and ten and K_p is increased by two or four. That is,

$$K_p^{i+1} = K_p^{i} + \begin{bmatrix} 2 \\ \text{or} \\ 4 \end{bmatrix} . \tag{4.6}$$

More ambitious policies usually result in failure of the algorithm.

Sub-problems are solved until a second stopping criterion is satisfied. Several criteria are possible to end the problem. A method used successfully involves observing

$$J_s^{*} + J_p^{*} \tag{4.7}$$

and stopping when this sum, which represents the penalty terms due to the equality and inequality constraints without weighting factors, ceases to decrease significantly between sub-problems.

5. Flow Chart

A flow chart of the algorithm is given in Figure 5.

6. Integration

At the completion of the last sub-problem a check on the degree of satisfaction of the state equations is obtained by comparing the state expansions with the state trajectory obtained by integrating the state equations with the control expansions.

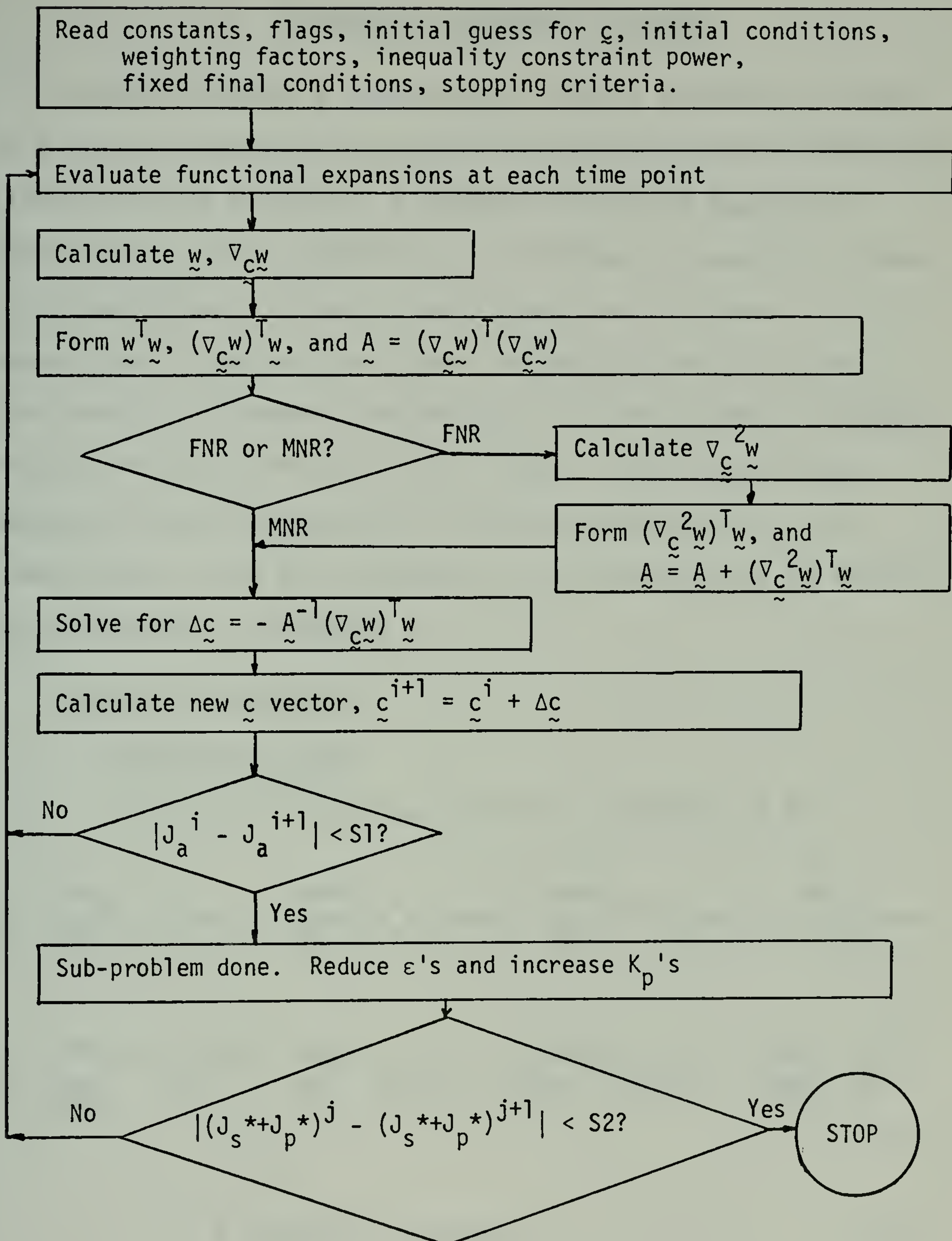

Figure 5
Algorithm Flow Chart

V. A MISSILE INTERCEPT PROBLEM

In this section a short-range missile intercept problem is solved. An air-to-air missile launched from an attacking airplane is to intercept a constant-velocity target in minimum time. The missile is restricted to move in a plane. The orientation of this plane is defined in three-dimensional space as the plane containing the position of the missile at launch, the position of the target at launch, and the velocity vector of the target. The assumptions applied to the problem, the coorinate systems used, the nomenclature, and the derivation of the equations of motion are presented in Appendix A.

A. PROBLEM FORMULATION

1. State Equations

The state equations derived in Appendix A are

$$\dot{M} = \frac{gTh_M}{aW_e} Th \cos\alpha - \frac{g\rho Sa}{2W_e} M^2 C_A \cos\alpha - \frac{g\rho Sa}{2W_e} M^2 C_N \sin\alpha - \frac{gW_c}{aW_e} \sin\theta \tag{5.1}$$

$$\dot{\theta} = \frac{gTh_M}{aW_e} \frac{Th \sin\alpha}{M} - \frac{g\rho Sa}{2W_e} MC_A \sin\alpha + \frac{g\rho Sa}{2W_e} MC_N \cos\alpha - \frac{gW_c}{aW_e} \frac{\cos\theta}{M} \tag{5.2}$$

$$\dot{X} = aM\cos\theta - aM_T\cos\gamma \tag{5.3}$$

$$\dot{Y} = aM\sin\theta - aM_T\sin\gamma \quad . \tag{5.4}$$

[illegible]

[illegible]

[illegible]

$$[illegible]$$

$$[illegible]$$

[illegible]

[illegible]

The states are Mach number M, flight path angle θ, relative range X, and relative cross-range Y as defined in Figure 40. The control is angle of attack α.

The normalized missile thrust Th is considered constant until missile engine burnout t_B and zero thereafter. That is,

$$Th = 1 \qquad , \ t \in [0, t_B] \tag{5.5}$$

$$Th = 0 \qquad , \ t \in (t_B, T] \ . \tag{5.6}$$

Other parameters considered constant are

$$\begin{aligned}
g &= 32.1725 && \text{ft./sec.}^2 \\
Th_M &= 3500 && \text{lbs.} \\
W_e &= 200 && \text{lbs.} \\
S &= 0.35 && \text{ft.}^2 \\
t_B &= 7 && \text{sec.} \\
a &= 1077.8 && \text{ft./sec.} \\
\rho &= 0.001756 && \text{slugs/ft.}^3
\end{aligned} \tag{5.7}$$

The values of the constants in equations (5.7) are based on an engagement at 10,000 feet altitude. It is convenient to group these constants as

$$C_1 = \frac{gTh_M}{aW_e} \tag{5.8}$$

[illegible]

$$C_2 = \frac{g\rho Sa}{2W_e} \tag{5.9}$$

$$C_3 = \frac{g}{aW_e} \quad . \tag{5.10}$$

In addition, the computer solution is aided by normalizing the states X and Y by defining

$$x \triangleq \frac{X}{\mathcal{X}} \tag{5.11}$$

$$y \triangleq \frac{Y}{\mathcal{Y}} \tag{5.12}$$

where $\mathcal{X}$ and $\mathcal{Y}$ are assigned nominal values of 10,000 feet.

With these adjustments the state equations are

$$\dot{M} = C_1 Th\cos\alpha - C_2 M^2 C_A \cos\alpha - C_2 M^2 C_N \sin\alpha - C_3 W_c \sin\theta \tag{5.13}$$

$$\dot{\theta} = C_1 \frac{Th\ \sin\alpha}{M} - C_2 M C_A \sin\alpha + C_2 M C_N \cos\alpha - C_3 \frac{W_c \cos\theta}{M} \tag{5.14}$$

$$\dot{x} = \frac{a}{\mathcal{X}} M \cos\theta - \frac{a}{\mathcal{X}} M_T \cos\gamma \tag{5.15}$$

$$\dot{y} = \frac{a}{\mathcal{Y}} M \sin\theta - \frac{a}{\mathcal{Y}} M_T \sin\gamma \quad . \tag{5.16}$$

2. <u>Tabular Functions</u>

The axial and normal force coefficients C_A and C_N are given in Appendix B as tabular functions of Mach number and angle of attack. This data is based on a typical air-to-air missile.

3. Performance Measure

The performance measure for this problem is

$$J = \int_0^T dt \quad . \tag{5.17}$$

4. Inequality Constraints

Four inequality constraints are required. The angle of attack must satisfy

$$-\frac{\pi}{2} \leq \alpha \leq \frac{\pi}{2} \quad . \tag{5.18}$$

From structural considerations the load factor must satisfy

$$-50 \leq \frac{a}{g}\,(\dot{\theta}M) \leq 50 \quad . \tag{5.19}$$

5. End Conditions

In order to describe the initial conditions for the problem it is necessary first to pose the problem in the ($\underline{X}$,$\underline{Y}$,$\underline{Z}$) coordinate system shown in Figures 41 and 42 of Appendix A. The problem chosen for presentation in this section involves a target in a shallow climb at short range with a slight altitude disadvantage crossing the attacker's flight path extension at 90°; i.e.

$$R_T = 15000 \text{ ft.} \tag{5.20}$$
$$h_T = -3000 \text{ ft.} \tag{5.21}$$
$$\beta_T = 90° \tag{5.22}$$
$$\delta_T = 10° \tag{5.23}$$

Following the procedure outlined in Appendix A, the remaining unknown parameters are

$$M_T = 0.8 \tag{5.24}$$

$$\gamma = 42.35° \tag{5.25}$$

$$W_c = 51.526 \text{ lbs.} \tag{5.26}$$

The initial conditions as computed by this procedure are

$$M(0) = 0.8 \tag{5.27}$$

$$\theta(0) = -49.573° \tag{5.28}$$

$$x(0) = 0 \tag{5.29}$$

$$y(0) = 0 \quad . \tag{5.30}$$

The final conditions as computed by this procedure are

$$x(T) = 0.9920 \tag{5.31}$$

$$y(T) = -1.1645 \quad . \tag{5.32}$$

Note that x and y are the normalized relative range and relative cross-range, respectively, as defined by equations (5.11) and (5.12). The states X and Y in equations (5.11) and (5.12) are defined as the position of the missile in the (X,Y) coordinate system shown in Figure 40. At t = 0 the missile is at the origin of the (X,Y) system, hence equations (5.29) and (5.30) apply. At t = T the missile must intercept the target. Since the (X,Y) system becomes fixed with respect to the target at launch, x(T) and y(T)

[illegible]

are equal to the normalized coordinates of the target in the (X,Y) system at launch and are given by equations (A.93) and (A.95).

B. THE EPSILON METHOD FORMULATION

1. The Augmented Performance Measure

Using the penalty functionals described in Section III for inequality constraints, the augmented performance measure is

$$
\begin{aligned}
J_a = & \int_0^T dt \\
& + \frac{1}{\varepsilon}\int_0^T \left[\dot{M} - C_1 Th\cos\alpha + C_2 M^2 C_A \cos\alpha + C_2 M^2 C_N \sin\alpha + C_3 W_c \sin\theta\right]^2 dt \\
& + \frac{1}{\varepsilon}\int_0^T \left[\dot{\theta} - C_1 \frac{Th\sin\alpha}{M} + C_2 M C_A \sin\alpha - C_2 M C_N \cos\alpha + C_3 \frac{W_c \cos\theta}{M}\right]^2 dt \\
& + \frac{1}{\varepsilon}\int_0^T \left[\dot{x} - \frac{a}{X} M\cos\theta + \frac{a}{X} M_T \cos\gamma\right]^2 dt \\
& + \frac{1}{\varepsilon}\int_0^T \left[\dot{y} - \frac{a}{y} M\sin\theta + \frac{a}{y} M_T \sin\gamma\right]^2 dt \\
& + r\int_0^T \left[\frac{2\alpha}{\pi\delta}\right]^{2K_p} dt + r\int_0^T \left[\frac{a\dot{\theta}M}{50g\delta}\right]^{2K_p} dt \; .
\end{aligned}
\tag{5.33}
$$

where ε and r are weighting factors and δ is a constant used to make minor adjustments in the admissible regions. In all problems δ is given a value of 1.03. This adjustment is applied to all admissible regions of constrained states and

controls. The power K_p is limited in computation to approximately 30 before computer exponent overflow problems develop. With this value of K_p it is desirable to adjust all admissible regions slightly as can be seen from Figure 6.

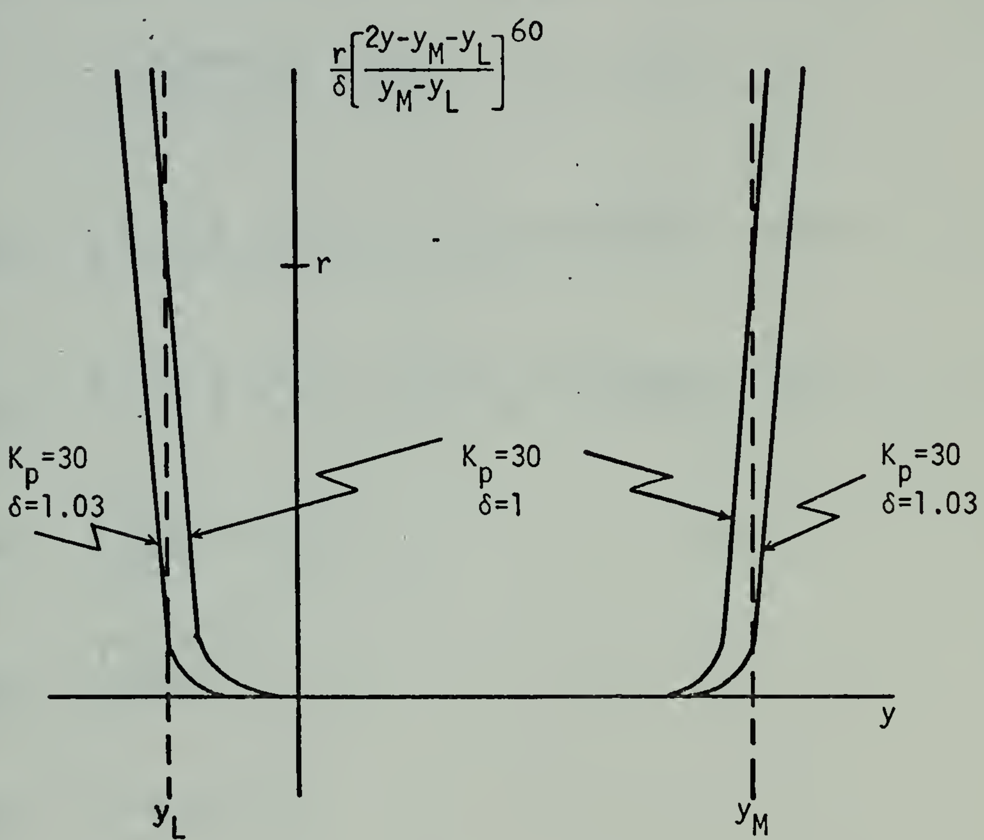

Figure 6

Adjusted admissible regions

The required elements of $\underset{\sim}{w}$ are

$$w_k = \left[\dot{M}_k - C_1 Th\cos\alpha_k + C_2 M_k^{\,2} C_{A_k} \cos\alpha_k + C_2 M_k^{\,2} C_{N_k} \sin\alpha_k + C_3 W_c \sin\theta_k\right] \left[\frac{\Delta t}{\varepsilon}\right]^{1/2} , \quad k = 1,2,\ldots,K \tag{5.34}$$

$$w_{K+k} = \left[\dot{\theta}_k - C_1 \frac{Th\sin\alpha_k}{M_k} + C_2 M_k C_{A_k} \sin\alpha_k - C_2 M_k C_{N_k} \cos\alpha_k + C_3 \frac{W_c \cos\theta_k}{M_k}\right] \left[\frac{\Delta t}{\varepsilon}\right]^{1/2} , \quad k = 1,2,\ldots,K \tag{5.35}$$

$$w_{2K+k} = \left[\dot{x}_k - \frac{a}{X} M_k \cos\theta_k + \frac{a}{X} M_T \cos\gamma\right] \left[\frac{\Delta t}{\varepsilon}\right]^{1/2} , \quad k=1,2,\ldots,K \tag{5.36}$$

$$w_{3K+k} = \left[\dot{y}_k - \frac{a}{y} M_k \sin\theta_k + \frac{a}{y} M_T \sin\gamma\right] \left[\frac{\Delta t}{\varepsilon}\right]^{1/2} , \quad k=1,2,\ldots,K \tag{5.37}$$

$$w_{4K+k} = \left[\frac{2\alpha_k}{\pi\delta}\right]^{K_p} (r\Delta t)^{1/2} , \quad k = 1,2,\ldots,K \tag{5.38}$$

$$w_{5K+k} = \left[\frac{a\dot{\theta}_k M_k}{50g\delta}\right]^{K_p} (r\Delta t)^{1/2} , \quad k = 1,2,\ldots,K \tag{5.39}$$

$$w_{6K+1} = [(K-1)\Delta t]^{1/2} \tag{5.40}$$

where

$$M_k \triangleq M(t)\Big|_{t=(k-1)\Delta t} \quad \text{etc.}$$

2. Functional Expansions

The state and control expansions written in discrete form are

$$M_k = M_1 + \frac{M_K - M_1}{K-1}(k-1) + \sum_{m=1}^{M} a_m \sin\frac{m\pi(k-1)}{K-1}, \quad k=1,2,\ldots,K \tag{5.41}$$

$$\theta_k = \theta_1 + \frac{\theta_K - \theta_1}{K-1}(k-1) + \sum_{m=1}^{M} b_m \sin\frac{m\pi(k-1)}{K-1}, \quad k=1,2,\ldots,K \tag{5.42}$$

$$x_k = x_1 + \frac{x_K - x_1}{K-1}(k-1) + \sum_{m=1}^{M} c_m \sin\frac{m\pi(k-1)}{K-1}, \quad k=1,2,\ldots,K \tag{5.43}$$

$$y_k = y_1 + \frac{y_K - y_1}{K-1}(k-1) + \sum_{m=1}^{M} d_m \sin\frac{m\pi(k-1)}{K-1}, \quad k=1,2,\ldots,K \tag{5.44}$$

$$\alpha_k = \alpha_1 + \frac{\alpha_K - \alpha_1}{K-1}(k-1) + \sum_{m=1}^{M} e_m \sin\frac{m\pi(k-1)}{K-1}, \quad k=1,2,\ldots,K. \tag{5.45}$$

3. Vector of Unknowns

The elements of the vector $\underset{\sim}{c}$ are

$$\begin{aligned}\underset{\sim}{c}^T = (&a_1,a_2,\ldots,a_M,b_1,b_2,\ldots,b_M,c_1,c_2,\ldots,c_M,\\ &d_1,d_2,\ldots,d_M,e_1,e_2,\ldots,e_M,M_K,\theta_K,\alpha_1,\alpha_K,\Delta t)\ .\end{aligned} \tag{5.46}$$

4. Partial Derivatives of the Tabular Function

The values of C_A and C_N are obtained from the tables by parabolic interpolation along with the values of $\frac{\partial C_A}{\partial M}$, $\frac{\partial C_A}{\partial \alpha}$,

$\frac{\partial^2 C_A}{\partial M^2}$, $\frac{\partial^2 C_A}{\partial \alpha^2}$, $\frac{\partial^2 C_A}{\partial M \partial \alpha}$, $\frac{\partial C_N}{\partial M}$, $\frac{\partial C_N}{\partial \alpha}$, $\frac{\partial^2 C_N}{\partial M^2}$, $\frac{\partial^2 C_N}{\partial \alpha^2}$, and $\frac{\partial^2 C_N}{\partial M \partial \alpha}$. The procedure is outlined in Appendix C.

5. First Partial Derivatives

The first partial derivatives indicated in equation (2.34) are required. These partial derivatives are easily obtained from equations (5.34) thru (5.40) by taking the partials of these expressions with respect to the vector $\underset{\sim}{c}$. The expressions are too numerous to include. A typical term is

$$\frac{\partial w_k}{\partial a_m} = \frac{\partial w_k}{\partial \dot{M}_k} \frac{\partial \dot{M}_k}{\partial a_m} + \frac{\partial w_k}{\partial M_k} \frac{\partial M_k}{\partial a_m} \quad . \tag{5.47}$$

For $1 \leq k \leq K$, w_k is given by equation (5.34) and the partial derivatives indicated above are

$$\frac{\partial w_k}{\partial \dot{M}_k} = \left[\frac{\Delta t}{\varepsilon}\right]^{1/2} \tag{5.48}$$

$$\frac{\partial w_k}{\partial M_k} = \left[2C_2 M_k C_{A_k} \cos\alpha_k + C_2 M_k^2 \frac{\partial C_{A_k}}{\partial M_k} \cos\alpha_k + 2C_2 M_k C_{N_k} \sin\alpha_k \right.$$
$$\left. + \; C_2 M_k^2 \frac{\partial C_{N_k}}{\partial M_k} \sin\alpha_k \right] \left[\frac{\Delta t}{\varepsilon}\right]^{1/2} \tag{5.49}$$

$$\frac{\partial \dot{M}_k}{\partial a_m} = \frac{m\pi}{(K-1)\Delta t} \cos \frac{m\pi(k-1)}{K-1} \tag{5.50}$$

$$\frac{\partial M_k}{\partial a_m} = \sin \frac{m\pi(k-1)}{K-1} \quad . \tag{5.51}$$

Notice that C_{A_k} and C_{N_k} are functions of M_k as well as α_k.

6. Second Partial Derivatives

The second partial derivatives indicated in the three-dimensional array (2.35) are also required. Again the expressions are too numerous to list. A typical term for $1 \leq k \leq K$ is

$$\frac{\partial^2 w_k}{\partial a_\ell \partial a_m} = \frac{\partial}{\partial a_\ell}\left[\frac{\partial w_k}{\partial a_m}\right] \quad . \tag{5.52}$$

Letting $\frac{\partial w_k}{\partial a_m} \overset{\Delta}{=} R$, we have

$$\frac{\partial^2 w_k}{\partial a_\ell \partial a_m} = \frac{\partial R}{\partial a_\ell} = \frac{\partial R}{\partial \dot{M}_k}\frac{\partial \dot{M}_k}{\partial a_\ell} + \frac{\partial R}{\partial M_k}\frac{\partial M_k}{\partial a_\ell} \quad . \tag{5.53}$$

The partial derivatives indicated above are

$$\frac{\partial R}{\partial \dot{M}_k} = 0 \tag{5.54}$$

$$\frac{\partial R}{\partial M_k} = \Bigg[2C_2 C_{A_k}\cos\alpha_k + 4C_2 M_k \frac{\partial C_{A_k}}{\partial M_k}\cos\alpha_k + C_2 M_k{}^2 \frac{\partial^2 C_{A_k}}{\partial M_k{}^2}\cos\alpha_k$$

$$+ 2C_2 C_{N_k}\sin\alpha_k + 4C_2 M_k \frac{\partial C_{N_k}}{\partial M_k}\sin\alpha_k + C_2 M_k{}^2 \frac{\partial^2 C_{N_k}}{\partial M_k{}^2}\sin\alpha_k\Bigg]$$

$$\left[\frac{\Delta t}{\varepsilon}\right]^{1/2}\sin\frac{m\pi(k-1)}{K-1} \tag{5.55}$$

$$\frac{\partial \dot{M}_k}{\partial a_\ell} = \frac{\ell\pi}{(K-1)\Delta t} \cos \frac{\ell\pi(k-1)}{K-1} \tag{5.56}$$

$$\frac{\partial M_k}{\partial a_\ell} = \sin \frac{\ell\pi(k-1)}{K-1} \quad . \tag{5.57}$$

C. RESULTS

The problem was solved twice: once using 8 coefficients for each expansion (problem A) and once using 12 coefficients for each expansion (problem B). In both cases K = 21 time points (20 time intervals) were used. The initial guess for the $\underset{\sim}{c}$ vector was:

$$\begin{aligned} &\text{all expansion coefficients} = 0 \\ &M(T) = 1.4 \\ &\theta(T) = 0° \\ &\alpha(0) = 20° \\ &\alpha(T) = 0° \\ &\Delta t = 7/20 \text{ sec. } (T = 7 \text{ sec.}) \end{aligned} \tag{5.58}$$

1. Problem A - 8 Coefficients for each Expansion

Four sub-problems were required to solve the problem. Table 3 gives the weighting factor values, optimization strategy, and computer time for each sub-problem. Table 4 gives the components of the minimum augmented performance measure for each sub-problem where

$$J_a^* = J^* + \frac{1}{\varepsilon} J_s^* + r J_p^* \tag{5.59}$$

sub-problem	ε	R	K_p	I*	optimization strategy**	C.P.U. time
1	1.0×10^{-5}	100	4	8	MMMMMMMM	2'28"
2	0.67×10^{-5}	100	6	6	FFFFFF	3'38"
3	0.5×10^{-5}	100	8	2	FF	1'54"
4	0.5×10^{-5}	100	32	1	F	1'32"

* number of iterations required
** M - MNR method
F - FNR method

Table 3

Weighting factors, optimization strategy, and C.P.U. time for missile intercept problem A.

sub-problem	$J_a{}^*$	J^*	$J_s{}^*$	$J_p{}^*$
1	16.95	7.538	0.6853×10^{-4}	0.2554×10^{-1}
2	14.52	7.585	0.4626×10^{-4}	0.1287×10^{-9}
3	16.83	7.585	0.4624×10^{-4}	0.4619×10^{-13}
4	16.83	7.585	0.4624×10^{-4}	0.3691×10^{-53}

Table 4

Components of the minimum augmented performance measure for missile intercept problem A.

Figure 7 is a plot of the augmented performance measure vs. iteration number.

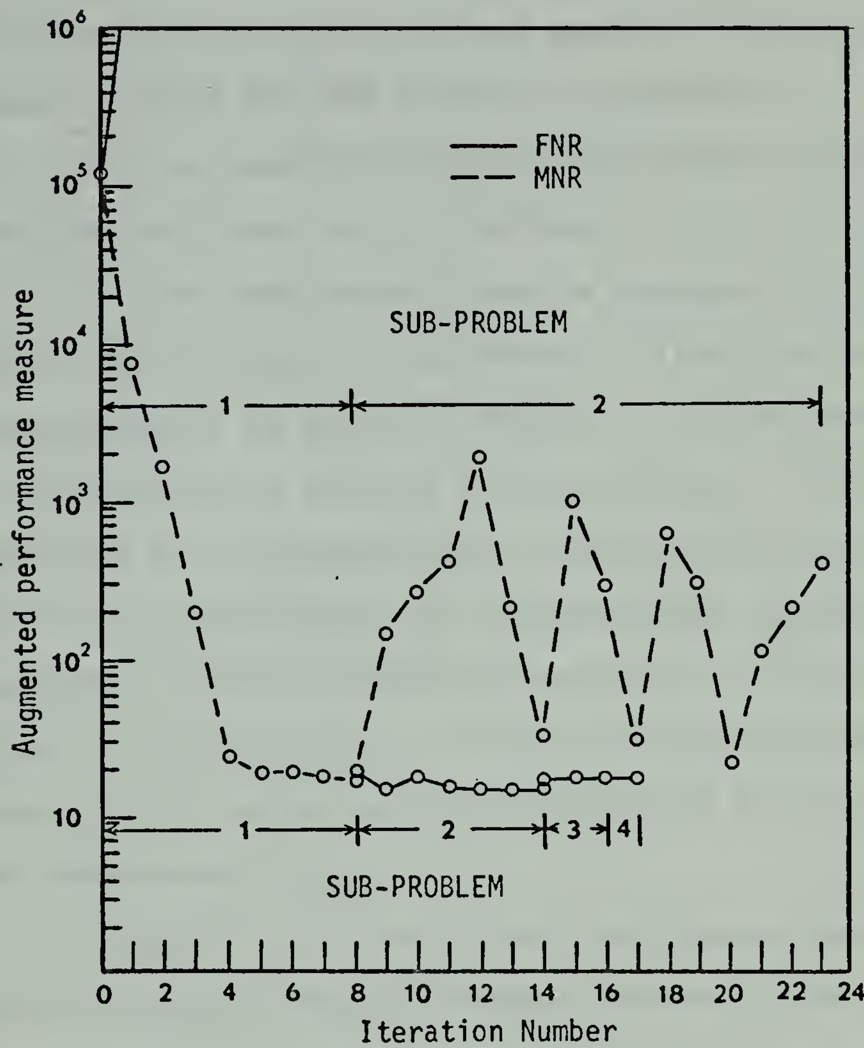

Figure 7

Augmented performance measure vs. iteration number for missile intercept problem A

Iterations performed by the FNR method are indicated by a solid line. Iterations performed by the MNR equations are indicated by a broken line. The figure shows several significant characteristics:

a. the failure of the FNR method on the first iteration of the problem (the initial guess is too far from optimum to allow the FNR method to converge);

b. the superior terminal convergence produced by the FNR method close to the minimum;

c. the oscillatory results produced by the MNR method as the minimum is approached. After the commencement of sub-problem 2 as shown in Figure 7, the FNR method is used exclusively to the end of the problem. For comparison, sub-problem 2 is commenced with the MNR method and allowed to run to 23 iterations. At the beginning of sub-problem 3, J_a increases slightly and never returns to the minimum value obtained in sub-problem 2. This is an indication that ε has reached a point where smaller values have little influence on the reduction of J_s.

Figure 8 is a plot of the performance measure vs. iteration number. The performance measure (final time) increases with iteration number. As the algorithm iterates, Δt is being increased to reduce J_s (the term in the augmented performance measure reflecting the degree of non-satisfaction of the state equations) while insuring that constrained states and controls are kept within admissible bounds by reducing or holding down J_p. With small values of ε and

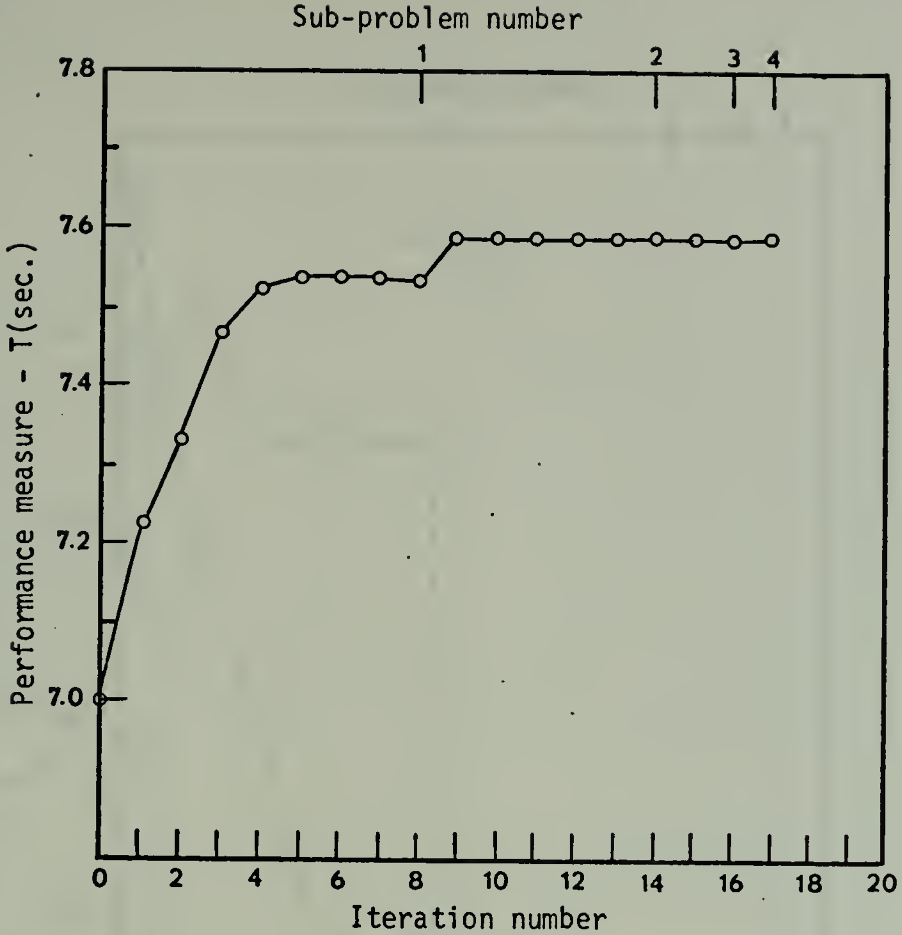

Figure 8

Performance measure vs. iteration number for missile intercept problem A.

large values of K_p the end result of minimizing the augmented performance measure is a control history and state trajectory which minimizes the time to intercept while satisfying the state equations and inequality constraints; all to a reasonable degree of accuracy.

Figure 9 is a plot of J_s and J_p vs. iteration number.

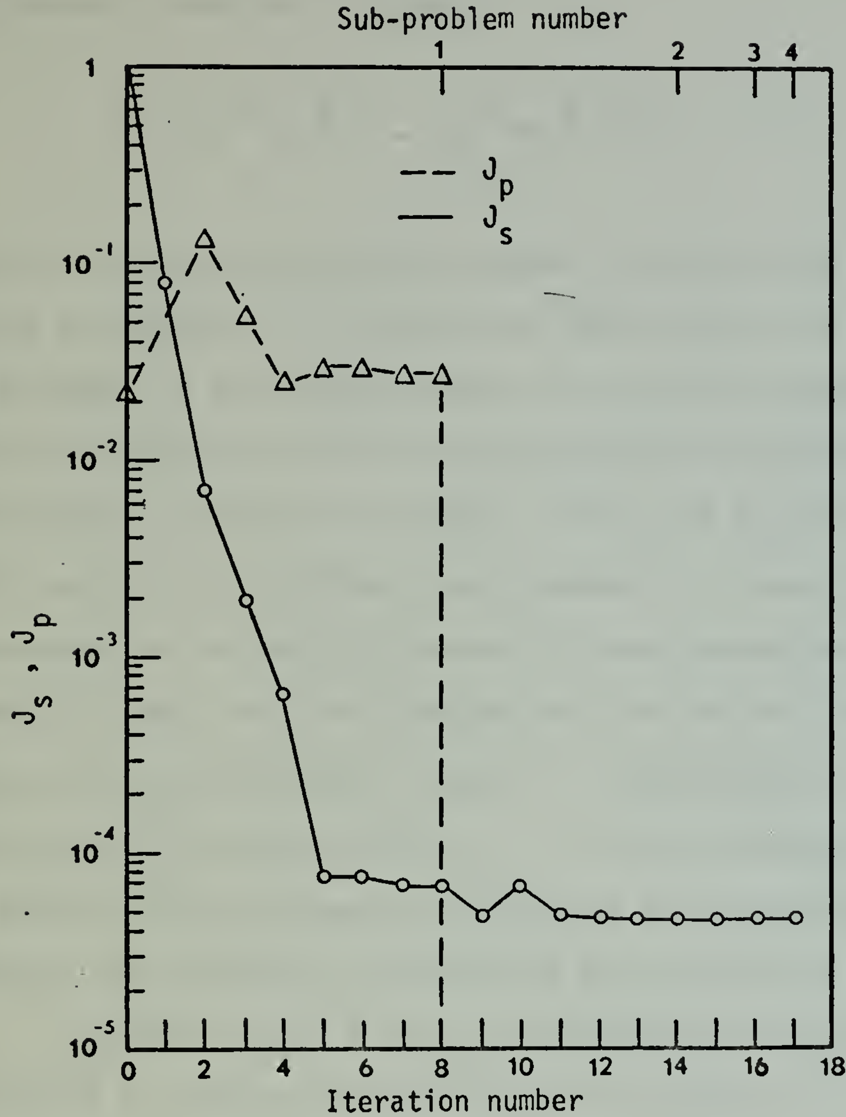

Figure 9

J_s and J_p vs. iteration number for missile intercept problem A.

After K_p is increased at the beginning of sub-problem 2, the inequality constraint penalty terms J_p become very small. This is because the angle of attack is well within its admissible region.

It is evident from Figures 7, 8, and 9 that two sub-problems are sufficient to obtain a reasonable solution. The overal stopping criterion

$$|(J_s^* + J_p^*)^i - (J_s^* + J_p^*)^{i+1}| < 10^{-6} \tag{5.60}$$

where i is the sub-problem number is satisfied after the third sub-problem. However, at this point the value of K_p is 8 which is not large enough to provide desirable penalty functionals for the inequality constraints. It is necessary to provide as large a value of K_p as the computer will allow for the final sub-problem to insure that the minimization is not influenced by the inequality constraint penalty terms when the constrained states and controls are within their admissible regions. Accordingly, a final sub-problem is performed with $K_p = 32$. The algorithm is able to handle the increase in K_p from 8 to 32 in one step only because no constraint boundaries are active in the solution.

Figure 10 is a plot of the angle of attack expansion computed at the end of the last sub-problem. The region of admissible angles of attack is shown.

Figures 11 and 12 are plots of Mach number and flight path angle vs. time. In each plot two curves are shown; one is the expansion for the state as computed at the end of the last sub-problem; the other is the state trajectory obtained by numerically integrating the state equations with the optimal control expansion.

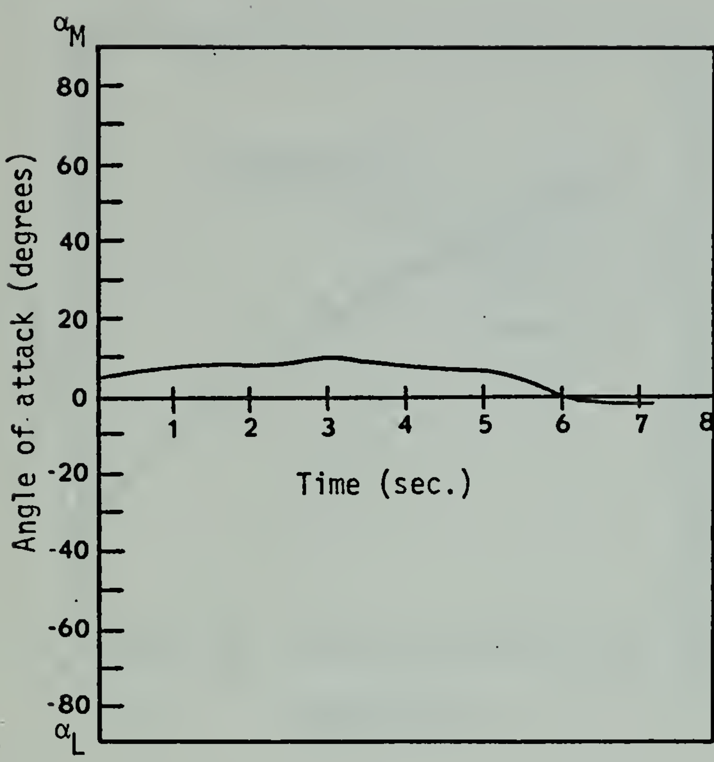

Figure 10

Angle of attack vs. time for missile intercept problem A.

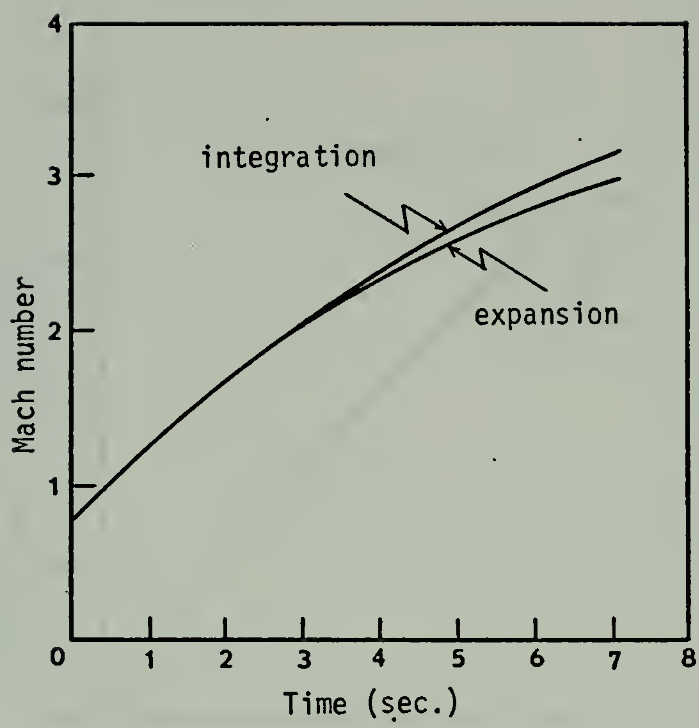

Figure 11

Mach number vs. time for missile intercept problem A.

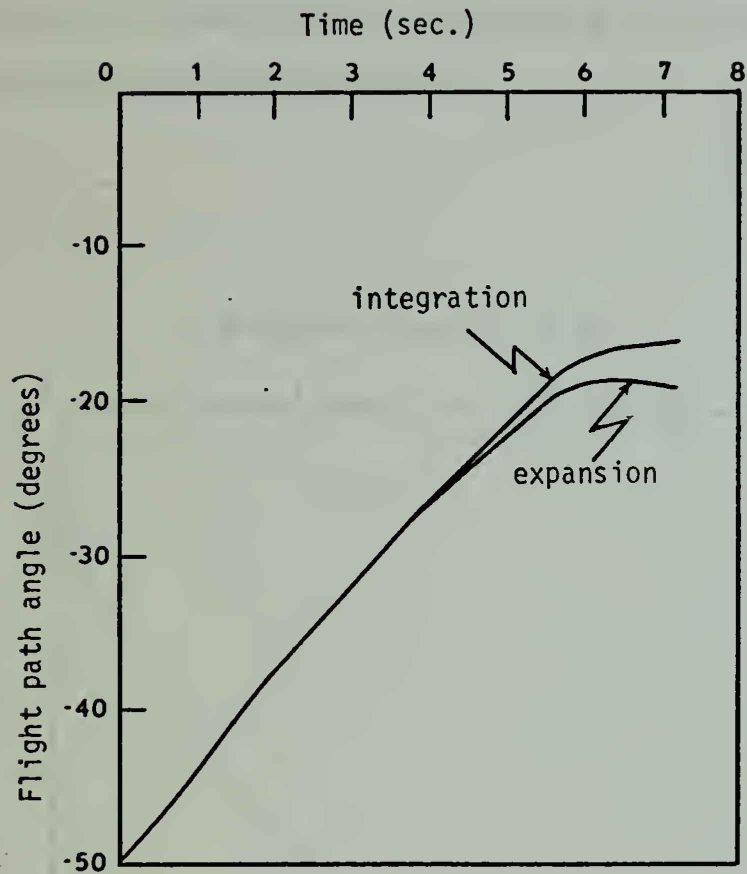

Figure 12

Flight path angle vs. time for missile intercept problem A.

Figure 13 is a plot of relative range X vs. relative cross-range Y. As before two curves are presented: one represents the expansions of the states as computed at the end of the last sub-problem; the other is the state trajectory obtained by numerically integrating the state equations with the optimal control expansion.

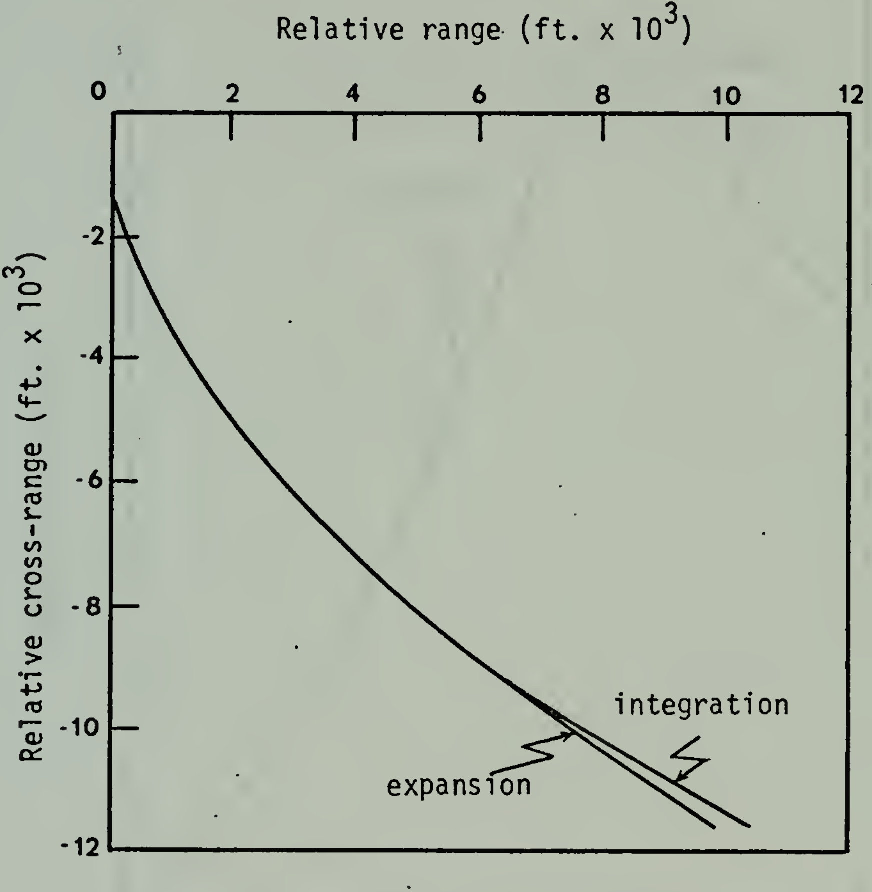

Figure 13

Relative range vs. relative cross-range for missile intercept problem A.

Figure 14 is a plot of range X' vs. cross-range Y' where both quantities are obtained by transforming the expansions of the states X and Y obtained at the end of the last sub-problem from the (X,Y) coordinate system to the inertial coordinate system (X',Y') fixed at the missile launch point (Figure 40).

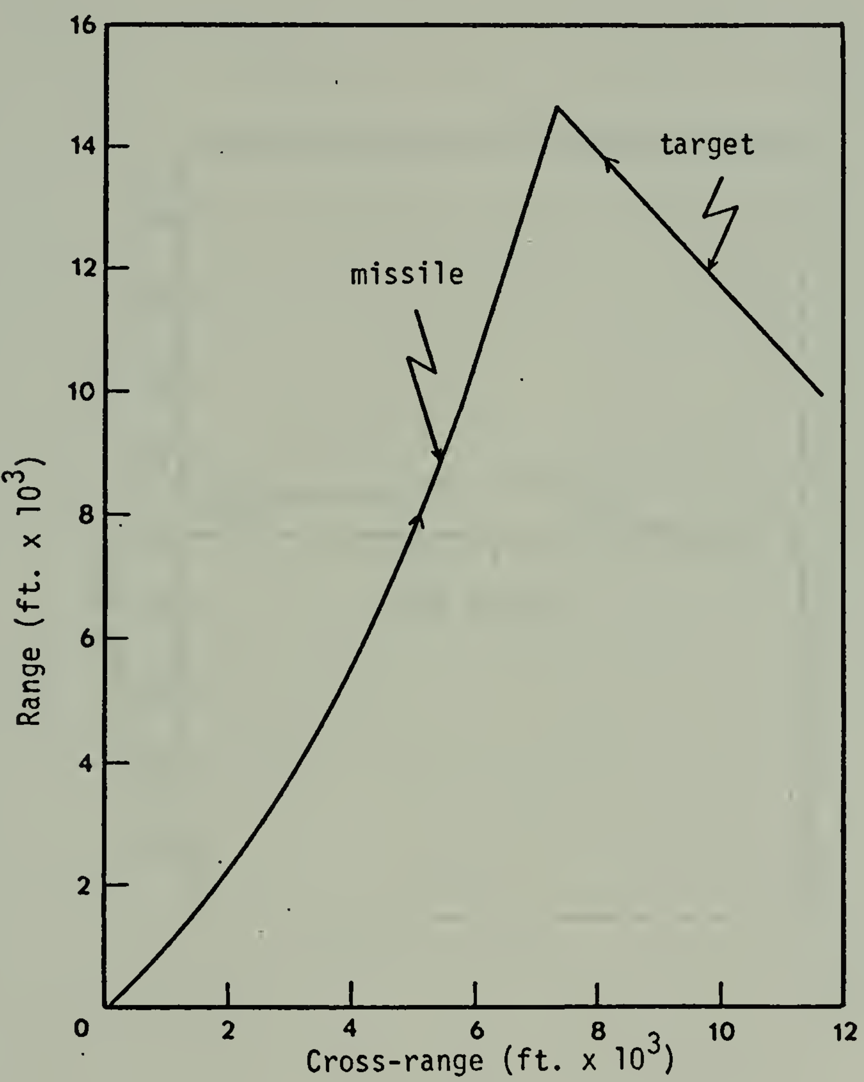

Figure 14

Range vs. cross-range for
missile intercept problem A.

Figure 15 is a plot of load factor vs. time where the load factor is given by

$$n = \frac{a}{g} (\dot{\theta} M) \tag{5.61}$$

and the states used in equation (5.61) are the state expansions obtained at the end of the last sub-problem.

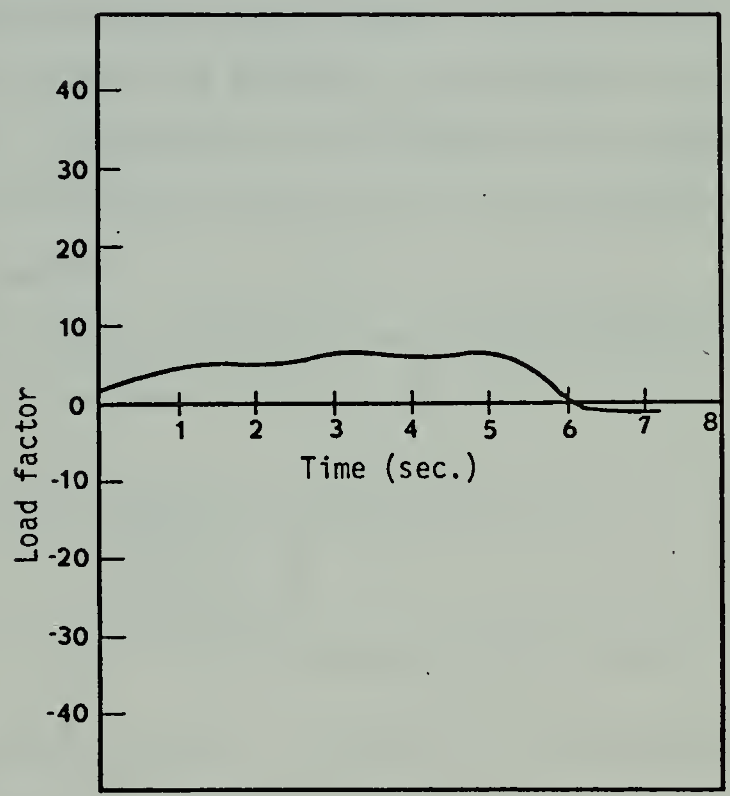

Figure 15

Load factor vs. time for missile intercept problem A.

Although load factor is not a state but a function of states, the plot is important because it shows that the load factor constraints as given by (5.19) are not active.

It might be suspected that the optimal trajectory is a maximum performance turn limited by a constraint boundary (angle of attack or load factor) followed by a straight line path to intercept. This is not the case. The initial turn rate of the missile is small compared to its maximum turn rate capability. This is due to the high induced drag associated with high angle of attack turns which would reduce the missile's longitudinal acceleration capability. Also there is no straight line segment to the trajectory although the turn rate of the missile is very small at intercept.

The first sub-problem was also solved with an initial guess for the $\underset{\sim}{c}$ vector of:

$$\begin{aligned} &\text{all expansion coefficients} = 0 \\ M(T) &= 2.5 \\ \theta(T) &= 0° \\ \alpha(0) &= 10° \\ \alpha(T) &= 0° \\ \Delta t &= 8/20 \text{ sec. } (T = 8 \text{ sec.}) \end{aligned} \tag{5.62}$$

The sub-problem reached a minimum of 7.544 which compared favorably with the minimum reached by the first initial guess given by equations (5.58). This gives an indication that the minimum attained is the global minimum.

2. Problem B - 12 Coefficients for each Expansion

Four sub-problems were required to solve this problem also. Tables 5 and 6 summarize the performance of the algorithm.

sub-problem	ε	r	K_p	I*	optimization strategy**	C.P.U. time
1	1.0×10^{-5}	100	4	8	MMMMMMMM	3'34"
2	0.67×10^{-5}	100	6	2	FF	2'20"
3	0.5×10^{-5}	100	8	2	FF	2'19"
4	0.5×10^{-5}	100	32	2	FF	2'20"

* number of iterations required
** M - MNR method
F - FNR method

Table 5

Weighting factors, optimization strategy, and C.P.U. time for missile intercept problem B.

sub-problem	J_a*	J*	J_s*	J_p*
1	11.51	7.537	0.2125×10^{-4}	0.1849×10^{-1}
2	9.69	7.612	0.1385×10^{-4}	0.3412×10^{-8}
3	10.65	7.628	0.1513×10^{-4}	0.3474×10^{-11}
4	10.31	7.631	0.1339×10^{-4}	0.6139×10^{-43}

Table 6

Components of the minimum augmented measure for missile intercept problem B.

Figure 16 is a plot of the augmented performance measure vs. iteration number and corresponds to Figure 7 for problem A.

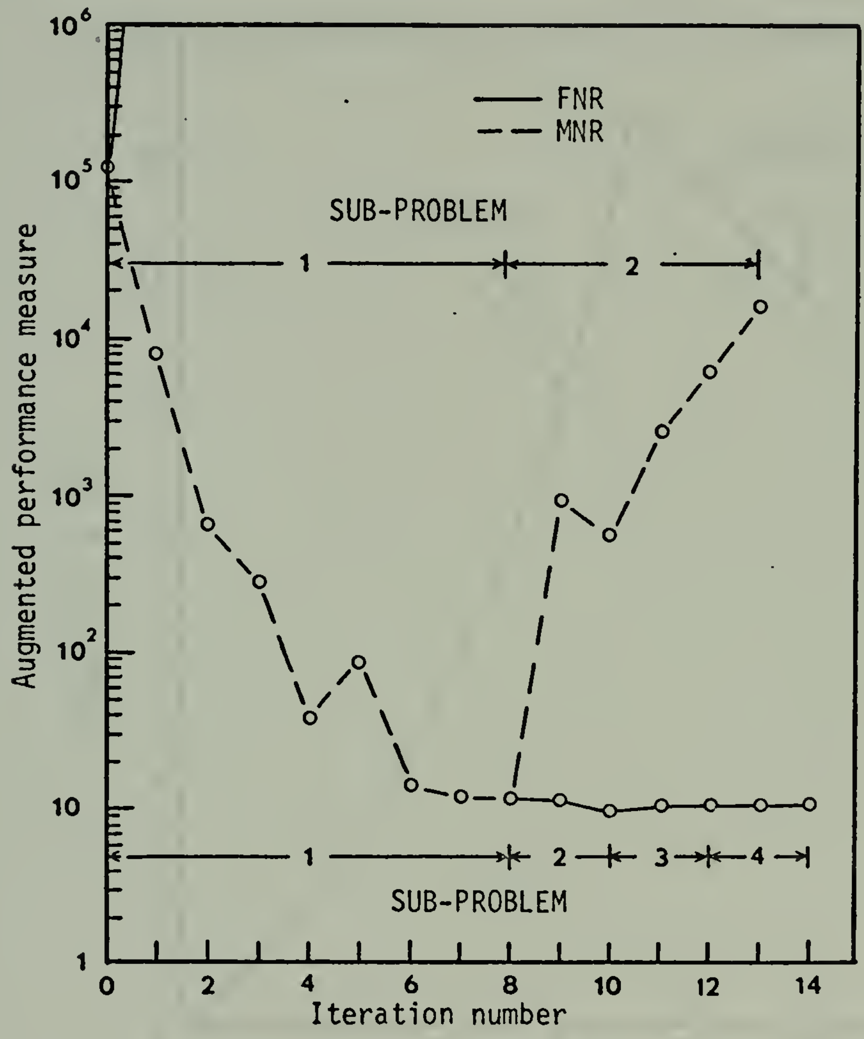

Figure 16

Augmented performance measure vs. iteration number for missile intercept problem B.

A second failure mode of the MNR method close to the minimum is shown. The MNR method produces a divergent J_a in the second sub-problem.

Figure 17 is a plot of range X' vs. cross-range Y' obtained in the same manner as in problem A (Figure 14).

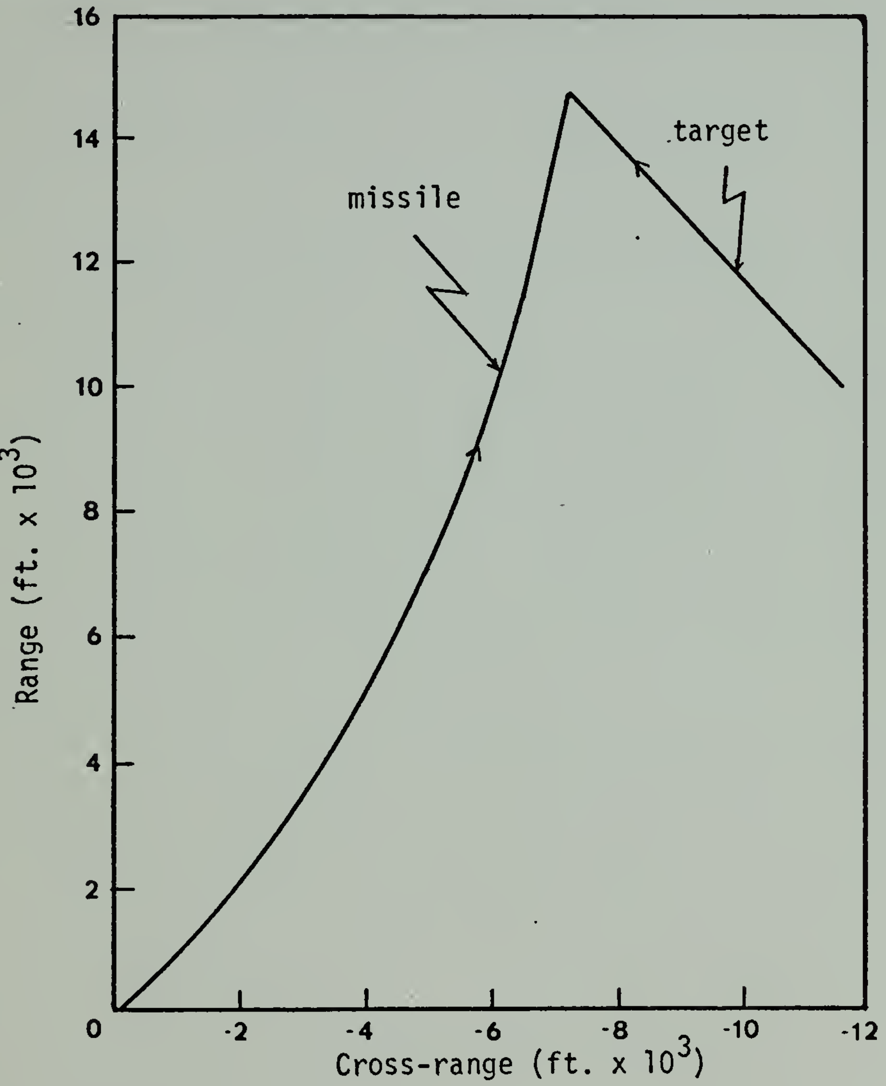

Figure 17

Range vs. cross-range for missile intercept problem B.

A comparison of the tables and figures for problems A and B show that the optimal control and trajectory have not been markedly affected by the increase in the number of coefficients from 8 to 12 for each expansion. It is prohibitive in terms of computation time and storage requirements to increase the number of coefficients further.

VI. A CLIMB PERFORMANCE PROBLEM

In this section a climb performance problem is solved. A supersonic fighter aircraft is to climb from sea level to high altitude in minimum time.

Flight test experience has shown that to climb to altitudes above the tropopause in minimum time a supersonic fighter must execute a maneuver which typically includes:

a. a subsonic climb to an altitude near the tropopause;

b. a level or near level acceleration to some supersonic Mach number;

c. a "zoom" climb to the desired altitude trading kinetic energy for potential energy. This technique has been used extensively in the past decade for establishing climb records and in fighter-interceptor tactics to attain altitudes higher than the aircraft's service ceiling for short periods of time.

Several factors contribute to the optimality of this type of maneuver. They are:

a. a fighter's maximum Mach number or "placard" limit which arises from dynamic pressure and/or thermal limitations and is a function of altitude;

b. a fighter's transonic drag characteristics;

c. air temperature variation with altitude;

d. air density variation with altitude;

e. turbojet engine maximum thrust variation with altitude.

Optimization techniques were first applied successfully to this problem by Bryson [Refs. 1 and 2]. The method of steepest descent was used successfully to predict the type maneuver described above for a typical supersonic aircraft.

The epsilon method is applied to the problem herein to demonstrate the method's power. A direct comparison of methods is not made as the mathematical model used here has been improved considerably over that used in Reference 2.

A. PROBLEM FORMULATION

1. State Equations

The state equations for this problem derived in Appendix A are

$$\dot{M} = \frac{gTh}{a} \cos\alpha - \frac{g}{a} \sin\gamma - \frac{g\rho_o Sa}{2W_e} \sigma M^2 C_D \tag{6.1}$$

$$\dot{\gamma} = \frac{gTh}{a} \frac{\sin\alpha}{M} + \frac{g\rho_o Sa}{2W_e} \sigma M C_L - \frac{g\cos\gamma}{aM} \tag{6.2}$$

$$\dot{h} = \frac{aM}{H_L} \sin \gamma \; . \tag{6.3}$$

The states are Mach number M, vertical flight path angle γ, and normalized altitude h. The control is angle of attack α. Parameters considered constant are the gravitational constant g, sea level standard density ρ_o, aircraft wing area S, aircraft weight W_e, and the altitude of the tropopause under standard atmospheric conditions H_L. These constants are

$$
\begin{aligned}
g &= 32.1725 \quad \text{ft./sec.}^2 \\
\rho_o &= 0.002378 \text{ slugs/ft.}^3 \\
S &= 400 \text{ ft.}^2 \\
W_e &= 39{,}000 \text{ lbs.} \\
H_L &= 36{,}089 \text{ ft.}
\end{aligned}
\tag{6.4}
$$

The remaining parameters in equations (6.1) thru (6.3) vary with flight and atmospheric conditions. These variations are represented in either tabular form or by empirical relations. These tabular and empirical relations are critical to the problem as they represent the mathematical equivalents of the factors a through e listed in the introduction to this section.

It is convenient to define the constant

$$c \overset{\Delta}{=} \frac{g\rho_o S}{2W_e} \quad . \tag{6.5}$$

With the definition (6.5) incorporated the state equations are

$$\dot{M} = \frac{gTh}{a}\cos\alpha - \frac{g}{a}\sin\gamma - ca\sigma M^2 C_D \tag{6.6}$$

$$\dot{\gamma} = \frac{gTh}{a}\frac{\sin\alpha}{M} + ca\sigma MC_L - \frac{g\cos\gamma}{aM} \tag{6.7}$$

$$\dot{h} = \frac{aM}{H_L}\sin\gamma \quad . \tag{6.8}$$

2. <u>Empirical Relations</u>

Empirical relations are used for air density ratio σ, maximum Mach number M_M, and the speed of sound a as functions of normalized altitude h. Air density ratio and normalized altitude are defined by

$$\sigma \stackrel{\Delta}{=} \frac{\rho}{\rho_o} \tag{6.9}$$

and

$$h \stackrel{\Delta}{=} \frac{H}{H_L} \tag{6.10}$$

These empirical relations which are discussed in Appendix D are repeated here for convenience. They are

$$\sigma = e^{-c_1 h} + c_3 h e^{-c_2 h} \tag{6.11}$$

$$M_M = 2.1 - 1.1e^{-2.4h} \tag{6.12}$$

$$a = a_o(1 - c_7 h) \quad , \quad h < 1 \tag{6.13}$$

$$= 971 \text{ ft./sec.} \quad , \quad h \geq 1 \quad . \tag{6.14}$$

where

$$c_1 = 1.54100 \tag{6.15}$$

$$c_2 = 1.80445 \tag{6.16}$$

$$c_3 = 0.4130 \tag{6.17}$$

$$c_4 = 0.1331 \quad . \tag{6.18}$$

3. Tabular Functions

In situations where parameter variations cannot be adequately represented by empirical formulas, a table of values is used. Tables are used for lift and drag coefficients as functions of Mach number and angle of attack for a typical supersonic fighter. Excerpts from these tables are presented in Appendix B.

The thrust Th appearing in equations (6.6) and (6.7) is normalized maximum thrust as it is assumed that since the aircraft must climb to altitude in minimum time, its power plant will always be operated at maximum thrust. Maximum thrust is normalized with respect to sea level static maximum thrust Th_{M_o} and is given by

$$Th = \frac{Th_M}{Th_{M_o}} \qquad (6.19)$$

where

$$Th_{M_o} = 34{,}000 \text{ lbs.} \qquad (6.20)$$

Maximum thrust is given as a tabular function of Mach number and altitude for the fighter under consideration.

4. Performance Measure

The performance measure for this problem is

$$J = \int_0^T dt \quad . \qquad (6.21)$$

5. Inequality Constraints

The following state and control inequality constraints are imposed:

$$0 \leq M \leq M_M \tag{6.22}$$

$$-6° = \alpha_L \leq \alpha \leq \alpha_M = 24° \quad . \tag{6.23}$$

The maximum Mach number M_M constraint represents the "placard" limit. M_M is a function of altitude and is given by an empirical relation as discussed in Section VI.2.

The angle of attack constraint α_M is set at an angle of attack slightly above that for maximum lift coefficient. The minimum angle of attack α_L is set slightly below that for minimum lift coefficient thus simulating aerodynamic stall.

6. End Conditions

The initial conditions are

$$M(0) = M_o = 0.6 \tag{6.24}$$

$$\gamma(0) = 0 \tag{6.25}$$

$$h(0) = h_o = 0 \quad . \tag{6.26}$$

The final condition is

$$h(T) = h_F = \frac{60{,}000 \text{ ft.}}{H_L} \quad . \tag{6.27}$$

B. THE EPSILON METHOD FORMULATION

1. The Augmented Performance Measure

Using the penalty functional described in Section III for inequality constraints, the augmented performance measure is

$$
\begin{aligned}
J_a = & \int_0^T dt \\
& + \frac{1}{\varepsilon}\int_0^T \left[\dot{M} - \frac{gTh}{a}\cos\alpha + \frac{g}{a}\sin\gamma + ca\sigma M^2 C_D\right]^2 dt \\
& + \frac{1}{\varepsilon}\int_0^T \left[\dot{\gamma} - \frac{gTh}{a}\frac{\sin\alpha}{M} - ca\sigma MC_L + \frac{g\cos\gamma}{aM}\right]^2 dt \\
& + \frac{1}{\varepsilon}\int_0^T \left[\dot{h} - \frac{aM}{H_L}\sin\gamma\right]^2 dt \\
& + r\int_0^T \left[\frac{2M}{\delta M_M} - 1\right]^{2K_p} dt \quad + \quad r\int_0^T \left[\frac{\alpha - d}{\alpha_M - d}\right]^{2K_p} dt
\end{aligned}
\qquad (6.28)
$$

where ε and r are weighting factors, δ is a constant used to make minor adjustments to the admissible regions, and d is the midpoint of the admissible angle of attack region; that is

$$
d = \frac{\alpha_M + \alpha_L}{2} \qquad (6.29)
$$

The required elements of $\underset{\sim}{w}$ are

$$w_k = \left[\dot{M}_k - \frac{gTh_k}{a_k} \cos\alpha_k + \frac{g}{a_k} \sin\gamma_k + ca_k\sigma_k M_k^2 C_{D_k} \right] \left[\frac{\Delta t}{\varepsilon}\right]^{1/2} , \quad k=1,2,\ldots,K \tag{6.30}$$

$$w_{K+k} = \left[\dot{\gamma}_k - \frac{gTh_k}{a_k} \frac{\sin\alpha_k}{M_k} - ca_k\sigma_k M_k C_{L_k} + \frac{g\cos\gamma_k}{a_k M_k} \right] \left[\frac{\Delta t}{\varepsilon}\right]^{1/2} , \quad k=1,2,\ldots,K \tag{6.31}$$

$$w_{2K+k} = \left[\dot{h}_k - \frac{a_k M_k}{H_L} \sin\gamma_k \right] \left[\frac{\Delta t}{\varepsilon}\right]^{1/2} , \quad k=1,2,\ldots,K \tag{6.32}$$

$$w_{3K+k} = \left[\frac{2M_k}{\delta M_{M_k}} - 1 \right]^{K_p} (r\Delta t)^{1/2} , \quad k=1,2,\ldots,K \tag{6.33}$$

$$w_{4K+k} = \left[\frac{\alpha_k - d}{\alpha_M - d} \right]^{K_p} (r\Delta t)^{1/2} , \quad k=1,2,\ldots,K \tag{6.34}$$

$$w_{5K+1} = [(K-1)\Delta t]^{1/2} \tag{6.35}$$

2. Functional Expansions, Unknowns, and Partial Derivatives

The state and control expansions are of the same form as the problem in Section V and are not shown. The elements of the $\underset{\sim}{c}$ vector are

$$\underset{\sim}{c}^T = (a_1, a_2, \ldots, a_M, b_1, b_2, \ldots, b_M, c_1, c_2, \ldots, c_M, d_1, d_2, \ldots, d_M, M_K, \gamma_K, \alpha_1, \alpha_K, \Delta t) \tag{6.36}$$

where the a_m's represent the Mach number expansion coefficients, the b_m's represent the vertical flight path angle coefficients, the c_m's represent the altitude coefficients, and the d_m's represent the angle of attack coefficients.

The first and second derivatives of the empirical relations (6.11) thru (6.14) are required. These expressions are

$$\frac{d\sigma}{dh} = -c_1 e^{-c_1 h} + (c_3 - c_2 c_3 h) e^{-c_2 h} \tag{6.37}$$

$$\frac{d^2\sigma}{dh^2} = c_1{}^2 e^{-c_1 h} - [(c_3 - c_2 c_3 h)c_2 + c_2 c_3] e^{-c_2 h} \tag{6.38}$$

$$\frac{dM_M}{dh} = 2.64 e^{-2.4h} \tag{6.39}$$

$$\frac{d^2 M_M}{dh^2} = -6.336 e^{-2.4h} \tag{6.40}$$

$$\frac{da}{dh} = -a_o c_7 \quad , \quad h < 1 \tag{6.41}$$

$$= 0 \quad , \quad h \geq 1 \tag{6.42}$$

$$\frac{d^2 a}{dh^2} = 0 \ . \tag{6.43}$$

The first and second partials of the tabular functions for lift coefficient, drag coefficient, and maximum thrust with respect to their independent variables and the elements

of $\underset{\sim}{w}$ given by equations (6.30) thru (6.35) with respect to $\underset{\sim}{c}$ are obtained in the same manner as in the problem in Section V.

C. RESULTS

Two problems were solved. In problem A the aircraft was to climb from sea level to 60,000 feet in minimum time. Problem B encompassed a series of problems. The results of problem A were used as a first guess for the solution of a minimum-time-to-climb profile from sea level to 61,000 feet, which in turn was used as a first guess for a climb to 62,000 feet, etc. In this manner optimal control and state trajectories were obtained for minimum-time-to-climb profiles from sea level to altitudes from 60,000 to 70,000 feet in thousand-foot increments. In both problems 8 coefficients for each expansion and 41 time points (40 time intervals) were used.

1. Problem A - A Climb from 0 to 60,000 Feet

The initial guess for the $\underset{\sim}{c}$ vector was:

$$\begin{aligned} &\text{all expansion coefficients} = 0 \\ M(T) &= 0.9 \\ \gamma(T) &= 45° \\ \alpha(0) &= 1° \\ \alpha(T) &= 1° \\ \Delta t &= 120/40 \text{ sec. } (T = 2 \text{ min.}) \end{aligned} \tag{6.44}$$

Four sub-problems were required to solve the problem. Tables 7 and 8 summarize the performance of the algorithm.

sub-problem	ε	r	K_p	I*	optimization strategy**	C.P.U.
1	0.2×10^{-4}	100	4	9	FMMMFFFFF	3'33"
2	0.1×10^{-4}	100	6	9	FMMMMMMFF	3'24"
3	0.67×10^{-5}	100	8	8	MFFFFFFF	3'38"
4	0.5×10^{-5}	100	32	3	FFF	2'59"

* number of iterations required
** M - MNR method
F - FNR method

Table 7

Weighting factors, optimization strategy, and C.P.U. time for climb performance problem A.

sub-problem	J_a*	J*	J_s*	J_p*
1	422.5	129.1	0.4496×10^{-2}	0.6855
2	442.2	199.3	0.2154×10^{-2}	0.2742
3	489.3	238.6	0.1544×10^{-2}	0.1904
4	451.5	258.0	0.9677×10^{-3}	0.8838×10^{-12}

Table 8

Components of the minimum augmented performance measure for climb performance problem A.

Neither the angle of attack or maximum Mach number constraints are active in this problem. The largest Mach number attained in the climb is 1.53 at an altitude of 23,000 feet. Consulting Appendix D, the maximum Mach number at this altitude is 1.88. However, since both constrained parameters approach their boundaries, a large value of K_p is required to obtain small J_p contributions to the augmented performance measure.

Figure 18 is a plot of the augmented performance measure vs. iteration number.

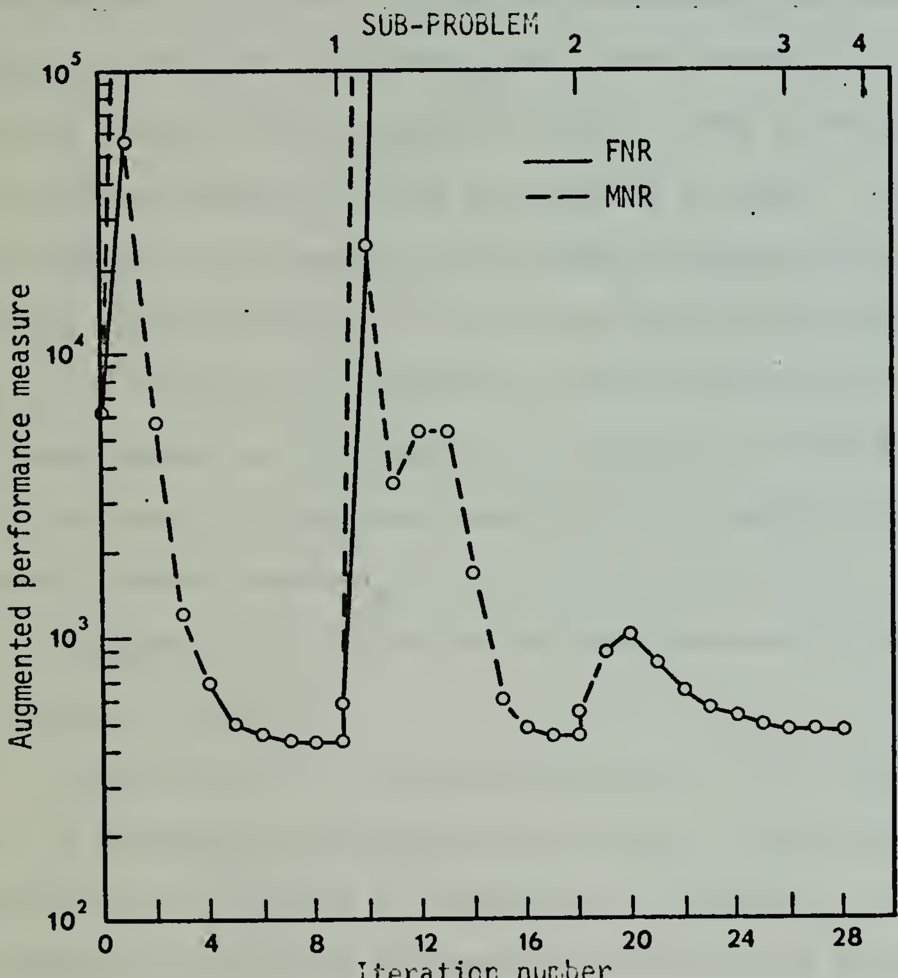

Figure 18

Augmented performance measure vs. iteration number for climb performance problem A.

[illegible]

[illegible]

Iterations performed by the FNR method are indicated by a solid line. Iterations performed by the MNR method are indicated by a broken line. As observed in the previous problem, the FNR method results in excellent terminal convergence. The MNR method performs well when the $\underset{\sim}{c}$ vector is far from optimum as indicated by relatively large augmented performance measures. At the commencement of sub-problem 1 the MNR method fails presumably because the initial guess for the $\underset{\sim}{c}$ vector is too close to optimum. The FNR method does not reduce the augmented performance measure but manages to salvage the first iteration. On iteration number 2 the opposite occurs. The $\underset{\sim}{c}$ vector is too far from optimum for the FNR method to work. The MNR method comes to the rescue. The same thing occurs at the beginning of sub-problem 2. In these two sub-problems the use of both methods in combination has allowed the algorithm to proceed where the exclusive use of either method by itself produces a divergent condition from which the algorithm cannot recover.

Figure 19 is a plot of the performance (final time) vs. iteration number.

Figures 20, 21, and 22 are plots of the states vs. time. In each plot two curves are shown: one is the expansion for the state as computed at the end of the last sub-problem; the second is the state trajectory obtained by integrating the state equations with the optimal control expansion.

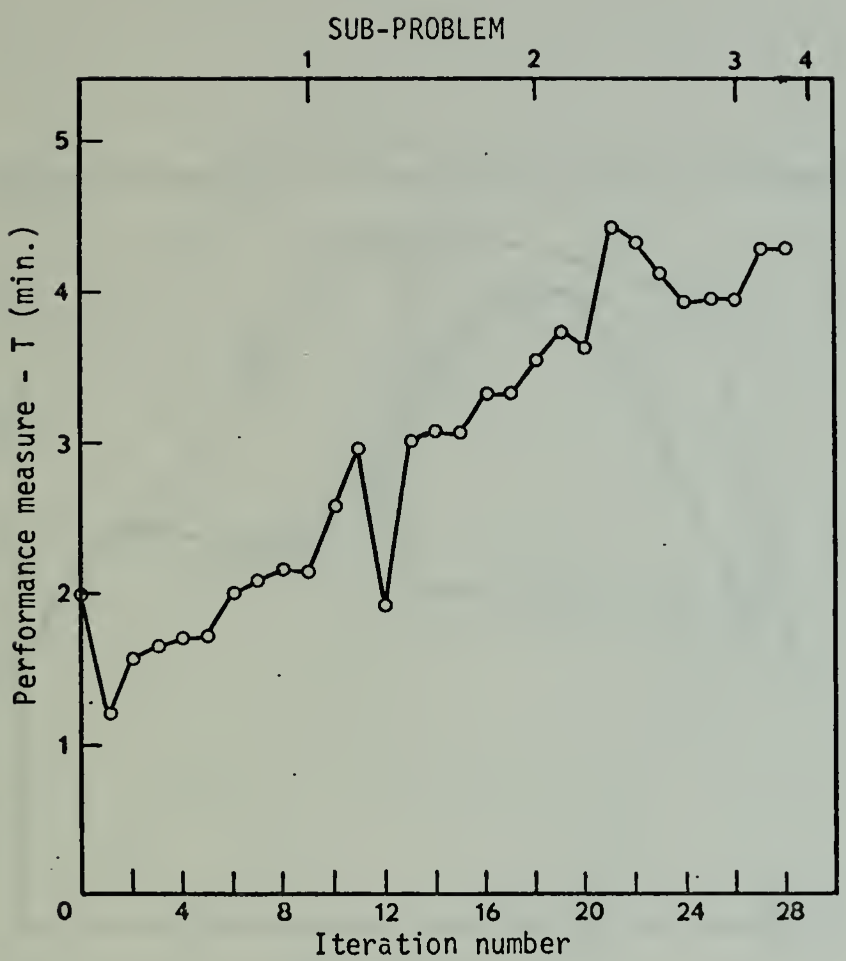

Figure 19

Performance measure vs. iteration number
for climb performance problem A.

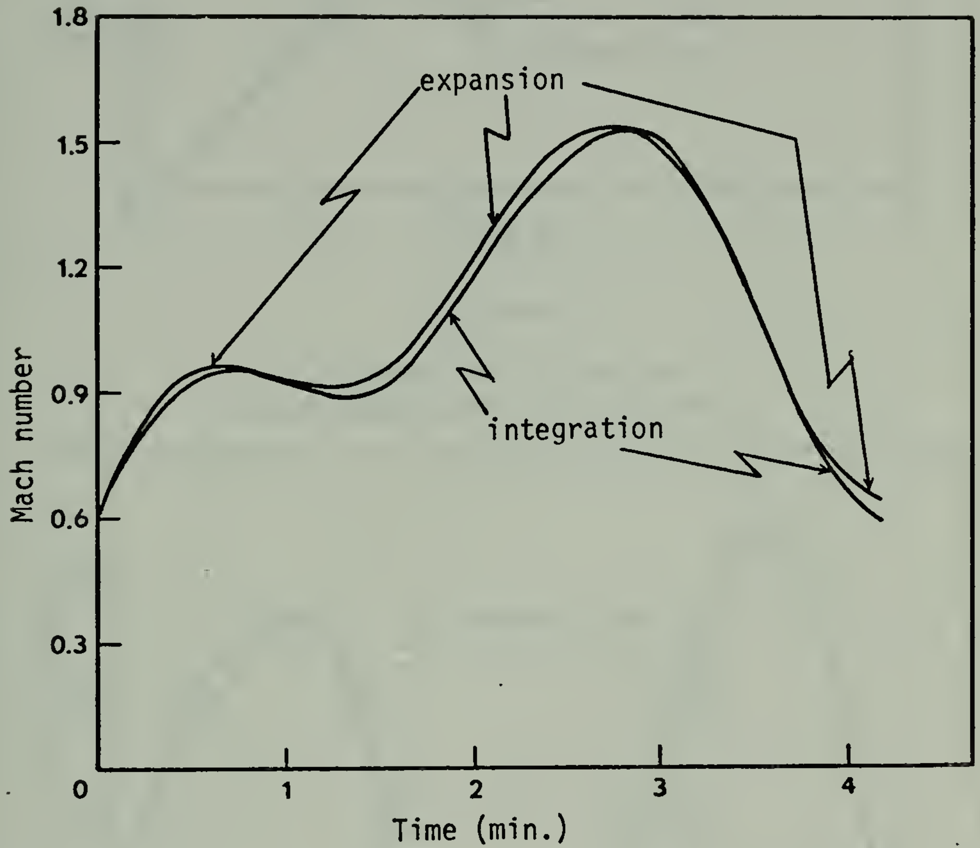

Figure 20

Mach number vs. time for
climb performance problem A.

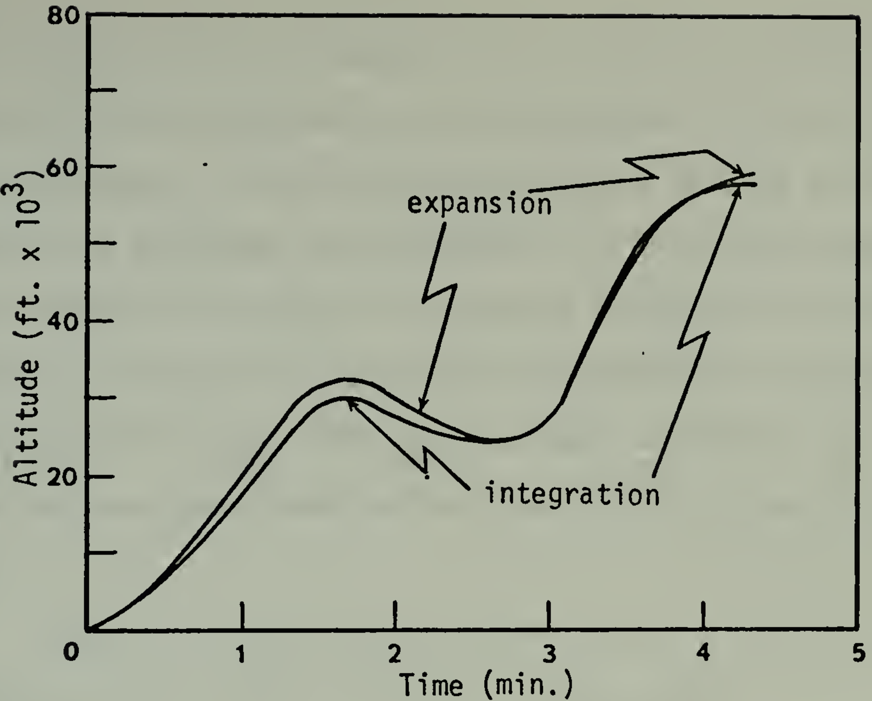

Figure 21

Altitude vs. time for
climb performance problem A.

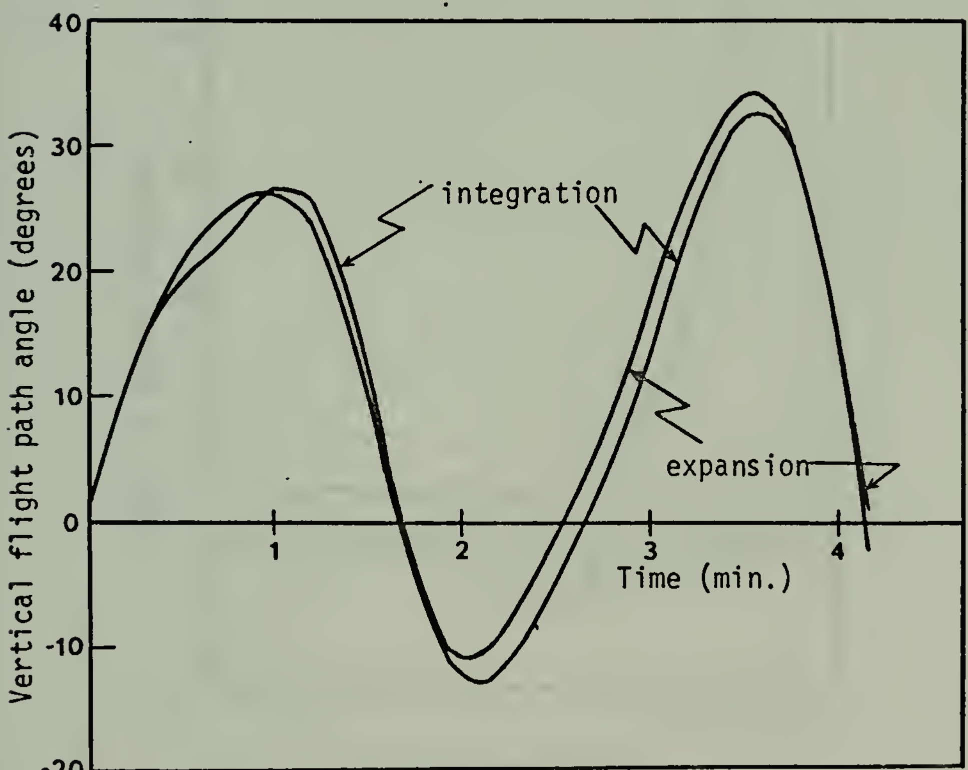

Figure 22

Vertical flight path angle vs.
time for climb performance problem A.

Close observation of Figures 20, 21, and 22 reveals a trajectory very similar to that described in the introduction to this problem. The trajectory begins with a sub-sonic climb to an altitude of 33,000 feet. The climb angle during this portion of the climb reaches a maximum of 27 degrees. At this point an acceleration is performed to a Mach number of 1.53 with the aircraft in a slight descent. A "zoom" climb is then performed to the desired altitude of 60,000 feet.

Figure 23 is a plot of the angle of attack expansion computed at the end of the last sub-problem.

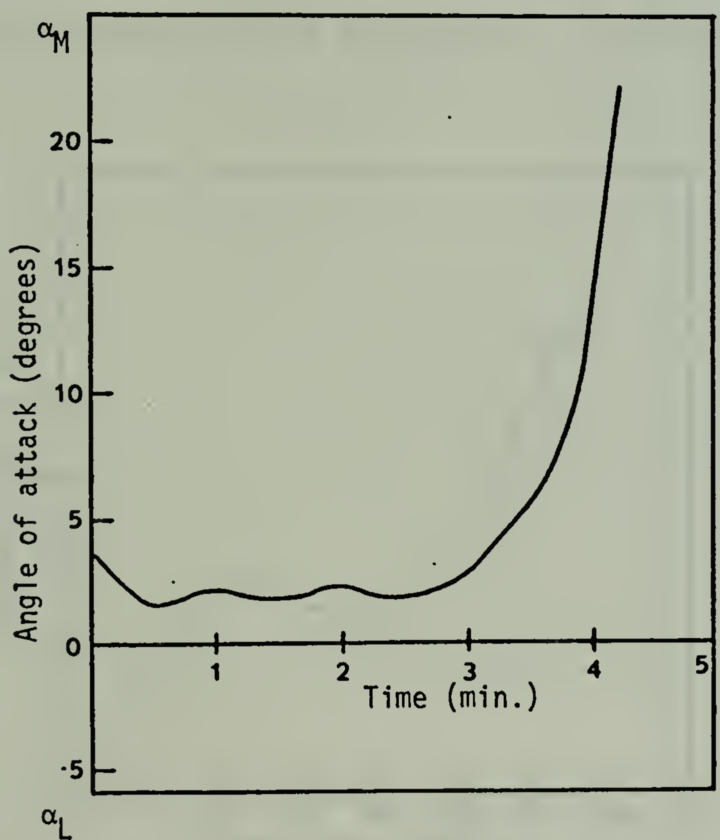

Figure 23

Angle of attack vs. time
for climb performance problem A.

Initially, the angle of attack is decreasing corresponding to the initial acceleration of the aircraft from a starting Mach number of 0.6. As the aircraft rotates to climb attitude, the angle of attack increases. As the aircraft levels off for the supersonic acceleration, the angle of attack decreases correspondingly. The angle of attack begins to increase again as the "zoom" climb attitude is established. A further increase is evident as the aircraft slows down in the climb until as the final altitude is approached, the aircraft is near stall. The climb was completed in 4 minutes and 18 seconds.

Figure 24 is a plot of altitude vs. range where both quantities are obtained by integration. The scales are not the same.

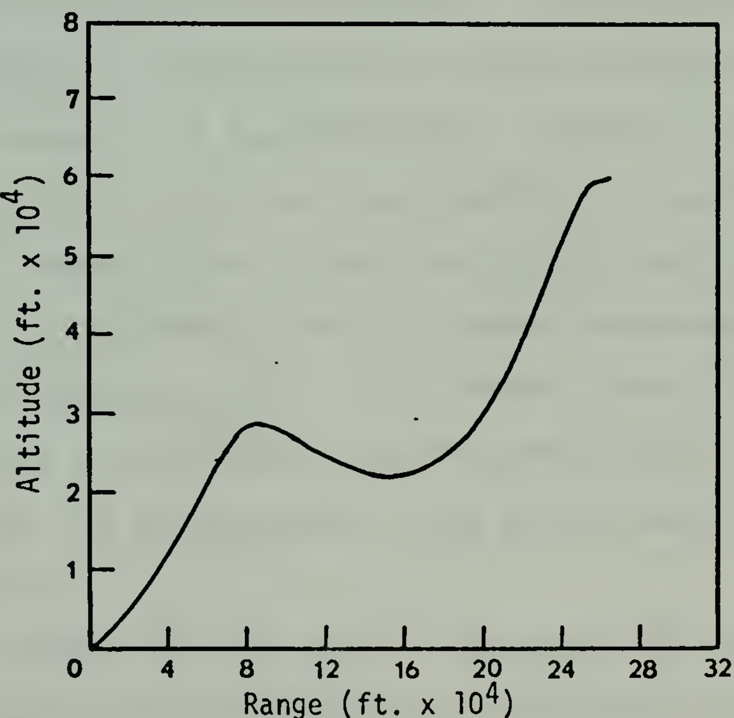

Figure 24

Altitude vs. range for climb performance problem A.

The problem was also solved with the maximum Mach number restricted to 1.0 throughout the flight regime to obtain a comparison of the "zoom" climb technique to a totally subsonic climb to 60,000 feet. The aircraft was not able to complete the climb. The altitude of 60,000 feet is apparently above the service ceiling of the model. After 4 minutes and 18 seconds, which was the time required to complete the climb by the "zoom" technique, the aircraft was passing 43,000 feet and climbing very slowly.

2. Problem B - Optimum Climbs to Altitudes from 60,000 to 70,000 Feet

Table 9 depicts the results for each sub-problem as minimum time-to-climb profiles are generated for final altitudes of 60,000 to 70,000 feet in thousand-foot increments. For each sub-problem the results of the previous sub-problem were used as a first guess for the new trajectory. The stable behavior of the FNR method near the minimum is responsible for the ability of the algorithm to generate neighboring optimal trajectories. Thus, in effect, ten problems were solved with minimum effort by taking advantage of the results of each problem in turn. If, however, the change in end conditions is too large, the MNR method may be required to start the new sub-problem. This is the case in sub-problems 11 thru 14.

Figure 25 is a plot of altitude vs. range where both quantities are obtained by numerical integration showing the climb trajectories for several of the final altitudes.

sub-problem	number of iterations required	optimization strategy *	final altitude (feet)	time to climb (J*)	C.P.U. time
4	3	FFF	60,000	4'18"	2'59"
5	4	FFFF	61,000	4'24"	3'11"
6	5	FFFFF	62,000	4'31"	3'16"
7	12	FFFFFFFFFFFF	63,000	4'36"	5'02"
8	4	FFFF	64,000	4'41"	3'05"
9	3	MFF	65,000	4'44"	2'52"
10	5	FFFFF	66,000	4'54"	3'29"
11	4	MFFF	67,000	4'57"	3'04"
12	3	MFF	68,000	5'00"	2'50"
13	4	MFFF	69,000	5'03"	2'55"
14	4	MFFF	70,000	5'09"	2'53"

* F - FNR method
M - MNR method

Table 9

Results of climb performance problem B.

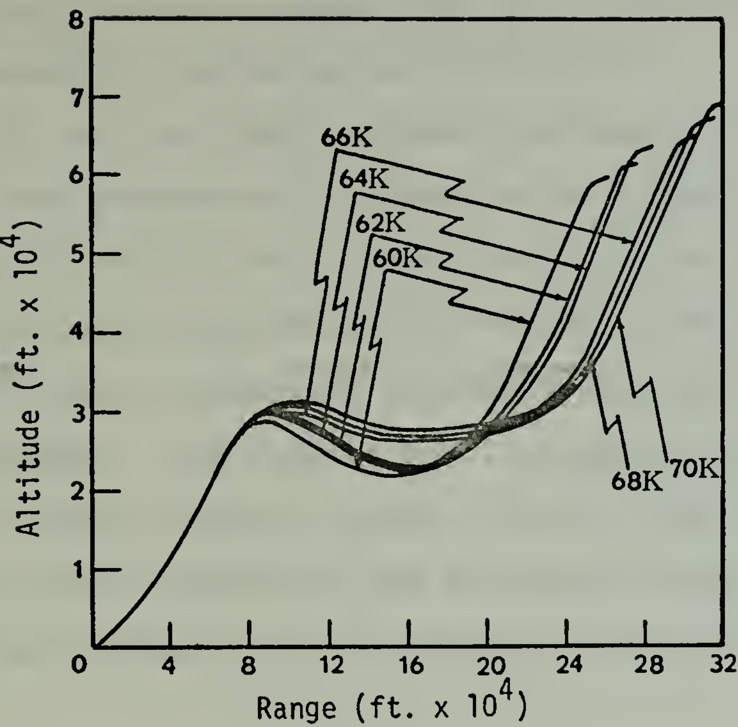

Figure 25

Altitude vs. range for
climb performance problem B.

The climb profiles shown in Figure 25 reveal the following characteristics:

a. The sub-sonic climb profiles are identical for all final altitudes for the initial portion of the climb;

b. as the final altitude increases, the altitude at which the aircraft levels off for the supersonic acceleration increases by approximately 15 to 18 percent of the final altitude;

c. the aircraft performcs a diving maneuver to transit the transonic region with the maximum dive angle (13°) reached in the climb to 60,000 feet;

d. as the final altitude increases, the aircraft performs the supersonic acceleration at higher altitudes with less altitude loss in acceleration. The results are not in agreement with standard practice in which the accelerations are generally performed in level flight at the tropopause. The results are in agreement with the results of Bryson [Ref. 2] which clearly show the dive associated with transiting the transonic region. Bryson's results were obtained by the method of steepest descent.

VII. AN AIR COMBAT MANEUVERING PROBLEM

In this section the turning performance of a supersonic fighter is considered. First, the basic aircraft limitations on maneuvering flight are reviewed. Second, turning performance in the horizontal plane is reviewed from a theoretical point of view. The "corner" velocity concept familiar to fighter pilots is presented. Third, turning performance in three-dimensions is discussed. Finally, a three-dimensional problem is solved in which a supersonic fighter is required to execute a 180° course reversal in minimum time with the initial and final altitudes specified.

A. THEORETICAL TURNING PERFORMANCE

1. Aircraft Performance and Maneuvering Limitations

A tactical fighter must be highly maneuverable. An important consideration in maneuverability is the ability of the fighter to turn. Two basic performance criteria in turning performance are:

a. radius of turn, and

b. rate of turn.

In air combat situations it is often desirable to perform a turn so that the aircraft's radius of turn (curvature) is minimized or the aircraft's rate of turn is maximized. The ability of a fighter to minimize radius of turn or maximize rate of turn is limited by:

a. maximum thrust,

b. aerodynamic stall, or

c. maximum allowable load factor.

2. Turns in the Horizontal Plane

If an aircraft is restricted to move in a horizontal plane only, turning performance is easily analyzed. Using the assumptions given in Appendix A and the added assumption that

$$T \sin \alpha << L, \tag{7.1}$$

equations for lift coefficient, radius of turn, rate of turn, and the thrust required to maintain level flight at constant velocity are easily derived and well known. They are

$$C_L = \frac{2W_e n}{\rho S v^2} , \tag{7.2}$$

$$R = \frac{v^2}{g(n^2-1)^{1/2}} , \tag{7.3}$$

$$\dot{\psi} = \frac{g(n^2-1)^{1/2}}{v} , \tag{7.4}$$

and

$$T = \frac{\rho S}{2 \cos \alpha} v^2 C_D . \tag{7.5}$$

where

T = thrust,
α = angle of attack,
L = lift,
C_L = lift coefficient,
W_e = aircraft weight,
n = load factor
ρ = air density,
S = wing area,
v = aircraft velocity,
g = gravitational constant,
C_D = drag coefficient,
R = radius of turn, and
ψ = horizontal flight path angle (heading angle).

Figure 26 is a plot of lines of constant thrust, constant radius of turn, constant rate of turn, and maximum lift coefficient on velocity-load factor (V-n) diagrams.

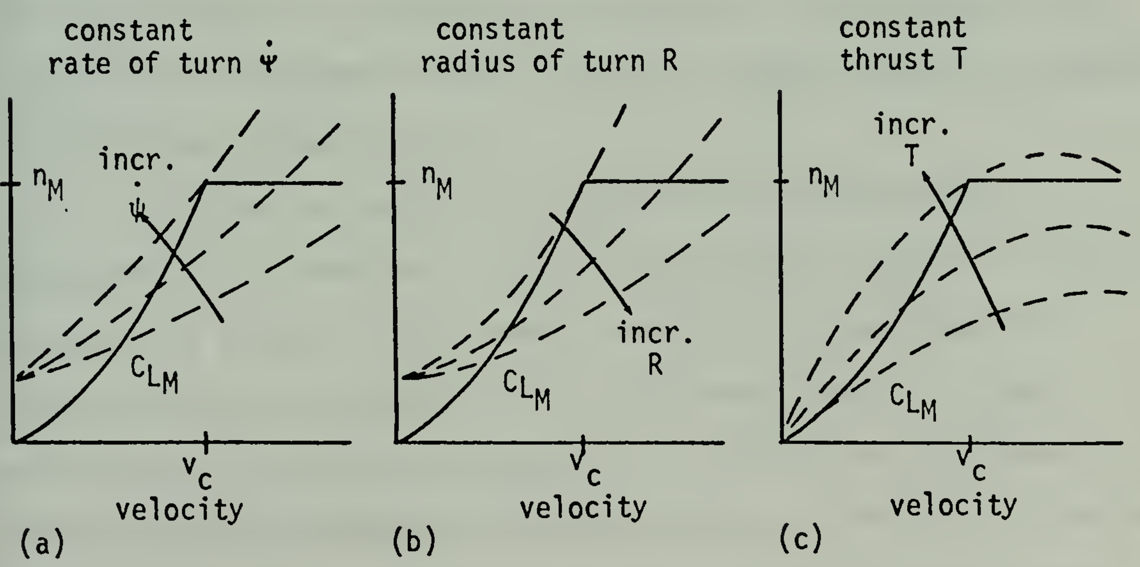

Figure 26

Velocity-Load Factor Diagrams

In Figure 26(c) the constant thrust lines indicate the thrust required to maintain a steady state turn at a specific load factor and velocity. The corner velocity v_c is defined as that velocity at which an aircraft is capable of operating at maximum lift coefficient C_{L_M} and maximum structural load factor n_M at the same time. This is the velocity which produces minimum radius of turn and maximum rate of turn as can be seen from Figures 26(a) and 26(b). The corner velocity can only be maintained in the steady state if the aircraft has enough thrust available to allow the maximum thrust curve to pass above the corner created by the $C_{L_M} - n_M$ boundary intersection. If sufficient thrust is not available to allow the corner velocity to be maintained in the steady state, which is typically the case, the aircraft must either degrade its turning performance by moving off the boundary intersection until the maximum thrust curve is encountered, or sacrifice altitude. In this case the velocity for maximum rate of turn is larger than the velocity for minimum radius of turn.

As can be seen from the previous discussion, optimization techniques are not required to analyze turns in the horizontal plane. This arena, however, is an excellent place to test an optimization technique which is being considered for use in solving more complicated problems involving three-dimensional maneuvering. With this in mind, two problems involving turns in the horizontal plane were solved by the epsilon method and the answers compared to

[illegible]

[illegible]

[illegible]

[illegible]

[illegible]

theoretical results. In one problem an aircraft was required to perform a horizontal turn with minimum radius. In a second problem the aircraft was required to turn through a given heading change in minimum time which is equivalent to maximizing rate of turn. The aircraft was given a large thrust capability so that the turns were not thrust limited. The mathematical model used in the problems is given in Appendix A. The model is an accurate three-degree-of-freedom model of the aircraft's motion with maneuvering limitations included. From the previous discussion the aircraft should have performed the turn in both cases at the corner velocity where

$$v_c = \left[\frac{2n_M W_e}{\rho S(C_{D_M}\tan\alpha_s + C_{L_M})}\right]^{\frac{1}{2}} . \tag{7.6}$$

In this equation α_s is the angle of attack for maximum lift coefficient and C_{D_M} is the drag coefficient for maximum lift coefficient. The epsilon method solved both problems successfully. In each case the optimum trajectory involved a turn at the corner velocity. Thus, the ability of the second-order epsilon method to handle problems of this type was demonstrated.

3. Turns in Three Dimensions

The analysis of turning performance in three dimensions is quite complicated. In this regime modern optimization techniques are the only method of solving

meaningful problems. Even optimization techniques are apt to have a difficult time with three-dimensional maneuvering problems using realistic models of the aircraft's motion because of large computer time and storage requirements. In this section the epsilon method is used to solve an important three-dimensional maneuvering problem often encountered in air combat.

In many air combat situations a fighter pilot is faced with the requirement to reverse his course as rapidly as possible. Generally, the pilot has in mind a specific altitude at which he would like to complete the maneuver which is dictated by his desire to track an enemy aircraft or perform some attacking maneuver. With this in mind, the problem posed for solution by the epsilon method involves a supersonic fighter which is required to execute a 180° reversal in minimum time. The aircraft must begin the maneuver in level flight and recover in level flight at the entry altitude. The accepted maneuvers used to accomplish this task developed over years of combat experience are the high-speed yo-yo and the low-speed yo-yo maneuvers. If the aircraft begins a reversal at a flight speed higher than its corner velocity a high-speed yo-yo is called for and vice-versa. A high speed yo-yo consists of a climbing turn followed by a descending turn. A low speed yo-yo consists of a descending turn followed by a climbing turn. If the aircraft begins a reversal at its corner velocity, a level turn is called for. The purpose of applying the epsilon

method to this problem is to either confirm or challenge the effectiveness of these experimentally developed maneuvers by the use of an optimization technique. The assumptions applied to the problem, the coordinate system and nomenclature used, and the derivation of the equations of motion are presented in Appendix A.

B. PROBLEM FORMULATION

1. State Equations

The state equations derived in Appendix A are

$$\dot{M} = \frac{gTh_M}{W_e a} Th\cos\alpha - \frac{g}{a}\sin\gamma - \frac{g\rho Sa}{2W_e} M^2 C_D \tag{7.7}$$

$$\dot{\psi} = \frac{g}{a}\frac{n\sin\phi}{M\cos\gamma} \tag{7.8}$$

$$\dot{\gamma} = \frac{g}{a}\frac{n\cos\phi}{M} - \frac{g}{a}\frac{\cos\gamma}{M} \tag{7.9}$$

$$\dot{h} = \frac{aM}{H_L}\sin\gamma \quad . \tag{7.10}$$

The states are Mach number M, horizontal flight path angle ψ, vertical flight path angle γ, and normalized altitude h. The controls are bank angle ϕ, normalized thrust Th, angle of attack α, and load factor n.

In addition to the four state equations, an equality constraint which must be satisfied is

$$0 = \frac{Th_M}{W_e} Th\sin\alpha + \frac{\rho Sa^2}{2W_e} M^2 C_L - n \quad . \tag{7.11}$$

This equation is a result of the definition of load factor n and is derived in Appendix A. It is possible to use equation (7.11) to eliminate the load factor control from the state equations, but this is not desirable for two reasons: first, the resulting state equations would be further complicated thus increasing the analytic workload required to compute first and second partial derivatives; second, the incorporation of the important load factor inequality constraint would be unnecessarily complicated.

Parameters considered constant for this problem are the gravitational constant g, aircraft maximum thrust Th_M, aircraft weight W_e, speed of sound a, base altitude H_L, air density ρ, and aircraft wing area S. These constants are

$$\begin{aligned}
g &= 32,1725 \text{ ft./sec.}^2 \\
Th_M &= 21,000 \text{ lbs.} \\
W_e &= 39,000 \text{ lbs.} \\
a &= 1077.8 \text{ ft./sec.} \\
H_L &= 10,000 \text{ ft.} \\
\rho &= 0.001756 \text{ slugs/ft.}^3 \\
S &= 400 \text{ ft.}^2
\end{aligned} \tag{7.12}$$

It is convenient to define the constants

$$c_1 \stackrel{\Delta}{=} \frac{g}{a} \tag{7.13}$$

$$c_2 \stackrel{\Delta}{=} \frac{gTh_M}{W_e a} \tag{7.14}$$

$$c_3 \stackrel{\Delta}{=} \frac{g\rho Sa}{2W_e} \tag{7.15}$$

$$c_4 \triangleq \frac{Th_M}{W_e} \tag{7.16}$$

$$c_5 \triangleq \frac{\rho S a^2}{2W_e} \; . \tag{7.17}$$

With these simplifying definitions incorporated the state equations are

$$\dot{M} = c_2 Th\cos\alpha - c_1\sin\gamma - c_3 M^2 C_D \tag{7.18}$$

$$\dot{\psi} = c_1 \frac{n\sin\phi}{M\cos\gamma} \tag{7.19}$$

$$\dot{\gamma} = c_1 \frac{n\cos\phi}{M} - c_1 \frac{\cos\gamma}{M} \tag{7.20}$$

$$\dot{h} = \frac{aM}{H_L} \sin\gamma \tag{7.21}$$

and the additional equality constraint is

$$0 = c_4 Th\sin\alpha + c_5 M^2 C_L - n \quad . \tag{7.22}$$

2. Tabular Functions

Tables are used for lift and drag coefficient as functions of Mach number and angle of attack for a typical supersonic fighter. Excerpts from these tables are provided in Appendix B.

3. Performance Measure

The performance measure for this problem is

$$J = \int_0^T dt. \tag{7.23}$$

4. Inequality Constraints

The controls must satisfy

$$0 \leq Th \leq 1 \tag{7.24}$$

$$0 \leq \alpha \leq \alpha_M = 24° \tag{7.25}$$

$$0 \leq n \leq n_M = 6.5 \text{ g's} \tag{7.26}$$

$$0 \leq \phi \leq \pi \,. \tag{7.27}$$

The minimum allowable normalized thrust, angle of attack, and load factor are approximated by zero as these constraints are not anticipated to be active. A zero value of the lower bound simplifies the associated penalty term in the augmented performance measure. The maximum angle of attack is fixed at a value slightly higher than the angle of attack for maximum lift coefficient as given in the tabular data thus simulating aerodynamic stall. The structural load factor upper bound is 6.5 g's, a standard value from fighter aircraft operational limitations. The bank angle constraints

were required to keep the algorithm from generating bank angles greater than 180°.

5. End Conditions

The initial conditions are

$$M(0) = 0.9 \tag{7.28}$$

$$\psi(0) = 0 \tag{7.29}$$

$$\gamma(0) = 0 \tag{7.30}$$

$$h(0) = h_o = 15{,}000 \text{ ft.} \tag{7.31}$$

The final conditions are

$$\psi(T) = \pi \tag{7.32}$$

$$\gamma(T) = 0 \tag{7.33}$$

$$h(T) = h_o \quad . \tag{7.34}$$

C. THE EPSILON METHOD FORMULATION

1. The Augmented Performance Measure

Using the penalty functionals described in Section III for the inequality constraints, the augmented performance measure is

$$J_a = \int_0^T dt$$

$$+ \frac{1}{\varepsilon}\int_0^T \left[\dot{M} - c_2 Th\cos\alpha + c_1\sin\gamma + c_3 M^2 C_D\right]^2 dt$$

$$+ \frac{1}{\varepsilon}\int_0^T \left[\dot{\psi} - c_1 \frac{n\sin\phi}{M\cos\gamma}\right]^2 dt$$

$$+ \frac{1}{\varepsilon}\int_0^T \left[\dot{\gamma} - c_1 \frac{n\cos\phi}{M} + c_1 \frac{\cos\gamma}{M}\right]^2 dt$$

$$+ \frac{1}{\varepsilon}\int_0^T \left[\dot{h} - \frac{aM}{H_L}\sin\gamma\right]^2 dt \tag{7.35}$$

$$+ \frac{1}{\varepsilon}\int_0^T \left[c_4 Th\sin\alpha + c_5 M^2 C_L - n\right]^2 dt$$

$$+ r\int_0^T \left[\frac{2Th}{\delta} - 1\right]^{2K_p} dt + r\int_0^T \left[\frac{2\alpha}{\delta\alpha_M} - 1\right]^{2K_p} dt$$

$$+ r\int_0^T \left[\frac{2n}{\delta n_M} - 1\right]^{2K_p} dt + r\int_0^T \left[\frac{2\phi}{\delta\pi} - 1\right]^{2K_p} dt$$

where ε and r are weighting factors, and δ is a constant used to make minor adjustments to the admissible regions. The required elements of $\underset{\sim}{w}$ are

$$w_k = \left[\dot{M}_k - c_2 Th_k\cos\alpha_k + c_1\sin\gamma_k + c_3 M_k^{\,2} C_{D_k}\right]\left[\frac{\Delta t}{\varepsilon}\right]^{1/2}, \; k=1,2,\ldots,K \tag{7.36}$$

$$w_{K+k} = \left[\dot{\psi}_k - c_1 \frac{n_k\sin\phi_k}{M_k\cos\gamma_k}\right]\left[\frac{\Delta t}{\varepsilon}\right]^{1/2}, \; k=1,2,\ldots,K \tag{7.37}$$

$$w_{2K+k} = \left[\dot{\gamma}_k - c_1 \frac{n_k \cos\phi_k}{M_k} + c_1 \frac{\cos\gamma_k}{M_k}\right]\left[\frac{\Delta t}{\varepsilon}\right]^{\frac{1}{2}}, \quad k=1,2,\ldots,K \tag{7.38}$$

$$w_{3K+k} = \left[\dot{h}_k - \frac{aM_k}{H_L}\sin\gamma_k\right]\left[\frac{\Delta t}{\varepsilon}\right]^{\frac{1}{2}}, \quad k=1,2,\ldots,K \tag{7.39}$$

$$w_{4K+k} = \left[c_4 Th_k \sin\alpha_k + c_5 M_k^{\,2} C_{L_k} - n_k\right]\left[\frac{\Delta t}{\varepsilon}\right]^{\frac{1}{2}}, \quad k=1,2,\ldots,K \tag{7.40}$$

$$w_{5K+k} = \left[\frac{2Th_k}{\delta} - 1\right]^{K_p}(r\Delta t)^{\frac{1}{2}}, \quad k=1,2,\ldots,K \tag{7.41}$$

$$w_{6K+k} = \left[\frac{2\alpha_k}{\delta\alpha_M} - 1\right]^{K_p}(r\Delta t)^{\frac{1}{2}}, \quad k=1,2,\ldots,K \tag{7.42}$$

$$w_{7K+k} = \left[\frac{2n_k}{\delta n_M} - 1\right]^{K_p}(r\Delta t)^{\frac{1}{2}}, \quad k=1,2,\ldots,K \tag{7.43}$$

$$w_{8K+k} = \left[\frac{2\phi_k}{\delta\pi} - 1\right]^{K_p}(r\Delta t)^{\frac{1}{2}}, \quad k=1,2,\ldots,K \tag{7.44}$$

$$w_{9K+1} = [(K-1)\Delta t]^{\frac{1}{2}} \tag{7.45}$$

2. Functional Expansions, Unknowns, and Partial Derivatives

The state and control expansions are of the same form as in previous problems and are not shown. The elements of the $\underset{\sim}{c}$ vector are

$$\underset{\sim}{c}^T = (a_1, a_2, \ldots, a_m, b_1, b_2, \ldots, b_m, c_1, c_2, \ldots, c_M, d_1, d_2, \ldots, d_M,$$
$$e_1, e_2, \ldots, e_M, f_1, f_2, \ldots, f_M, g_1, g_2, \ldots, g_M, h_1, h_2, \ldots, h_M,$$
$$M_K, \phi_1, \phi_K, Th_1, Th_K, \alpha_1, \alpha_K, n_1, n_K, \Delta t) \tag{7.46}$$

where the a_m's represent the Mach number expansion coefficients, the b_m's represent the horizontal flight path coefficients, the c_m's represent the vertical flight path angle coefficients, the d_m's represent the altitude coefficients, the e_m's represent the bank angle coefficients, the f_m's represent the thrust coefficients, the g_m's represent the angle of attack coefficients, and the h_m's represent the load factor coefficients.

The first and second partial derivatives of the tabular functions for lift coefficient and drag coefficient with respect to their independent variables and equations (7.36) thru (7.45) with respect to the $\underset{\sim}{c}$ vector are obtained in the same manner as in previous problems.

D. RESULTS

Three problems were solved. In problem A the aircraft must perform the 180° reversal in minimum time starting from an initial Mach number of 0.9. In problem B the aircraft must perform the reversal starting from its corner Mach number which from equation (7.6) is 0.708. In problem C the aircraft must perform the reversal starting from an initial Mach number of 0.5. In all problems 8 coefficients for each expansion and 21 time points (20 time intervals) are used.

1. Problem A

Since the initial Mach number is above the corner Mach number, a high-speed yo-yo maneuver is called for by

accepted tactics. With this in mind an initial guess of the $\underset{\sim}{c}$ vector was made to reflect this type of maneuver. Accordingly, the following coefficients were given non-zero initial values:

$$\begin{aligned} a_1 &= -0.309 \\ c_1 &= 0.524 \\ d_1 &= 0.333 \\ e_1 &= 1.047 \\ g_1 &= 0.262 \\ h_1 &= 3.000 \end{aligned} \tag{7.47}$$

The remaining initial values for the $\underset{\sim}{c}$ vector were:

$$\begin{aligned} &\text{remaining expansion coefficients} = 0 \\ M(T) &= 0.9 \\ \phi(0) &= 0° \\ \phi(T) &= 0° \\ Th(0) &= 0.88 \ (30{,}000 \text{ lbs.}) \\ Th(T) &= 0.88 \ (30{,}000 \text{ lbs.}) \\ \alpha(0) &= 5° \\ \alpha(T) &= 5° \\ n(0) &= 1.0 \\ n(T) &= 1.0 \\ \Delta t &= 12/20 \text{ sec. } (T = 12 \text{ sec.}) \end{aligned} \tag{7.48}$$

The problem was solved in six sub-problems. It took 17.65 seconds to complete the turn. Figures 27 thru 30 are plots of the control expansions as computed at the end of the last sub-problem.

From Figure 28 it is seen that the maximum thrust constraint is active for the first 10 seconds of the turn. At $t \approx 6$ seconds there is a short period in which the thrust is slightly inadmissible. This is due to the use

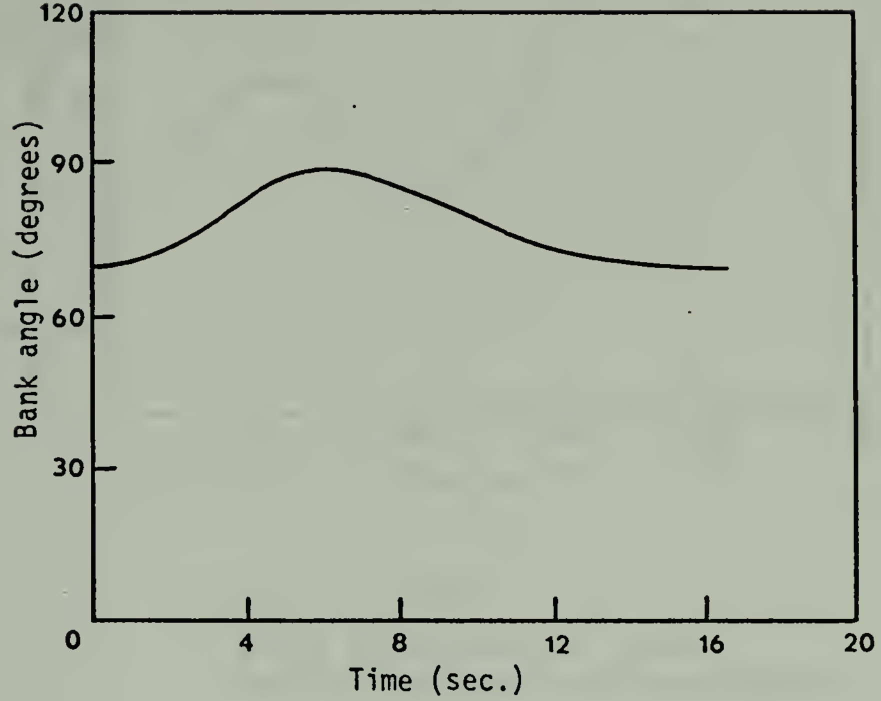

Figure 27

Bank angle vs. time for
turning performance problem A.

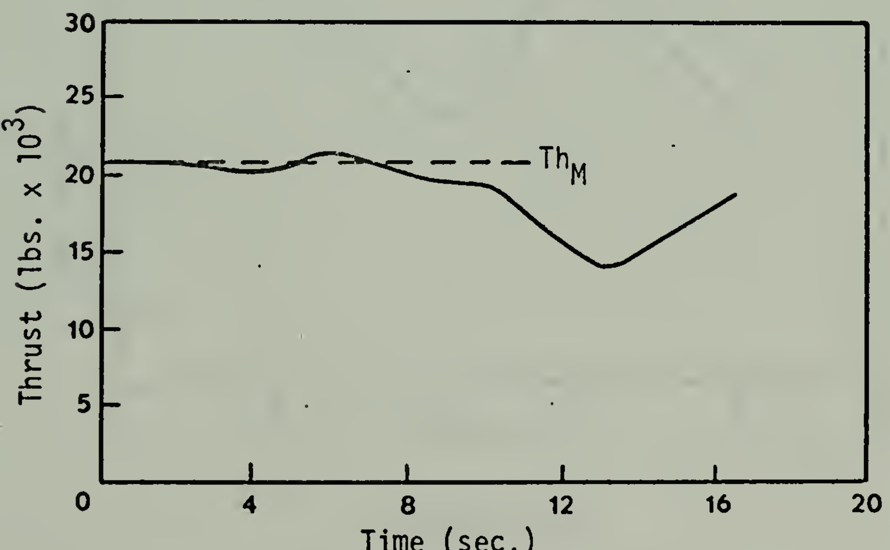

Figure 28

Thrust vs. time for
turning performance problem A.

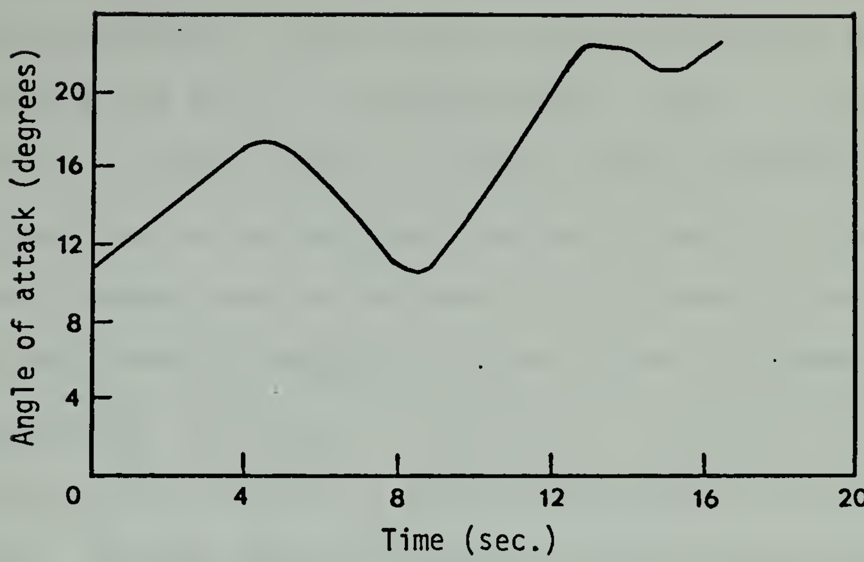

Figure 29

Angle of attack vs. time
for turning performance problem A.

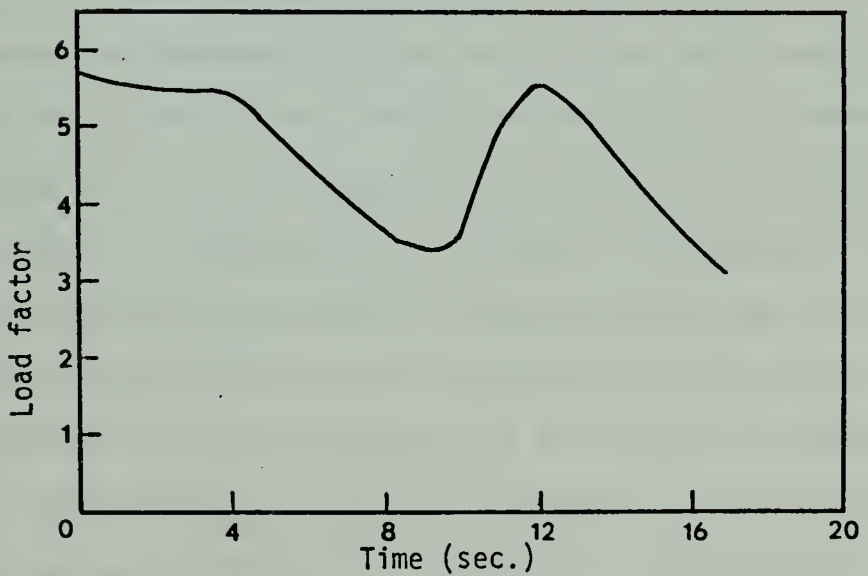

Figure 30

Load factor vs. time for
turning performance problem A.

of the factor δ = 1.03 in the inequality constraint penalty terms in equation (7.35) which has the effect of slightly increasing the size of the admissible region. This is desirable, however, as the epsilon method generates only an approximation to the optimal control from which the true optimal control must be deduced. It is easier to recognize an optimal control expansion which is on a constraint boundary with the factor δ included. As shown in Figure 6 in Section V, δ = 1.03 is the proper choice for a final K_p = 30. During the last portion of the turn, the aircraft is operated at the angle of attack for maximum lift coefficient (approximately 22°). The bank angle and load factor constraints are not active during the maneuver.

Figures 31 thru 34 are plots of the states vs. time. In each plot two curves are shown: one is the expansion for the states as computed at the end of the last sub-problem; the second is the state trajectory obtained by numerically integrating the state equations with the optimal control expansions. An observation of these plots reveals that a high-speed yo-yo maneuver is performed although the altitude excursions are not as large as this author expected. The optimization procedure settles on a nearly level hard turn at high load factors, steep bank angles, and maximum thrust for the majority of the turn. When the maximum thrust boundary is not active, the aircraft flies at the angle of attack for maximum lift coefficient.

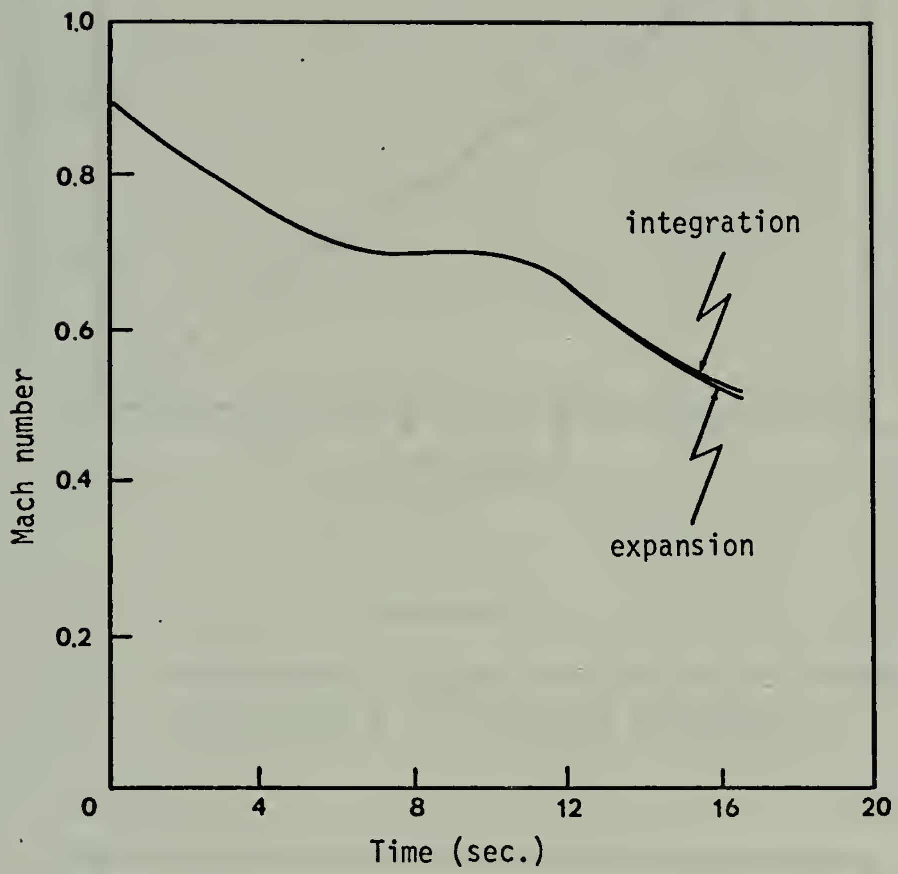

Figure 31

Mach number vs. time
for turning performance problem A.

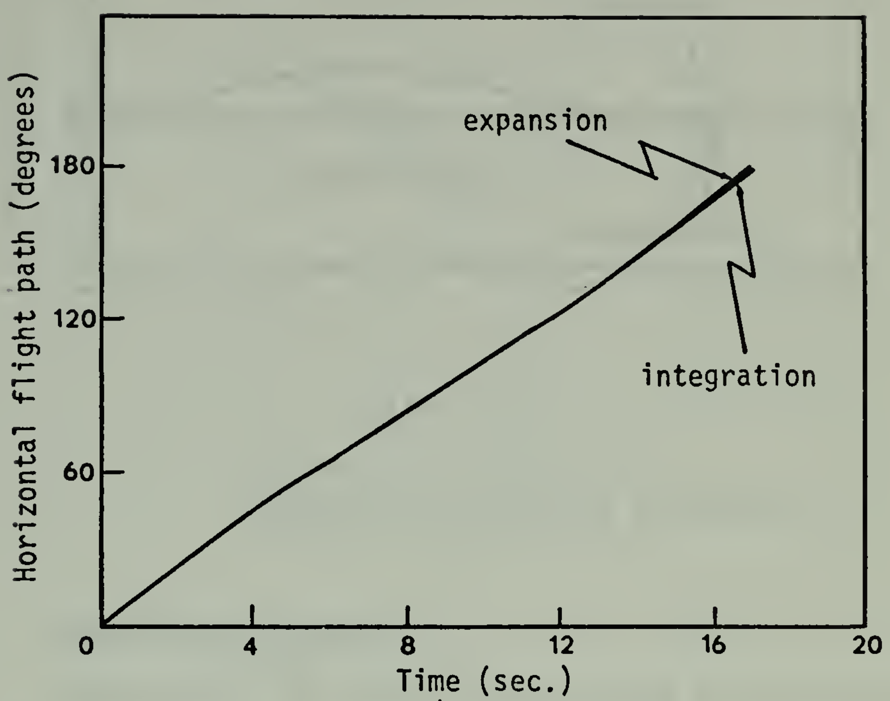

Figure 32

Horizontal flight path angle vs. time for turning performance problem A.

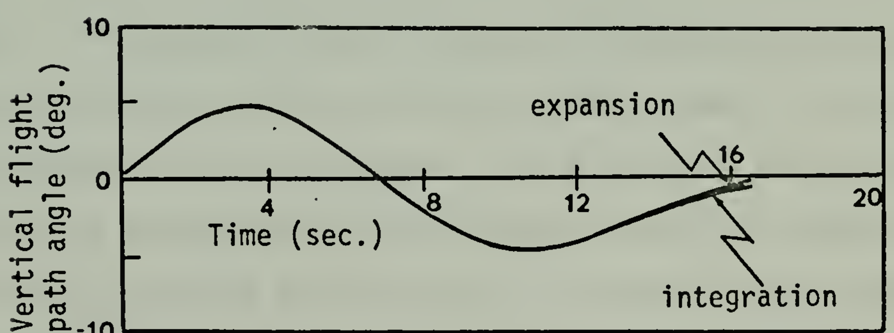

Figure 33

Vertical flight path angle vs. time for turning performance problem A.

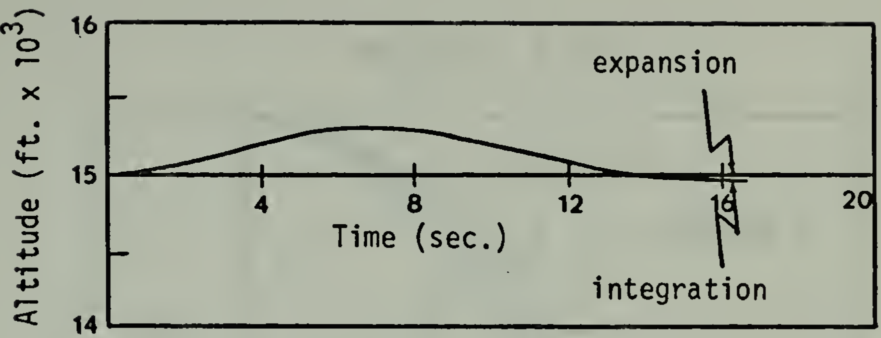

Figure 34

Altitude vs. time for
turning performance problem A.

2. Problems B and C

Figures 35, 36, and 37 are plots of cross-range vs. range, altitude vs. cross-range, and altitude vs. range obtained by integrating the equations of motion with the optimal control expansions found in problems A, B, and C. An observation of Figures 35, 36, and 37 reveals that the expected maneuvers are performed for each initial Mach number. In problem B the aircraft performs an essentially level turn from an initial Mach number equal to its corner Mach number at this altitude. In problem C the aircraft performs a low-speed yo-yo maneuver losing a maximum of 800 feet after 90° of turn from an initial Mach number below its corner Mach number. In problems A and C, however, the aircraft does not go through as much of an altitude excursion as anticipated by the author. Since in fighter

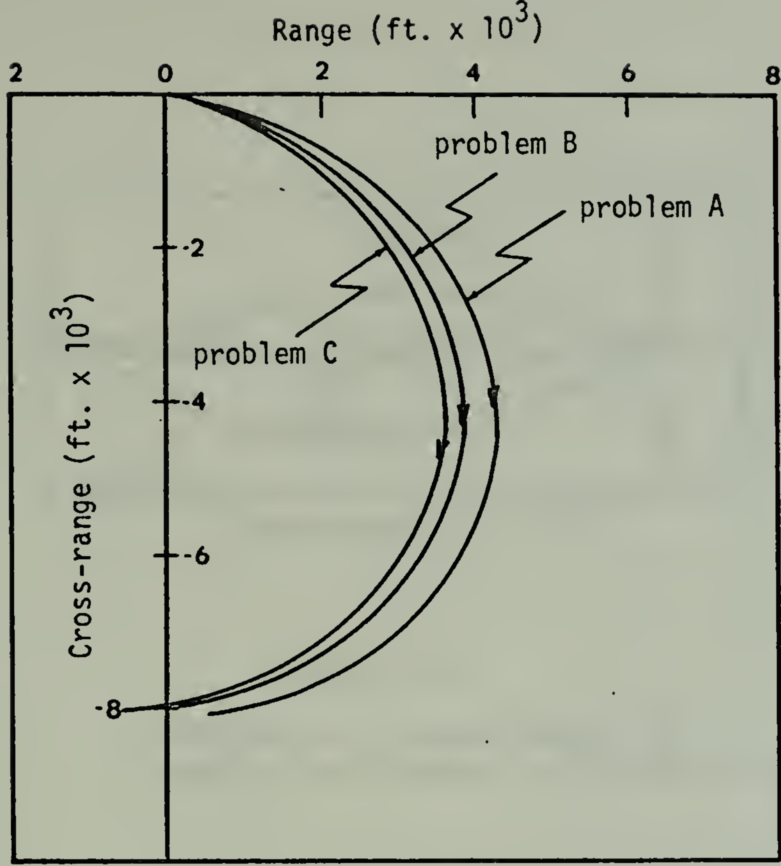

Figure 35

Cross-range vs. range for
turning performance problems A, B, and C.

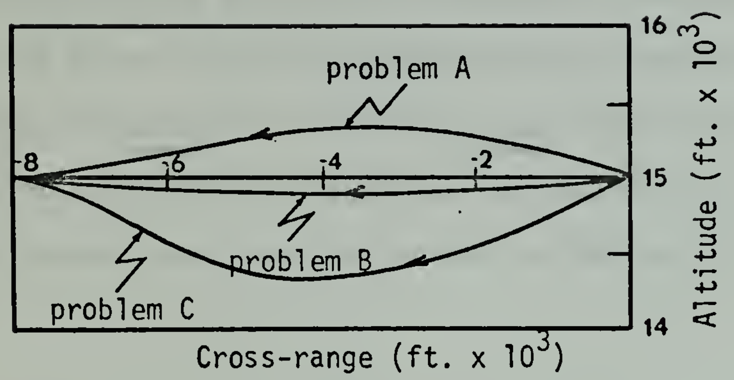

Figure 36

Altitude vs. cross-range for
turning performance problems A, B, and C.

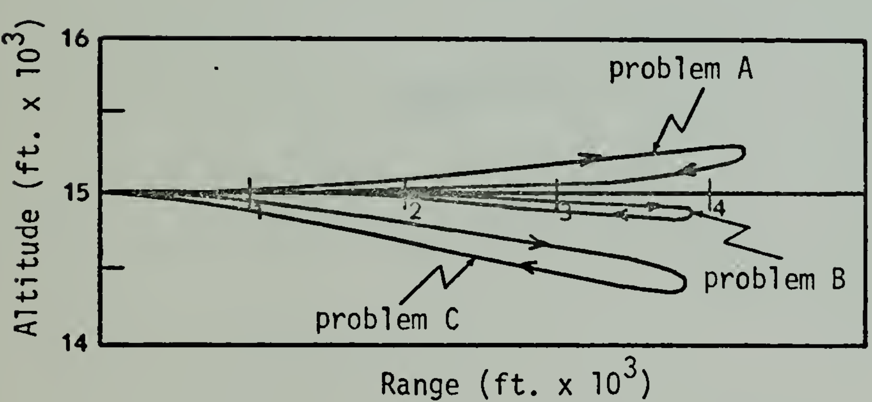

Figure 37

Altitude vs. range for
turning performance problem A, B, and C.

tactics, however, there are no rules on the amount of altitude which should be gained or lost in a yo-yo maneuver, a quantitative evaluation of the results is purely subjective. The important result is that the optimization technique did require the aircraft to perform the high-speed and low-speed yo-yo maneuvers predicted by accepted tactics. The accepted tactics are, therefore, qualitatively correct.

The optimal times required to complete the turn for each of the three problems are given in Table 10.

	Optimal time for reversal
problem A	17.6 sec.
problem B	20.8 sec.
problem C	24.9 sec.

Table 10

VIII. SUMMARY AND CONCLUSIONS

A number of realistic problems in aircraft and missile performance optimization have been solved by the use of a second-order epsilon method. The mathematical models have portrayed aircraft and missile dynamics in an accurate manner with particular emphasis placed on the modeling of performance and maneuvering limitations.

The state and control inequality constraints generated by these limitations have been handled by a new computationally superior penalty functional. Three desirable theoretical properties of this penalty functional have been shown.

A full Newton-Raphson method for minimizing the augmented performance measure has been shown to be computationally feasible and superior in certain situations to the "modified" Newton-Raphson method proposed elsewhere.

The following observations are significant with respect to the second-order epsilon method.

a. The MNR method is relatively insensitive to the starting values of the unknowns $\underset{\sim}{c}$. The FNR method diverges for starting values of $\underset{\sim}{c}$ which are far from optimum.

b. Once $\underset{\sim}{c}$ is close to optimum, the FNR method converges rapidly whereas typically the MNR method either diverges, oscillates, or converges slowly at best.

c. In relatively simple problems the MNR method is capable of obtaining a solution by itself. In more difficult

problems such as those solved in this dissertation, a combination of the two methods is required. Typically, the most effective procedure involves using the MNR method initially followed by the FNR method when successive iterations yield "small" improvements in the augmented performance measure. In other rare cases where the initial guess for the $\tilde{c}$ vector is close to optimum, the FNR method must be used initially.

d. The power of the FNR method close to the minimum can be used to advantage to obtain with minimum effort optimal control and state trajectories for problems with neighboring end conditions by using the solution to a basic problem as a first guess for the new problem.

The solutions to the problems solved have a number of applications. In the missile intercept problem (Section V) minimum-time optimal trajectories may be used as a basis for comparison with the performance of more practical suboptimal controllers such as proportional navigation for a short range air-to-air missile. In the three-dimensional turn-reversal problem the qualitative optimality of an experimentally developed air combat maneuver is shown for the first time. A significant lesson to be learned from the results of this problem is the importance of thrust in comparison to lift coefficient in the maneuvering capability of a fighter aircraft. Thus, an optimization method of the type used in this work applied to realistic performance

problems has application in the evaluation of tradeoffs in the design of future flight vehicles.

APPENDIX A

MATHEMATICAL MODELS

In this Appendix the mathematical models used in the problems are derived. In Section A.1 the basic equations of motion of an aircraft in three dimensions are derived under appropriate assumptions. This model is used in the problem solved in Section VII. In Section A.2 the aircraft is restricted to move in the horizontal plane only and the appropriate adjustments are made to the three-dimensional model. In Section A.3 the aircraft is restricted to move in the vertical plane only and the appropriate adjustments are made to the three-dimensional model. This model is used in the problem solved in Section VI. In Section A.4 the mathematical model for the missile intercept problem solved in Section V is derived.

1. The Mathematical Model for an Aircraft Maneuvering in Three Dimensions

In this section the basic three-degree-of-freedom equations of motion of an aircraft are derived. The assumptions are

a. the earth is flat,

b. the aircraft is a point mass,

c. the mass of the aircraft is a constant,

d. the aircraft is always in balanced flight,

e. the aircraft rolls about its velocity vector,

and f. acceleration due to gravity is a constant.

The coordinate system and notation are presented below.

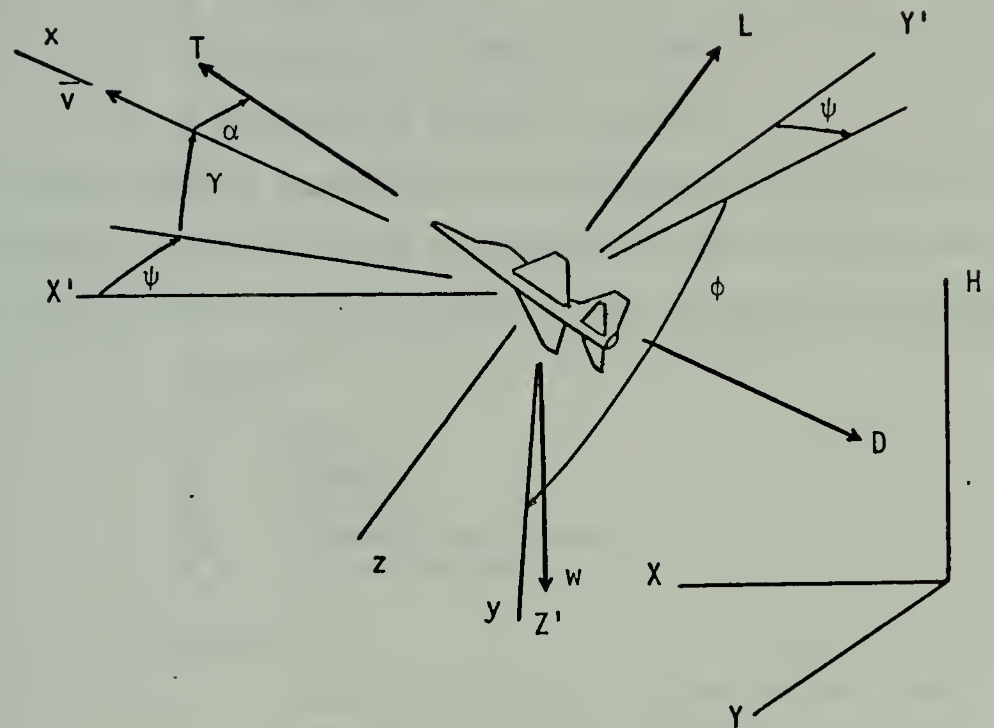

Figure 39
Aircraft Coordinate System

Three axis systems are drawn in Figure 39. They are:

a. (X, Y, H) a fixed inertial axis system;

b. (X', Y', Z') a non-rotating axis system fixed to the center of mass of the aircraft;

c. (x, y, z) a rotating axis system fixed to the center of mass of the aircraft; the x axis is oriented in the direction of the aircraft's velocity vector; the y axis points out the right wing.

The attitude of the aircraft is given by four angles as follows:

a. a rotation ψ in the X'Y' (horizontal) plane;

b. a rotation γ in the xZ' (vertical) plane;

c. a rotation ϕ in the yz plane;

d. a rotation α in the xz plane.

The three angles ψ, γ, and ϕ are the Euler angles (Ref. 19). The angle α is the angle of attack of the aircraft using the thrust line as a reference. The remaining notation is

a. forces;

L = lift,
D = drag,
T = thrust,
Th = normalized thrust,
W_e = gross weight,

b. angles;

α = angle of attack of the thrust line measured in the xz plane,

α_s = angle of attack for maximum lift coefficient,

γ = vertical flight path angle measured in the xZ' plane,

ϕ = bank angle measured in the yz plane,

ψ = horizontal flight path angle measured in the X'Y' plane,

c. rates;

p = roll rate measured in the yz plane,
q = pitch rate measured in the xz plane,
r = yaw rate measured in the xy plane,
ω = angular velocity of the xyz system with respect to the X'Y'Z' system,

d. other parameters;

v = velocity,
m = mass,
g = gravitational constant,

ρ = air density,
S = aircraft wing area,
C_L = lift coefficient,

C_D = drag coefficient,
H = altitude,
h = normalized altitude,

R = radius of turn,
M = Mach number,
M_c = Corner Mach number,
a = speed of sound,

v_c = corner velocity,
n = load factor,
$\underset{\sim}{e}$ = unit vector (with appropriate subscript indicating direction),

e. subscripts;

M = maximum value,
L = minimum value.

The equations of motion are derived following the methods used in Reference 19. Starting with Newton's second law

$$\underset{\sim}{F} = m \frac{d\underset{\sim}{v}}{dt} = m\left[\frac{\delta \underset{\sim}{v}}{\delta t} + \underset{\sim}{\omega} \times \underset{\sim}{v}\right], \tag{A.1}$$

where $\frac{\delta}{\delta t}$ is defined as the time derivative in the xyz system. The aircraft velocity and acceleration may be written

$$\underset{\sim}{v} = v\underset{\sim}{e}_x \tag{A.2}$$

$$\frac{d\underset{\sim}{v}}{dt} = \dot{\underset{\sim}{v}} = \dot{v}\underset{\sim}{e}_x + v\dot{\underset{\sim}{e}}_x , \tag{A.3}$$

where

$$\dot{\underset{\sim}{v}}e_x = \frac{\delta \underset{\sim}{v}}{\delta t} \tag{A.4}$$

and

$$\underset{\sim}{v}\dot{e}_x = \underset{\sim}{\omega} \times \underset{\sim}{v} \ . \tag{A.5}$$

The angular velocity of the xyz system with respect to the non-rotating frame X'Y'Z' is given by

$$\underset{\sim}{\omega} = p\underset{\sim}{e}_x + q\underset{\sim}{e}_y + r\underset{\sim}{e}_z \ . \tag{A.6}$$

At this point, relations between the angular rates p, q, and r and the angular rates of change of the Euler angles are required. These relations are purely trigonometric in nature and are derived in Reference 19. In matrix notation they are

$$\begin{bmatrix} p \\ q \\ r \end{bmatrix} = \begin{bmatrix} 1 & 0 & -\sin\gamma \\ 0 & \cos\phi & \sin\phi \cos\gamma \\ 0 & -\sin\phi & \cos\phi \cos\gamma \end{bmatrix} \begin{bmatrix} \dot{\phi} \\ \dot{\gamma} \\ \dot{\psi} \end{bmatrix} . \tag{A.7}$$

Substituting equations (A.7) into equation (A.6), we obtain

$$\begin{aligned} \underset{\sim}{\omega} = (\dot{\phi} - \dot{\psi}\sin\gamma)\underset{\sim}{e}_x + (\dot{\gamma}\cos\phi + \dot{\psi}\sin\phi \cos\gamma)\underset{\sim}{e}_y \\ + (\dot{\psi}\cos\phi \cos\gamma - \dot{\gamma}\sin\phi)\underset{\sim}{e}_z . \end{aligned} \tag{A.8}$$

Using equations (A.8) and (A.2) the product

$$\underset{\sim}{w} \times \underset{\sim}{v} = (\dot{\psi}\cos\phi \cos\gamma - \dot{\gamma}\sin\phi)v\underset{\sim}{e}_y - (\dot{\psi}\sin\phi \cos\gamma + \dot{\gamma}\cos\phi)v\underset{\sim}{e}_z \tag{A.9}$$

is formed. Isolating thrust and weight components in the xyz system,

$$T_x = T\cos\alpha \ , \tag{A.10}$$

$$T_y = 0 \ , \tag{A.11}$$

$$T_z = -T\sin\alpha \ , \tag{A.12}$$

$$W_{e_x} = -W_e\sin\gamma \ , \tag{A.13}$$

$$W_{e_y} = W_e\cos\gamma \sin\phi \ , \tag{A.14}$$

$$W_{e_z} = W_e\cos\gamma \cos\phi \ , \tag{A.15}$$

equation (A.1) may be written in component form as

$$T\cos\alpha - D - W_e\sin\gamma = m\dot{v} \ , \tag{A.16}$$

$$W_e\cos\gamma \sin\phi = mv(\dot{\psi}\cos\phi \cos\gamma - \dot{\gamma}\sin\phi), \tag{A.17}$$

$$W_e\cos\gamma \cos\phi - T\sin\alpha - L = -mv(\dot{\psi}\sin\phi \cos\gamma + \dot{\gamma}\cos\phi). \tag{A.18}$$

The equations (A.16) thru (A.18) are the basic equations of motion. To apply optimization methods, it is desirable to

transform these equations into state variable format. First, lift and drag coefficients are defined by the expressions

$$L = C_L \tfrac{1}{2}\rho v^2 S \ , \qquad (A.19)$$

$$D = C_D \tfrac{1}{2}\rho v^2 S \ . \qquad (A.20)$$

Second, it is convenient to introduce the normalizing expressions

$$v = aM \ , \qquad (A.21)$$

$$T = Th_M Th \ . \qquad (A.22)$$

Substituting equations (A.19) thru (A.22) into equations (A.16) thru (A.18) along with the expression

$$W_e = mg \ , \qquad (A.23)$$

we obtain

$$Th_M Th\cos\alpha - \tfrac{1}{2}C_D\rho(aM)^2 S - W_e\sin\gamma = \frac{W_e}{g}\, a\dot{M} \qquad (A.24)$$

$$W_e\cos\gamma\sin\phi = \frac{W_e}{g}\, aM(\dot{\psi}\cos\phi\,\cos\gamma - \dot{\gamma}\sin\phi) \qquad (A.25)$$

$$W_e\cos\gamma\,\cos\phi - Th_M Th\sin\alpha - \tfrac{1}{2}C_L\rho(aM)^2 S = \frac{W_e}{g}\, aM(\dot{\psi}\sin\phi\,\cos\gamma + \dot{\gamma}\cos\phi). \qquad (A.26)$$

Solving equations (A.24) thru (A.26) for $\dot{M}$, $\dot{\psi}$, and $\dot{\gamma}$ yields the state variable format

$$\dot{M} = \frac{gTh_M}{W_e a} Th\cos\alpha - \frac{g}{a}\sin\gamma - \frac{g\rho Sa}{2W_e} M^2 C_D \tag{A.27}$$

$$\dot{\psi} = \frac{gTh_M}{W_e a} \frac{Th\sin\alpha \sin\phi}{M\cos\gamma} + \frac{g\rho Sa}{2W_e} \frac{MC_L \sin\phi}{\cos\gamma} \tag{A.28}$$

$$\dot{\gamma} = \frac{gTh_M}{W_e a} \frac{Th\sin\alpha \cos\phi}{M} + \frac{g\rho Sa}{2W_e} MC_L\cos\phi - \frac{g}{a}\frac{\cos\gamma}{M} \tag{A.29}$$

In addition the position of the aircraft (center of mass location) may be required from some fixed reference point. To this end three additional state equations are

$$\dot{X} = aM\cos\gamma \cos\psi , \tag{A.30}$$

$$\dot{Y} = -aM\cos\gamma \sin\psi , \tag{A.31}$$

$$\dot{H} = aM\sin\gamma . \tag{A.32}$$

It is convenient, also, to define the load factor n as

$$n \equiv \frac{\text{TOTAL LIFTING FORCE}}{\text{WEIGHT}} \tag{A.33}$$

$$= \frac{L + T\sin\alpha}{W_e} \tag{A.34}$$

$$= \frac{Th_M}{W_e} Th\sin\alpha + \frac{\rho Sa^2}{2W_e} M^2 C_L \tag{A.35}$$

With equations (A.35) incorporated into equations (A.27) thru (A.29) the state equations are

$$\dot{M} = \frac{gTh_M}{W_e a} Th\cos\alpha - \frac{g}{a}\sin\gamma - \frac{g\rho Sa}{2W_e} M^2 C_D \qquad (A.36)$$

$$\dot{\psi} = \frac{g}{a} \frac{n\sin\phi}{M\cos\gamma} \qquad (A.37)$$

$$\dot{\gamma} = \frac{g}{a} \frac{n\cos\phi}{M} - \frac{g}{a} \frac{\cos\gamma}{M} \qquad (A.38)$$

The mathematical model for the three-dimensional reversal problem solved in Section VII includes the state equations (A.36), (A.37), (A.38), and (A.32). In addition, equation (A.35) must be satisfied. This equation is written in the form

$$0 = \frac{Th_M}{W_e} Th\sin\alpha + \frac{\rho Sa^2}{2W_e} M^2 C_L - n \ . \qquad (A.39)$$

The states are Mach number M, horizontal flight path angle ψ, and vertical flight path angle γ. The controls are bank angle ϕ, normalized thrust Th, angle of attack α, and load factor n. The purpose of introducing load factor as an independent control through equation (A.35) vice using the state equations (A.27) thru (A.29) is to simplify the state equations and the incorporation of the structural load factor constraint.

The following inequality constraints are imposed on the controls:

$$0 \leq Th \leq 1 \ , \tag{A.40}$$

$$0 \leq \alpha \leq \alpha_M \ , \tag{A.41}$$

$$0 \leq n \leq n_M \ . \tag{A.42}$$

The lift and drag coefficients are given as tabular functions of Mach number and angle of attack. Reynold's number effects are neglected. The parameters considered constant for the problem in Section VII are the gravitational constant g, maximum thrust Th_M, aircraft gross weight W_e, the speed of sound a, air density ρ, and wind area S.

2. <u>The Mathematical Model for an Aircraft Maneuvering in the Horizontal Plane</u>

In this section the state equations (A.36) thru (A.38) are applied to an aircraft restricted to maneuver in a horizontal plane. The appropriate assumptions are

$$\gamma = 0 \tag{A.43}$$

$$\dot{\gamma} = 0 \tag{A.44}$$

$$H = H_o \tag{A.45}$$

Applying equations (A.43) thru (A.45) to equation (A.38), we obtain

$$n = \frac{1}{\cos\phi} \, . \tag{A.46}$$

Substituting equations (A.43) and (A.46) into equations (A.36) and (A.37), we may write the state equations as

$$\dot{M} = \frac{gTh_M}{W_e a} Th\cos\alpha - \frac{g\rho Sa}{2W_e} M^2 C_D \, , \tag{A.47}$$

$$\dot{\psi} = \frac{g\tan\phi}{aM} \quad . \tag{A.48}$$

The mathematical model for the two dimensional minimum time and minimum radius of turn problems referred to in Section VII includes the state equations (A.47) and (A.48). In addition, equation (A.35) must be satisfied. Using equation (A.46), equation (A.35) is written in the form

$$0 = \frac{Th_M}{W_e} Th\sin\alpha \cos\phi + \frac{\rho Sa^2}{2W_e} C_L M^2 \cos\phi - 1 \, . \tag{A.49}$$

The states are Mach number M, and horizontal flight path angle ψ. The controls are bank angle ϕ, angle of attack α, and thrust Th. It is possible to eliminate one control by substituting equation (A.49) into equation (A.48). The use of equation (A.49) as an additional equality constraint is preferred, however, because the state equations are simpler

and the required control inequality constraints are simpler to incorporate.

The following inequality constraints are imposed on the controls:

$$0 \leq Th \leq 1 \quad , \tag{A.50}$$

$$0 \leq \phi \leq \phi_M = \cos^{-1}\left[\frac{1}{n_M}\right] , \tag{A.51}$$

$$0 \leq \alpha \leq \alpha_M \quad . \tag{A.52}$$

The lift and drag coefficients are given as tabular functions of Mach number and angle of attack. The parameters considered constant for the problem are the same as those listed for the three dimensional model described in Section A.1.

3. The Mathematical Model for an Aircraft Maneuvering in the Vertical Plane

In this section the state equations (A.27) thru (A.29) are applied to an aircraft restricted to maneuver in the vertical plane. The appropriate assumptions are

$$\phi = 0 \tag{A.53}$$

and

$$\dot{\psi} = 0 . \tag{A.54}$$

Substituting equations (A.53) and (A.54) into equations (A.28) and (A.29), we may write the state equations as

$$\dot{M} = \frac{gTh_M}{W_e a} Th\cos\alpha - \frac{g}{a}\sin\gamma - \frac{g\rho Sa}{2W_e} M^2 C_D \qquad (A.55)$$

$$\dot{\gamma} = \frac{gTh_M}{W_e a} \frac{Th\sin\alpha}{M} + \frac{g\rho Sa}{2W_e} MC_L - \frac{g}{a} \frac{\cos\gamma}{M} \qquad (A.56)$$

The mathematical model for the two dimensional climb performance problem solved in Section VI includes the state equations (A.55) and (A.56) along with state equation (A.32). It is convenient, however, to introduce the following relations into the state equations:

$$\sigma = \frac{\rho}{\rho_o} \qquad (A.57)$$

$$Th = \frac{Th_M}{W_e} \qquad (A.58)$$

$$h = \frac{H}{H_L} \qquad (A.59)$$

where σ = density ratio,

ρ_o = standard sea level density,

Th = normalized maximum thrust,

H_L = tropopause altitude,

and h = normalized altitude.

Substituting equations (A.57) thru (A.59) into equations (A.55) and (A.56), we obtain the revised state equations

$$\dot{M} = \frac{gTh}{a} \cos\alpha - \frac{g}{a} \sin\alpha - \frac{g\rho_o Sa}{2W_e} \sigma M^2 C_D \tag{A.60}$$

$$\dot{\gamma} = \frac{gTh}{a} \frac{\sin\alpha}{M} + \frac{g\rho_o Sa}{2W_e} \sigma M C_L - \frac{g\cos\gamma}{aM} \tag{A.61}$$

$$\dot{h} = \frac{aM}{H_L} \sin\gamma \ . \tag{A.62}$$

The states are Mach number M and vertical flight path angle γ. The control is angle of attack α.

The following inequality constraints are imposed on the states and controls:

$$0 \leq M \leq M_M \tag{A.63}$$

$$\alpha_{min} \leq \alpha \leq \alpha_M \ . \tag{A.64}$$

Thrust (Th) represents normalized maximum thrust for the problem in Section VI. This is given as a tabular function of Mach number and altitude. The lift and drag coefficients are given as tabular functions of Mach number and angle of attack.

Empirical relations are used for density ratio σ, speed of sound a, and maximum Mach number M_M as functions of altitude. These relations are given in Appendix D.

The parameters considered constant for the problem are the gravitational constant g, standard sea level density ρ_o, wing area S, gross weight W_e, and tropopause altitude H_L.

4. <u>The Mathematical Model for the Missile Intercept Problem</u>

In this section the mathematical model for the missile intercept problem solved in Section V is derived. An air-to-air missile launched from an attacking aircraft must intercept a constant-velocity target. The missile is restricted to maneuver in a plane. The orientation of this maneuver plane in three dimensional space is defined at launch as the plane containing the position of the missile at launch, the position of the target at launch, and the velocity vector of the target.

The assumptions applied to the problem include those presented in Section A.1 plus the following:

a. the initial velocity vector of the missile lies in the maneuver plane,

b. the attacking aircraft is tracking the target at missile launch so that the missile's initial velocity points at the target at $t = 0$,

c. the target moves with constant velocity,

d. components of out of plane forces perpendicular to the maneuver plane are ignored.

Figure 40 presents a view of the problem in the maneuver plane.

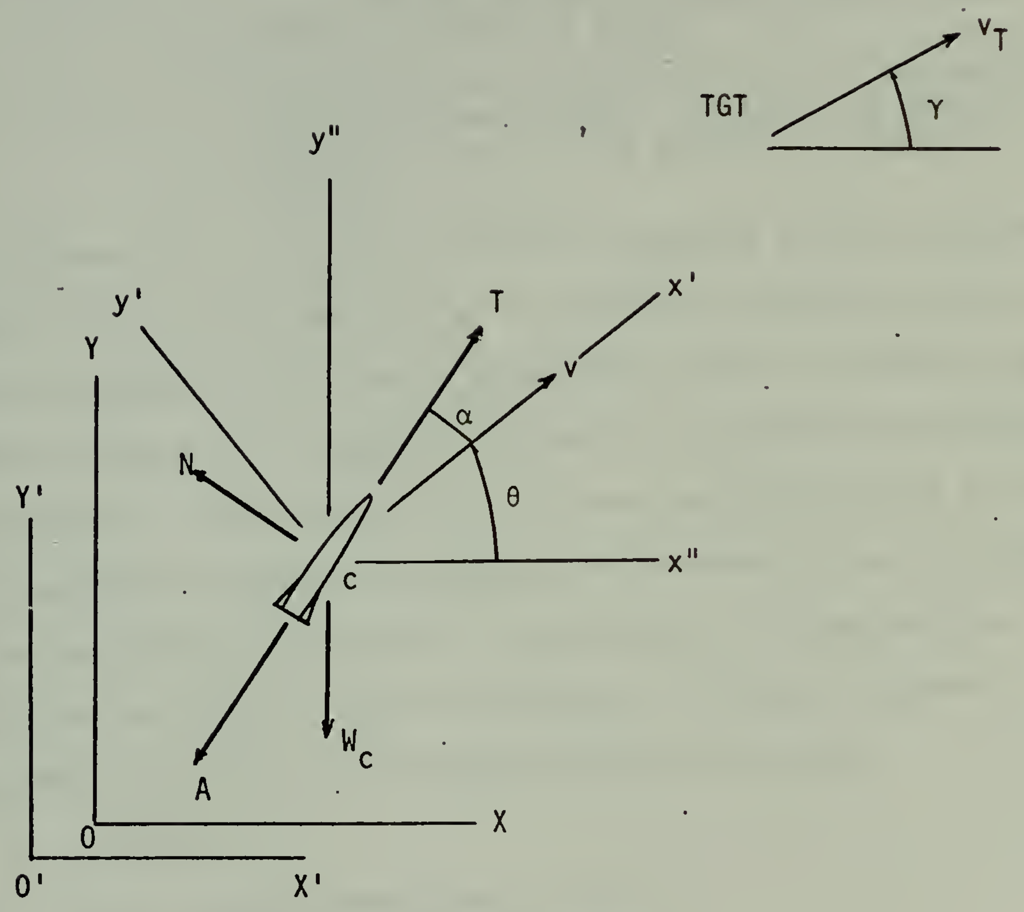

Figure 40

Missile Coordinate System

Four axis systems are drawn in Figure 40. They are:

a.	(X',Y')	a fixed inertial axis system in the maneuver plane with the origin at the missile launch point;
b.	(X,Y)	a Newtonian reference system in the maneuver plane with the origin at the missile launch point at $t = 0$; after launch the origin remains fixed with respect to the target (it moves with velocity v_T with respect to the X'Y' system);
c.	(x'',y'')	a non-rotating axis system fixed to the missile center of mass;
d.	(x',y')	a rotating axis system fixed to the missile center of mass; the x' axis is oriented in the direction of the missile's velocity vector.

The systems X'Y', XY, and x"y" are oriented in the maneuver plane so that the axes 0'X', 0X, and cx" form the intersection of the maneuver plane and a horizontal plane. These axes are chosen so that the target's initial X, X', and x" positions are positive. The axes 0'Y', 0Y, and cy" are chosen so that the component of missile weight in the maneuver plane is acting in the negative Y', Y, or y" direction. All angles are positive as they are shown in Figure 40 in the counter-clockwise direction. The remaining notation is:

a. forces;

N = normal aerodynamic force,
A = axial aerodynamic force,
T = thrust,
Th = normalized thrust,
W_c = component of missile weight in the maneuver plane,

b. angles;

α = angle of attack,
θ = missile flight path angle,
γ = target flight path angle,

c. other quantities;

v = missile velocity,

v_T = target velocity,

M = missile Mach number,

M_T = target Mach number,

W_e = missile gross weight,

C_N = normal force coefficient,

C_A = axial force coefficient,

ω = angular velocity of the x'y' system with respect to the x"y" system,

m = missile mass,

g = gravitational constant,

S = missile wing area,

ρ = air density,

n = load factor,

a = speed of sound,

The equations of motion are derived following the methods used in Section A.1. Equations (A.1) thru (A.5) are identical. The angular velocity of the x'y' system with respect to the non-rotating frame x"y" is given by

$$\underset{\sim}{\omega} = \dot{\theta}\, \underset{\sim}{e}_{z'} \; . \tag{A.65}$$

The product

$$\underset{\sim}{\omega} \times \underset{\sim}{v} = v\, \dot{\theta}\, \underset{\sim}{e}_{y'} \tag{A.66}$$

is formed. Summing forces in the x' and y' directions, we obtain from equation (A.1)

$$T\cos\alpha - N\sin\alpha - A\cos\alpha - W_c\sin\theta = m\dot{v} \quad , \tag{A.67}$$

$$T\sin\alpha + N\cos\alpha - A\sin\alpha - W_c\cos\theta = mv\dot{\theta} \quad . \tag{A.68}$$

Axial and normal force coefficients are defined by the expressions

$$A = C_A \frac{1}{2} \rho v^2 S \quad , \tag{A.69}$$

and

$$N = C_N \frac{1}{2} \rho v^2 S \quad . \tag{A.70}$$

Substituting equations (A.21), (A.22), and (A.23) into equations (A.69) and (A.70) and transforming the results into state variable format, the state equations become

$$\dot{M} = \frac{gTh_M}{aW_e} Th\cos\alpha - \frac{g\rho Sa}{2W_e} M^2 C_A \cos\alpha - \frac{g\rho Sa}{2W_e} M^2 C_N \sin\alpha - \frac{gW_c}{aW_e} \sin\theta \quad , \tag{A.71}$$

$$\dot{\theta} = \frac{gTh_M}{aW_e} \frac{Th\sin\alpha}{M} - \frac{g\rho Sa}{2W_e} MC_A \sin\alpha + \frac{g\rho Sa}{2W_e} MC_N \cos\alpha - \frac{gW_c}{aW_e} \frac{\cos\theta}{M} \quad . \tag{A.72}$$

Two additional state equations are required to impose end conditions on the relative positions of the missile and target in the optimization procedure. They are

$$\dot{X} = aM\cos\theta - aM_T\cos\gamma \tag{A.73}$$

$$\dot{Y} = aM\sin\theta - aM_T\sin\gamma \quad . \tag{A.74}$$

The states are missile Mach number M and missile flight path angle θ. The control is missile angle of attack α. Normalized thrust is given by

$$Th = 1 \qquad t \leq t_B \tag{A.75}$$

$$Th = 0 \qquad t > t_B$$

where t_B represents engine burnout. The following inequality constraints are imposed:

$$-\alpha_M \leq \alpha \leq \alpha_M \tag{A.77}$$

$$-n_M \leq \frac{a}{g} (\dot{\theta} M) \leq n_M \tag{A.78}$$

Equation (A.78) represents a structural load factor limit.

The axial and normal force coefficients are given as tabular functions of Mach number and angle of attack. Parameters considered constant for the problem are the gravitational constant g, maximum thrust Th_M, the speed of sound a, missile weight W_e, air density ρ, missile wing area S, the Mach number of the target M_T, and the flight path angle of the target γ.

In order to properly define the problem, it is necessary to perform several manipulations in analytic geometry. First, the three dimensional positions of the missile and target must be specified at launch. Second, the velocity

vector of the target and the Mach number of the missile at launch must be specified. Once this is done it is necessary to:

a. identify the maneuver plane,

b. identify the XY coordinate system,

c. calculate the target coordinates in that system,

d. calculate the target flight path angle γ, the initial missile flight path angle $\theta(0)$, and the component of the missile weight acting in the maneuver plane W_c. The optimization procedure can then be commenced.

To accomplish these calculations an initial coordinate system is established in which the problem can be easily visualized. The origin is situated at the missile. The $O\underline{X}$ axis is positioned in the horizontal plane. The $O\underline{Y}$ axis is positioned in the horizontal plane such that the target has no $\underline{Y}$ coordinate. The $O\underline{Z}$ axis is positioned in the vertical plane such that a target which has an altitude advantage over the missile has a positive $\underline{Z}$ component. This coordinate system is shown in figures 41 and 42. The angles δ_T and β_T are defined as shown above. The following relations may be written:

$$\underset{\sim}{a} = R_T \underset{\sim}{i} + h_T \underset{\sim}{k} \tag{A.79}$$

$$\underset{\sim}{M}_T = m_{x'} \underset{\sim}{i} + m_{y'} \underset{\sim}{j} + m_{z'} \underset{\sim}{k} \tag{A.80}$$

$$\tan\delta_T = \frac{m_{z'}}{m_{x'}} \tag{A.81}$$

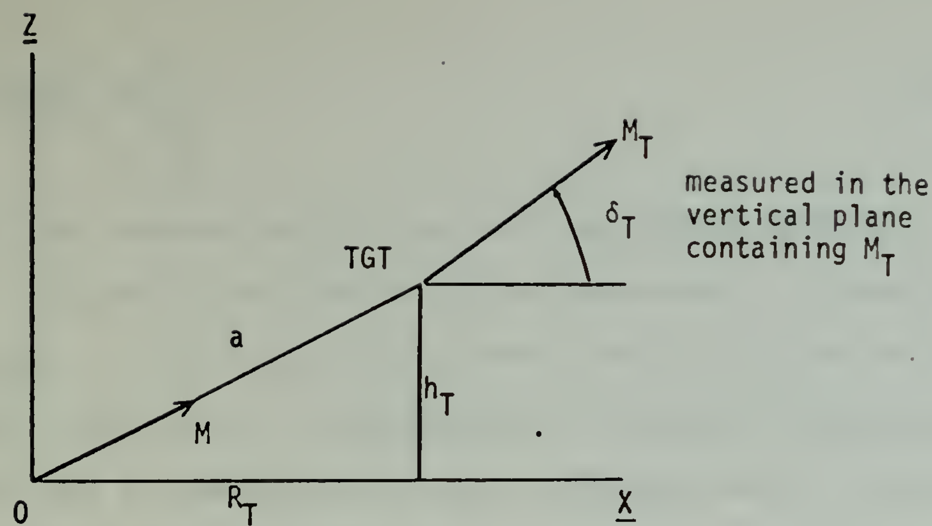

Figure 41

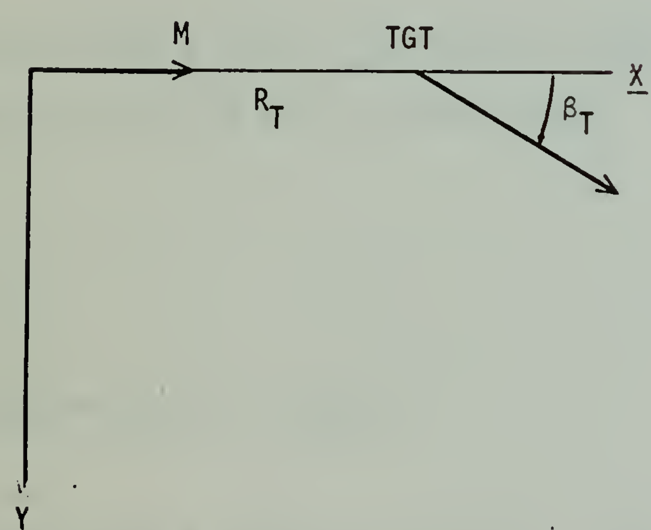

Figure 42

Initial Missile Coordinate System

$$\tan\beta_T = \frac{m_{y'}}{m_{x'}} \quad . \tag{A.82}$$

With the problem defined in the coordinate system shown in Figures 41 and 42 it is now necessary to transfer the problem to the coordinate system used in the optimization procedure. That is, it is necessary to identify the maneuver plane and the XY coordinate system. To this end, a vector normal to the maneuver plane is

$$\underset{\sim}{N} = \underset{\sim}{a} \times \underset{\sim}{M}_T \tag{A.83}$$

$$= -h_T m_{y'} \underset{\sim}{i} + (h_T m_{x'} - R_T m_{z'}) \underset{\sim}{j} + R_T m_{y'} \underset{\sim}{k} \quad . \tag{A.84}$$

To establish the X axis a vector is required which is in both the maneuver plane and a horizontal plane. Such a vector is

$$\underset{\sim}{X} = \underset{\sim}{N} \times \underset{\sim}{k} \tag{A.85}$$

$$= (h_T m_{x'} - R_T m_{z'}) \underset{\sim}{i} + h_T m_{y'} \underset{\sim}{j} \quad . \tag{A.86}$$

To establish the Y axis a vector is required which is in the maneuver plane and perpendicular to the X axis. Such a vector is

$$\underset{\sim}{Y} = \underset{\sim}{N} \times \underset{\sim}{X} \tag{A.87}$$

$$= -R_T h_T m_{h'}{}^2 \underset{\sim}{i} + R_T m_{y'}(h_T m_{x'} - R_T m_{z'})\underset{\sim}{j} \tag{A.88}$$

$$= [h_T{}^2 m_{y'}{}^2 + (h_T m_{x'} - R_T m_{z'})^2]\underset{\sim}{k} \quad .$$

The angle ϕ between the maneuver plane and a horizontal plane is required and is given by

$$\cos\phi = \left| \frac{\underset{\sim}{N} \cdot \underset{\sim}{k}}{|\underset{\sim}{N}| \ |\underset{\sim}{k}|} \right| \tag{A.89}$$

$$= \left| \frac{R_T m_{y'}}{[(h_T m_{y'})^2 + (h_T m_{x'} - R_T m_{z'})^2 + (R_T m_{y'})^2]^{\frac{1}{2}}} \right| \quad . \tag{A.90}$$

The missile weight component in the maneuver plane W_c may be found from

$$W_c = w_e \sin\phi \quad . \tag{A.91}$$

This is shown graphically in Figure 43.

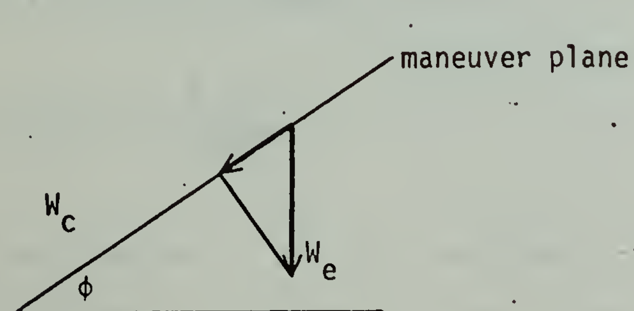

Figure 43
Missile Weight Component

The initial target coordinates are

$$X_T(0) = |PROJ_{\underset{\sim}{X}}\underset{\sim}{a}|$$

$$= \left| \frac{R_T(h_T m_{x'} - R_T m_{z'})}{[(h_T m_{x'} - R_T m_{z'})^2 + (h_T m_{y'})^2]^{1/2}} \right| , \qquad (A.93)$$

$$Y_T(0) = \pm PROJ_{\underset{\sim}{Y}}\underset{\sim}{a} \qquad (A.95)$$

$$= \pm \frac{-R_T{}^2 h_T m_{y'}{}^2 - h_T{}^3 m_{y'}{}^2 - h_T(h_T m_{x'} - R_T m_{z'})^2}{\left\{(R_T h_T m_{y'}{}^2)^2 + [R_T m_{y'}(h_T m_{x'} - R_T m_{z'})]^2 + [h_T^2 m_{y'}^2 + (h_T m_{x'} - R_T m_{z'})^2]^2\right\}^{1/2}} .$$

The sign of $Y_T(0)$ is resolved by:

if $h_T \geq 0$, Y_T is positive;

if $h_T < 0$, Y_T is negative.

The initial missile flight path angle $\theta(0)$ is

$$\tan\theta(0) = \frac{Y_T(0)}{X_T(0)} \qquad (A.96)$$

by assumption b at the beginning of this section. Before proceeding it is necessary to insure that the $\underset{\sim}{X}$ and $\underset{\sim}{Y}$ vectors given in equations (A.86) and (A.88) have the

correct sense. This may be checked by observing the sign of $PROJ_{\underset{\sim}{X}}\underset{\sim}{a}$ which should be positive and the sign of $PROJ_{\underset{\sim}{Y}}\underset{\sim}{a}$ which should be positive if $h_T > 0$ or negative if $h_T < 0$. After the senses of these vectors have been checked and altered as required, the target flight path angle γ may be calculated by

$$\cos\gamma = \frac{\underset{\sim}{M}_T \cdot \underset{\sim}{X}}{|\underset{\sim}{M}_T| \cdot |\underset{\sim}{X}|} \quad . \tag{A.97}$$

The possible range of γ is

$$-\pi \leq \gamma \leq \pi \quad . \tag{A.98}$$

If $\cos\gamma$ is positive, then

$$-\frac{\pi}{2} \leq \gamma \leq \frac{\pi}{2} \quad . \tag{A.99}$$

If $\cos\gamma$ is negative, then

$$\frac{\pi}{2} \leq \gamma \leq \pi \quad \text{or} \quad -\pi \leq \gamma \leq -\frac{\pi}{2} \quad . \tag{A.100}$$

To find which inequality applies in (A.100) the quantity

$$k = \frac{\underset{\sim}{M}_T \cdot \underset{\sim}{Y}}{|\underset{\sim}{M}_T| |\underset{\sim}{Y}|} \tag{A.101}$$

is formed. If k is positive, then

$$0 \leq \gamma \leq \pi \quad . \tag{A.102}$$

If k is negative, then

$$-\pi \leq \gamma \leq 0 \quad . \tag{A.103}$$

This logic completes the set up of the problem in the maneuver plane.

APPENDIX B

TABULAR FUNCTIONS

In this Appendix the tabular functions used in the problems are presented.

1. Three Dimensional Plots

Three dimensional plots of all tabular functions are presented here. Figure 44 gives the lift coefficient C_L as a function of Mach number M and angle of attack α for the the supersonic fighter aircraft used in the aircraft problems. Figure 45 gives the drag coefficient C_D as a function of Mach number M and angle of attack α for the same fighter. Figure 46 gives normalized maximum thrust Th as a function of Mach number M and altitude H for the supersonic aircraft performing the minimum-time climb in the problem in Section VI. Figure 47 gives the normal force coefficient C_N as a function of Mach number M and angle of attack α for the air-to-air missile used in the problem in Section V. Figure 48 gives the axial force coefficient C_A for this missile.

2. Tables

Following each plot a condensed version of the table used in the computation is presented.

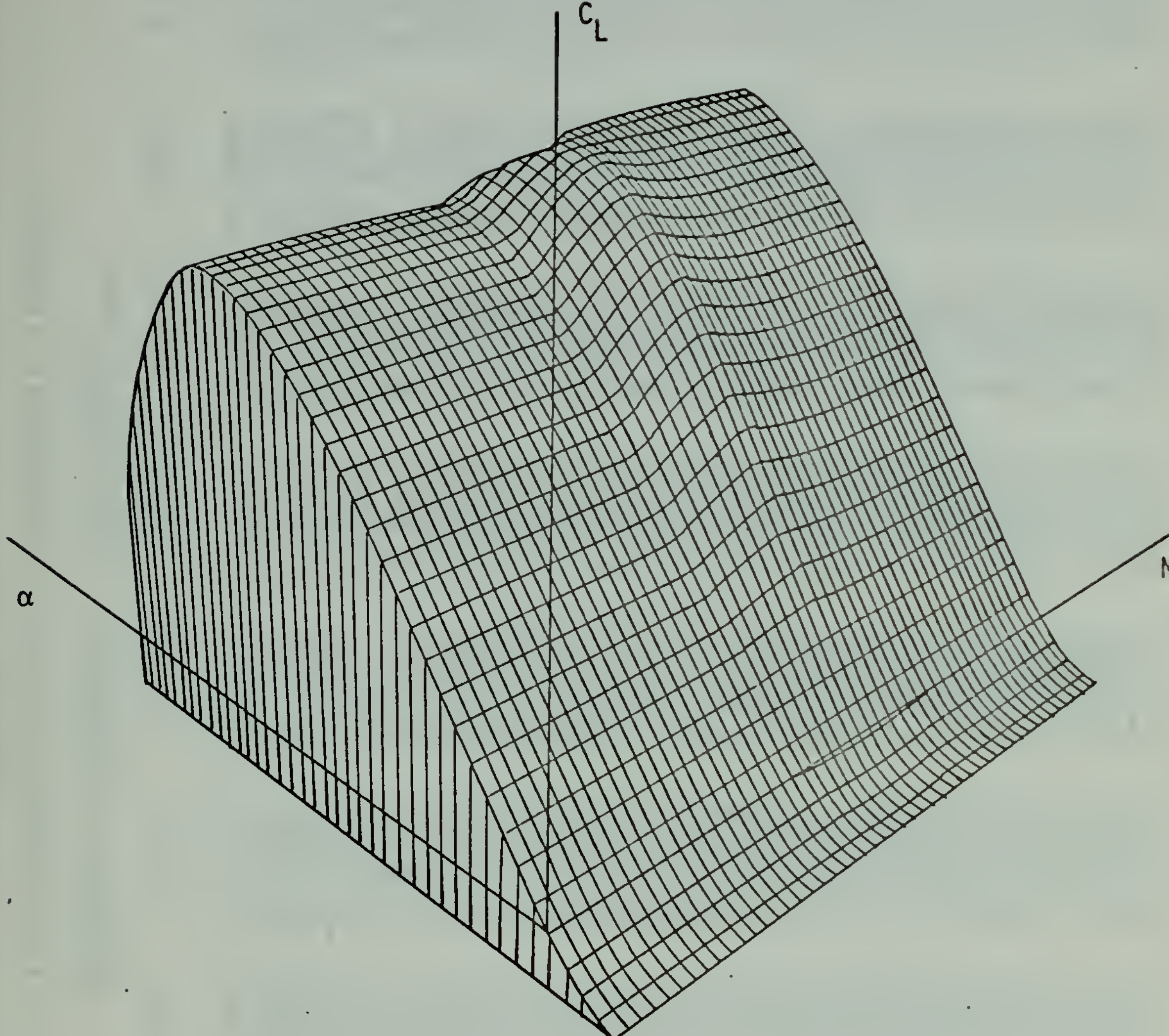

Figure 44

$C_L = f(M,\alpha)$

TABLE 11

LIFT COEFFICIENT FOR A SUPERSONIC AIRCRAFT

HORIZONTAL PARAMETER = MACH NUMBER
VERTICAL PARAMETER = ANGLE OF ATTACK

	0.0	0.100	0.200	0.300	0.400	0.500	0.600	0.700	0.800
-6.0	-0.2060	-0.2060	-0.2060	-0.2060	-0.2060	-0.2060	-0.2060	-0.2060	-0.2060
-5.0	-0.1963	-0.1963	-0.1963	-0.1963	-0.1963	-0.1963	-0.1963	-0.1968	-0.1980
-4.0	-0.1770	-0.1770	-0.1770	-0.1770	-0.1770	-0.1770	-0.1770	-0.1780	-0.1800
-3.0	-0.1486	-0.1486	-0.1486	-0.1486	-0.1486	-0.1486	-0.1486	-0.1503	-0.1525
-2.0	-0.1100	-0.1100	-0.1100	-0.1100	-0.1100	-0.1100	-0.1100	-0.1120	-0.1140
-1.0	-0.0583	-0.0583	-0.0583	-0.0583	-0.0583	-0.0583	-0.0563	-0.0594	-0.0605
0.0	0.0	0.0	0.0	0.0	0.0	0.0	0.0	0.0	0.0
1.0	0.0594	0.0594	0.0594	0.0594	0.0594	0.0594	0.0594	0.0599	0.0604
2.0	0.1200	0.1200	0.1200	0.1200	0.1200	0.1200	0.1200	0.1210	0.1220
3.0	0.1800	0.1800	0.1800	0.1800	0.1800	0.1800	0.1800	0.1814	0.1833
4.0	0.2400	0.2400	0.2400	0.2400	0.2400	0.2400	0.2400	0.2420	0.2450
5.0	0.3000	0.3000	0.3000	0.3000	0.3000	0.3000	0.3000	0.3034	0.3075
6.0	0.3600	0.3600	0.3600	0.3600	0.3600	0.3600	0.3600	0.3650	0.3700
7.0	0.4206	0.4206	0.4206	0.4206	0.4206	0.4206	0.4206	0.4267	0.4321
8.0	0.4800	0.4800	0.4800	0.4800	0.4800	0.4800	0.4800	0.4870	0.4930
9.0	0.5361	0.5361	0.5361	0.5361	0.5361	0.5361	0.5361	0.5443	0.5519
10.0	0.5900	0.5900	0.5900	0.5900	0.5900	0.5900	0.5900	0.5990	0.6080
11.0	0.6423	0.6423	0.6423	0.6423	0.6423	0.6423	0.6423	0.6511	0.6600
12.0	0.6920	0.6920	0.6920	0.6920	0.6920	0.6920	0.6920	0.7000	0.7090
13.0	0.7385	0.7385	0.7385	0.7385	0.7385	0.7385	0.7385	0.7443	0.7563
14.0	0.7820	0.7820	0.7820	0.7820	0.7820	0.7820	0.7820	0.7860	0.8000
15.0	0.8224	0.8224	0.8224	0.8224	0.8224	0.8224	0.8224	0.8273	0.8378
16.0	0.8600	0.8600	0.8600	0.8600	0.8600	0.8600	0.8600	0.8660	0.8720
17.0	0.8959	0.8959	0.8959	0.8959	0.8959	0.8959	0.8959	0.9011	0.9051
18.0	0.9280	0.9280	0.9280	0.9280	0.9280	0.9280	0.9280	0.9320	0.9350
19.0	0.9511	0.9511	0.9511	0.9511	0.9511	0.9511	0.9511	0.9559	0.9601
20.0	0.9750	0.9750	0.9750	0.9750	0.9750	0.9750	0.9750	0.9780	0.9810
21.0	1.0186	1.0186	1.0186	1.0186	1.0186	1.0186	1.0186	1.0094	1.0003
22.0	1.0500	1.0500	1.0500	1.0500	1.0500	1.0500	1.0500	1.0300	1.0100
23.0	1.0339	1.0339	1.0339	1.0339	1.0339	1.0339	1.0339	1.0176	1.0013
24.0	1.0000	1.0000	1.0000	1.0000	1.0000	1.0000	1.0000	0.9900	0.9800
25.0	0.9692	0.9692	0.9692	0.9692	0.9692	0.9692	0.9692	0.9589	0.9486
26.0	0.9320	0.9320	0.9320	0.9320	0.9320	0.9320	0.9320	0.9200	0.9080
27.0	0.8849	0.8849	0.8849	0.8849	0.8849	0.8849	0.8849	0.8730	0.8606
28.0	0.8300	0.8300	0.8300	0.8300	0.8300	0.8300	0.8300	0.8180	0.8050
29.0	0.7688	0.7688	0.7688	0.7688	0.7688	0.7688	0.7688	0.7549	0.7400
30.0	0.7000	0.7000	0.7000	0.7000	0.7000	0.7000	0.7000	0.6840	0.6670
31.0	0.6230	0.6230	0.6230	0.6230	0.6230	0.6230	0.6230	0.6054	0.5871
32.0	0.5380	0.5380	0.5380	0.5380	0.5380	0.5380	0.5380	0.5190	0.5000

TABLE 11 (continued)

LIFT COEFFICIENT FOR A SUPERSONIC AIRCRAFT

HORIZONTAL PARAMETER = MACH NUMBER
VERTICAL PARAMETER = ANGLE OF ATTACK

	0.900	1.000	1.100	1.200	1.300	1.400	1.500	1.600	1.700
-6.0	-0.2060	-0.2060	-0.2060	-0.2050	-0.2040	-0.2030	-0.2030	-0.2030	-0.2030
-5.0	-0.2013	-0.2044	-0.2044	-0.1999	-0.1954	-0.1916	-0.1916	-0.1916	-0.1916
-4.0	-0.1850	-0.1900	-0.1900	-0.1830	-0.1760	-0.1700	-0.1700	-0.1700	-0.1700
-3.0	-0.1576	-0.1632	-0.1632	-0.1543	-0.1453	-0.1369	-0.1369	-0.1369	-0.1369
-2.0	-0.1180	-0.1230	-0.1230	-0.1140	-0.1050	-0.0960	-0.0960	-0.0960	-0.0960
-1.0	-0.0629	-0.0659	-0.0654	-0.0603	-0.0552	-0.0497	-0.0497	-0.0497	-0.0497
0.0	0.0	0.0	0.0	0.0	0.0	0.0	0.0	0.0	0.0
1.0	0.0643	0.0681	0.0646	0.0604	0.0572	0.0500	0.0500	0.0500	0.0500
2.0	0.1300	0.1370	0.1300	0.1220	0.1150	0.1010	0.1010	0.1010	0.1010
3.0	0.1956	0.2018	0.1953	0.1838	0.1701	0.1531	0.1531	0.1531	0.1531
4.0	0.2600	0.2660	0.2600	0.2450	0.2250	0.2050	0.2050	0.2050	0.2050
5.0	0.3200	0.3324	0.3228	0.3042	0.2814	0.2551	0.2551	0.2551	0.2551
6.0	0.3800	0.3990	0.3850	0.3630	0.3380	0.3050	0.3050	0.3050	0.3050
7.0	0.4454	0.4653	0.4484	0.4234	0.3948	0.3561	0.3561	0.3561	0.3561
8.0	0.5100	0.5300	0.5110	0.4830	0.4500	0.4070	0.4070	0.4070	0.4070
9.0	0.5686	0.5921	0.5721	0.5403	0.5017	0.4569	0.4569	0.4569	0.4569
10.0	0.6230	0.6510	0.6300	0.5950	0.5510	0.5050	0.5050	0.5050	0.5050
11.0	0.6729	0.7056	0.6819	0.6467	0.5988	0.5496	0.5496	0.5496	0.5496
12.0	0.7200	0.7560	0.7300	0.6950	0.6440	0.5920	0.5920	0.5920	0.5920
13.0	0.7662	0.8018	0.7763	0.7393	0.6858	0.6335	0.6335	0.6335	0.6335
14.0	0.8100	0.8430	0.8190	0.7800	0.7250	0.6730	0.6730	0.6730	0.6730
15.0	0.8511	0.8792	0.8567	0.8177	0.7624	0.7099	0.7099	0.7099	0.7099
16.0	0.8880	0.9110	0.8900	0.8520	0.7970	0.7440	0.7440	0.7440	0.7440
17.0	0.9183	0.9398	0.9196	0.8831	0.8277	0.7746	0.7746	0.7746	0.7746
18.0	0.9440	0.9630	0.9440	0.9100	0.8550	0.8020	0.8020	0.8020	0.8020
19.0	0.9671	0.9792	0.9626	0.9320	0.8798	0.8270	0.8270	0.8270	0.8270
20.0	0.9850	0.9860	0.9740	0.9480	0.9000	0.8480	0.8480	0.8480	0.8480
21.0	0.9970	0.9806	0.9772	0.9579	0.9141	0.8636	0.8636	0.8636	0.8636
22.0	0.9990	0.9630	0.9700	0.9580	0.9220	0.8740	0.8740	0.8740	0.8740
23.0	0.9861	0.9321	0.9496	0.9441	0.9258	0.8806	0.8806	0.8806	0.8806
24.0	0.9600	0.8880	0.9160	0.9180	0.9180	0.8780	0.8780	0.8780	0.8780
25.0	0.9199	0.8311	0.8674	0.8798	0.8898	0.8603	0.8603	0.8603	0.8603
26.0	0.8680	0.7600	0.8060	0.8300	0.8470	0.8300	0.8300	0.8300	0.8300
27.0	0.8064	0.6748	0.7353	0.7701	0.7924	0.7876	0.7876	0.7876	0.7876
28.0	0.7350	0.5720	0.6500	0.6980	0.7260	0.7330	0.7330	0.7330	0.7330
29.0	0.6554	0.4498	0.5463	0.6123	0.6493	0.6671	0.6671	0.6671	0.6671
30.0	0.5650	0.3040	0.4230	0.5130	0.5600	0.5880	0.5880	0.5880	0.5880
31.0	0.4613	0.1291	0.2773	0.3999	0.4564	0.4938	0.4938	0.4938	0.4938
32.0	0.3450	-0.0730	0.1100	0.2730	0.3390	0.3850	0.3850	0.3850	0.3850

TABLE 11 (continued)

LIFT COEFFICIENT FOR A SUPERSONIC AIRCRAFT

HORIZONTAL PARAMETER = MACH NUMBER
VERTICAL PARAMETER = ANGLE OF ATTACK

	1.800	1.900	2.000	2.100	2.200	2.300	2.400
-6.0	-0.2030	-0.2030	-0.2030	-0.2030	-0.2030	-0.2030	-0.2030
-5.0	-0.1916	-0.1916	-0.1916	-0.1916	-0.1916	-0.1916	-0.1916
-4.0	-0.1700	-0.1700	-0.1700	-0.1700	-0.1700	-0.1700	-0.1700
-3.0	-0.1369	-0.1369	-0.1369	-0.1369	-0.1369	-0.1369	-0.1369
-2.0	-0.0960	-0.0960	-0.0960	-0.0960	-0.0960	-0.0960	-0.0960
-1.0	-0.0497	-0.0497	-0.0497	-0.0497	-0.0497	-0.0497	-0.0497
0.0	0.0	0.0	0.0	0.0	0.0	0.0	0.0
1.0	0.0500	0.0500	0.0500	0.0500	0.0500	0.0500	0.0500
2.0	0.1010	0.1010	0.1010	0.1010	0.1010	0.1010	0.1010
3.0	0.1531	0.1531	0.1531	0.1531	0.1531	0.1531	0.1531
4.0	0.2050	0.2050	0.2050	0.2050	0.2050	0.2050	0.2050
5.0	0.2551	0.2551	0.2551	0.2551	0.2551	0.2551	0.2551
6.0	0.3050	0.3050	0.3050	0.3050	0.3050	0.3050	0.3050
7.0	0.3561	0.3561	0.3561	0.3561	0.3561	0.3561	0.3561
8.0	0.4070	0.4070	0.4070	0.4070	0.4070	0.4070	0.4070
9.0	0.4569	0.4569	0.4569	0.4569	0.4569	0.4569	0.4569
10.0	0.5050	0.5050	0.5050	0.5050	0.5050	0.5050	0.5050
11.0	0.5496	0.5496	0.5496	0.5496	0.5496	0.5496	0.5496
12.0	0.5920	0.5920	0.5920	0.5920	0.5920	0.5920	0.5920
13.0	0.6335	0.6335	0.6335	0.6335	0.6335	0.6335	0.6335
14.0	0.6730	0.6730	0.6730	0.6730	0.6730	0.6730	0.6730
15.0	0.7099	0.7099	0.7099	0.7099	0.7099	0.7099	0.7099
16.0	0.7440	0.7440	0.7440	0.7440	0.7440	0.7440	0.7440
17.0	0.7746	0.7746	0.7746	0.7746	0.7746	0.7746	0.7746
18.0	0.8020	0.8020	0.8020	0.8020	0.8020	0.8020	0.8020
19.0	0.8270	0.8270	0.8270	0.8270	0.8270	0.8270	0.8270
20.0	0.8480	0.8480	0.8480	0.8480	0.8480	0.8480	0.8480
21.0	0.8636	0.8636	0.8636	0.8636	0.8636	0.8636	0.8636
22.0	0.8740	0.8740	0.8740	0.8740	0.8740	0.8740	0.8740
23.0	0.8806	0.8806	0.8806	0.8806	0.8806	0.8806	0.8806
24.0	0.8780	0.8780	0.8780	0.8780	0.8780	0.8780	0.8780
25.0	0.8603	0.8603	0.8603	0.8603	0.8603	0.8603	0.8603
26.0	0.8300	0.8300	0.8300	0.8300	0.8300	0.8300	0.8300
27.0	0.7876	0.7876	0.7876	0.7876	0.7876	0.7876	0.7876
28.0	0.7330	0.7330	0.7330	0.7330	0.7330	0.7330	0.7330
29.0	0.6671	0.6671	0.6671	0.6671	0.6671	0.6671	0.6671
30.0	0.5880	0.5880	0.5880	0.5880	0.5880	0.5880	0.5880
31.0	0.4938	0.4938	0.4938	0.4938	0.4938	0.4938	0.4938
32.0	0.3850	0.3850	0.3850	0.3850	0.3850	0.3850	0.3850

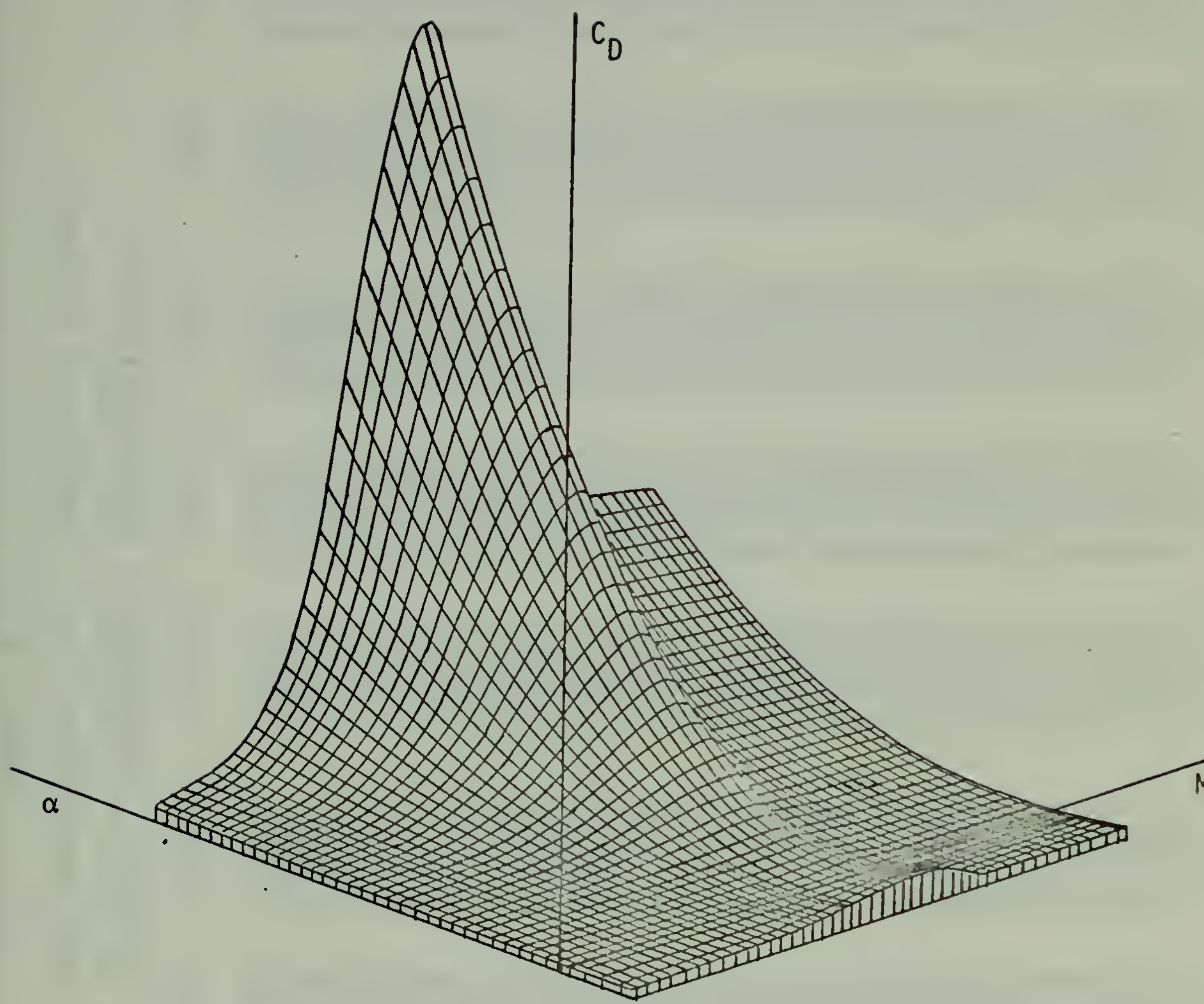

Figure 45

$C_D = f(M,\alpha)$

TABLE 12

DRAG COEFFICIENT FOR A SUPERSONIC AIRCRAFT

HORIZONTAL PARAMETER = MACH NUMBER
VERTICAL PARAMETER = ANGLE OF ATTACK

	0.0	0.100	0.200	0.300	0.400	0.500	0.600	0.700	0.800
-6.0	0.0527	0.0527	0.0527	0.0527	0.0527	0.0527	0.0527	0.0530	0.0576
-5.0	0.0421	0.0421	0.0421	0.0421	0.0421	0.0421	0.0421	0.0423	0.0455
-4.0	0.0334	0.0334	0.0334	0.0334	0.0334	0.0334	0.0334	0.0336	0.0356
-3.0	0.0267	0.0267	0.0267	0.0267	0.0267	0.0267	0.0267	0.0268	0.0279
-2.0	0.0219	0.0219	0.0219	0.0219	0.0219	0.0219	0.0219	0.0219	0.0224
-1.0	0.0190	0.0190	0.0190	0.0190	0.0190	0.0190	0.0190	0.0190	0.0191
0.0	0.0180	0.0180	0.0180	0.0180	0.0180	0.0180	0.0180	0.0180	0.0180
1.0	0.0190	0.0190	0.0190	0.0190	0.0190	0.0190	0.0190	0.0190	0.0191
2.0	0.0219	0.0219	0.0219	0.0219	0.0219	0.0219	0.0219	0.0219	0.0224
3.0	0.0267	0.0267	0.0267	0.0267	0.0267	0.0267	0.0267	0.0268	0.0279
4.0	0.0334	0.0334	0.0334	0.0334	0.0334	0.0334	0.0334	0.0336	0.0356
5.0	0.0421	0.0421	0.0421	0.0421	0.0421	0.0421	0.0421	0.0423	0.0455
6.0	0.0527	0.0527	0.0527	0.0527	0.0527	0.0527	0.0527	0.0530	0.0576
7.0	0.0653	0.0653	0.0653	0.0653	0.0653	0.0653	0.0653	0.0657	0.0719
8.0	0.0797	0.0797	0.0797	0.0797	0.0797	0.0797	0.0797	0.0803	0.0885
9.0	0.0961	0.0961	0.0961	0.0961	0.0961	0.0961	0.0961	0.0968	0.1072
10.0	0.1145	0.1145	0.1145	0.1145	0.1145	0.1145	0.1145	0.1153	0.1281
11.0	0.1347	0.1347	0.1347	0.1347	0.1347	0.1347	0.1347	0.1358	0.1512
12.0	0.1569	0.1569	0.1569	0.1569	0.1569	0.1569	0.1569	0.1582	0.1765
13.0	0.1811	0.1811	0.1811	0.1811	0.1811	0.1811	0.1811	0.1825	0.2040
14.0	0.2071	0.2071	0.2071	0.2071	0.2071	0.2071	0.2071	0.2088	0.2338
15.0	0.2351	0.2351	0.2351	0.2351	0.2351	0.2351	0.2351	0.2370	0.2657
16.0	0.2650	0.2650	0.2650	0.2650	0.2650	0.2650	0.2650	0.2672	0.2998
17.0	0.2968	0.2968	0.2968	0.2968	0.2968	0.2968	0.2968	0.2993	0.3361
18.0	0.3306	0.3306	0.3306	0.3306	0.3306	0.3306	0.3306	0.3333	0.3747
19.0	0.3663	0.3663	0.3663	0.3663	0.3663	0.3663	0.3663	0.3694	0.4154
20.0	0.4039	0.4039	0.4039	0.4039	0.4039	0.4039	0.4039	0.4073	0.4583
21.0	0.4435	0.4435	0.4435	0.4435	0.4435	0.4435	0.4435	0.4472	0.5035
22.0	0.4850	0.4850	0.4850	0.4850	0.4850	0.4850	0.4850	0.4891	0.5508
23.0	0.5284	0.5284	0.5284	0.5284	0.5284	0.5284	0.5284	0.5329	0.6003
24.0	0.5737	0.5737	0.5737	0.5737	0.5737	0.5737	0.5737	0.5786	0.6521
25.0	0.6210	0.6210	0.6210	0.6210	0.6210	0.6210	0.6210	0.6263	0.7060
26.0	0.6702	0.6702	0.6702	0.6702	0.6702	0.6702	0.6702	0.6759	0.7621
27.0	0.7213	0.7213	0.7213	0.7213	0.7213	0.7213	0.7213	0.7275	0.8205
28.0	0.7744	0.7744	0.7744	0.7744	0.7744	0.7744	0.7744	0.7810	0.8810
29.0	0.8294	0.8294	0.8294	0.8294	0.8294	0.8294	0.8294	0.8365	0.9438
30.0	0.8863	0.8863	0.8863	0.8863	0.8863	0.8863	0.8863	0.8939	1.0087
31.0	0.9452	0.9452	0.9452	0.9452	0.9452	0.9452	0.9452	0.9533	1.0759
32.0	1.0060	1.0060	1.0060	1.0060	1.0060	1.0060	1.0060	1.0146	1.1452

TABLE 12 (Continued)

DRAG COEFFICIENT FOR A SUPERSONIC AIRCRAFT

HORIZONTAL PARAMETER = MACH NUMBER
VERTICAL PARAMETER = ANGLE OF ATTACK

	0.900	1.000	1.100	1.200	1.300	1.400	1.500	1.600	1.700
-6.0	0.0972	0.1354	0.1389	0.1296	0.1172	0.1029	0.0889	0.0766	0.0666
-5.0	0.0739	0.1058	0.1100	0.1037	0.0947	0.0846	0.0747	0.0661	0.0591
-4.0	0.0549	0.0815	0.0865	0.0824	0.0762	0.0695	0.0631	0.0576	0.0530
-3.0	0.0401	0.0627	0.0681	0.0659	0.0619	0.0578	0.0541	0.0509	0.0483
-2.0	0.0296	0.0492	0.0550	0.0540	0.0517	0.0495	0.0477	0.0461	0.0449
-1.0	0.0232	0.0411	0.0471	0.0470	0.0455	0.0445	0.0438	0.0433	0.0429
0.0	0.0211	0.0384	0.0445	0.0446	0.0435	0.0428	0.0425	0.0423	0.0422
1.0	0.0232	0.0411	0.0471	0.0470	0.0455	0.0445	0.0438	0.0433	0.0429
2.0	0.0296	0.0492	0.0550	0.0540	0.0517	0.0495	0.0477	0.0461	0.0449
3.0	0.0401	0.0627	0.0681	0.0659	0.0619	0.0578	0.0541	0.0509	0.0483
4.0	0.0549	0.0815	0.0865	0.0824	0.0762	0.0695	0.0631	0.0576	0.0530
5.0	0.0739	0.1058	0.1100	0.1037	0.0947	0.0846	0.0747	0.0661	0.0591
6.0	0.0972	0.1354	0.1389	0.1296	0.1172	0.1029	0.0889	0.0766	0.0666
7.0	0.1247	0.1705	0.1730	0.1603	0.1438	0.1246	0.1056	0.0890	0.0754
8.0	0.1564	0.2109	0.2123	0.1958	0.1745	0.1497	0.1249	0.1033	0.0855
9.0	0.1923	0.2567	0.2569	0.2359	0.2093	0.1781	0.1468	0.1196	0.0970
10.0	0.2325	0.3079	0.3067	0.2808	0.2482	0.2098	0.1713	0.1377	0.1099
11.0	0.2769	0.3645	0.3618	0.3304	0.2911	0.2449	0.1983	0.1577	0.1241
12.0	0.3255	0.4265	0.4221	0.3847	0.3382	0.2833	0.2279	0.1797	0.1396
13.0	0.3783	0.4939	0.4876	0.4438	0.3894	0.3250	0.2601	0.2035	0.1565
14.0	0.4354	0.5666	0.5584	0.5076	0.4446	0.3701	0.2949	0.2293	0.1748
15.0	0.4967	0.6448	0.6344	0.5761	0.5040	0.4186	0.3322	0.2569	0.1944
16.0	0.5622	0.7283	0.7157	0.6493	0.5674	0.4703	0.3721	0.2865	0.2154
17.0	0.6320	0.8173	0.8023	0.7272	0.6350	0.5254	0.4146	0.3180	0.2377
18.0	0.7059	0.9116	0.8940	0.8099	0.7066	0.5839	0.4597	0.3514	0.2614
19.0	0.7842	1.0113	0.9910	0.8973	0.7823	0.6457	0.5073	0.3867	0.2865
20.0	0.8666	1.1164	1.0933	0.9894	0.8621	0.7108	0.5576	0.4239	0.3128
21.0	0.9532	1.2269	1.2008	1.0863	0.9460	0.7793	0.6103	0.4630	0.3406
22.0	1.0441	1.3428	1.3135	1.1878	1.0340	0.8511	0.6657	0.5040	0.3697
23.0	1.1393	1.4641	1.4315	1.2941	1.1261	0.9263	0.7237	0.5469	0.4001
24.0	1.2386	1.5908	1.5548	1.4052	1.2223	1.0048	0.7842	0.5917	0.4319
25.0	1.3422	1.7228	1.6832	1.5209	1.3226	1.0866	0.8473	0.6385	0.4651
26.0	1.4500	1.8603	1.8170	1.6414	1.4270	1.1718	0.9129	0.6871	0.4996
27.0	1.5620	2.0031	1.9559	1.7666	1.5354	1.2603	0.9812	0.7377	0.5355
28.0	1.6783	2.1513	2.1001	1.8965	1.6480	1.3521	1.0520	0.7902	0.5727
29.0	1.7987	2.3049	2.2496	2.0311	1.7647	1.4473	1.1254	0.8445	0.6112
30.0	1.9234	2.4640	2.4043	2.1705	1.8854	1.5459	1.2014	0.9008	0.6512
31.0	2.0524	2.6284	2.5642	2.3146	2.0102	1.6477	1.2799	0.9590	0.6924
32.0	2.1855	2.7981	2.7294	2.4634	2.1392	1.7529	1.3610	1.0191	0.7351

TABLE 12 (Continued)

DRAG COEFFICIENT FOR A SUPERSONIC AIRCRAFT

HORIZONTAL PARAMETER = MACH NUMBER
VERTICAL PARAMETER = ANGLE OF ATTACK

	1.800	1.900	2.000	2.100	2.200	2.300	2.400
-6.0	0.0587	0.0527	0.0479	0.0445	0.0419	0.0400	0.0382
-5.0	0.0536	0.0493	0.0458	0.0431	0.0410	0.0395	0.0379
-4.0	0.0494	0.0466	0.0441	0.0420	0.0403	0.0391	0.0377
-3.0	0.0462	0.0445	0.0427	0.0412	0.0398	0.0387	0.0375
-2.0	0.0439	0.0429	0.0418	0.0406	0.0394	0.0385	0.0373
-1.0	0.0425	0.0420	0.0412	0.0402	0.0392	0.0383	0.0372
0.0	0.0420	0.0417	0.0410	0.0401	0.0391	0.0383	0.0372
1.0	0.0425	0.0420	0.0412	0.0402	0.0392	0.0383	0.0372
2.0	0.0439	0.0429	0.0418	0.0406	0.0394	0.0385	0.0373
3.0	0.0462	0.0445	0.0427	0.0412	0.0398	0.0387	0.0375
4.0	0.0494	0.0466	0.0441	0.0420	0.0403	0.0391	0.0377
5.0	0.0536	0.0493	0.0458	0.0431	0.0410	0.0395	0.0379
6.0	0.0587	0.0527	0.0479	0.0445	0.0419	0.0400	0.0382
7.0	0.0647	0.0567	0.0504	0.0461	0.0429	0.0407	0.0386
8.0	0.0717	0.0613	0.0533	0.0479	0.0440	0.0414	0.0391
9.0	0.0796	0.0665	0.0565	0.0500	0.0453	0.0422	0.0396
10.0	0.0884	0.0723	0.0602	0.0523	0.0468	0.0431	0.0401
11.0	0.0982	0.0787	0.0642	0.0548	0.0484	0.0441	0.0407
12.0	0.1088	0.0857	0.0686	0.0576	0.0502	0.0452	0.0414
13.0	0.1205	0.0934	0.0734	0.0607	0.0521	0.0464	0.0421
14.0	0.1330	0.1016	0.0786	0.0640	0.0542	0.0477	0.0429
15.0	0.1464	0.1105	0.0841	0.0675	0.0564	0.0491	0.0437
16.0	0.1608	0.1200	0.0901	0.0713	0.0588	0.0506	0.0446
17.0	0.1762	0.1301	0.0964	0.0753	0.0614	0.0522	0.0456
18.0	0.1924	0.1408	0.1031	0.0796	0.0641	0.0539	0.0466
19.0	0.2096	0.1521	0.1102	0.0841	0.0669	0.0557	0.0477
20.0	0.2277	0.1640	0.1176	0.0888	0.0699	0.0576	0.0488
21.0	0.2467	0.1766	0.1255	0.0938	0.0731	0.0596	0.0500
22.0	0.2667	0.1897	0.1337	0.0990	0.0764	0.0616	0.0513
23.0	0.2876	0.2035	0.1424	0.1045	0.0799	0.0638	0.0526
24.0	0.3094	0.2179	0.1514	0.1102	0.0835	0.0661	0.0539
25.0	0.3321	0.2329	0.1608	0.1162	0.0873	0.0684	0.0553
26.0	0.3558	0.2485	0.1705	0.1224	0.0912	0.0709	0.0568
27.0	0.3804	0.2647	0.1807	0.1289	0.0953	0.0734	0.0584
28.0	0.4059	0.2815	0.1912	0.1356	0.0995	0.0761	0.0600
29.0	0.4324	0.2989	0.2022	0.1425	0.1039	0.0788	0.0616
30.0	0.4598	0.3170	0.2135	0.1497	0.1084	0.0817	0.0633
31.0	0.4881	0.3356	0.2251	0.1571	0.1131	0.0846	0.0651
32.0	0.5174	0.3549	0.2372	0.1648	0.1180	0.0877	0.0669

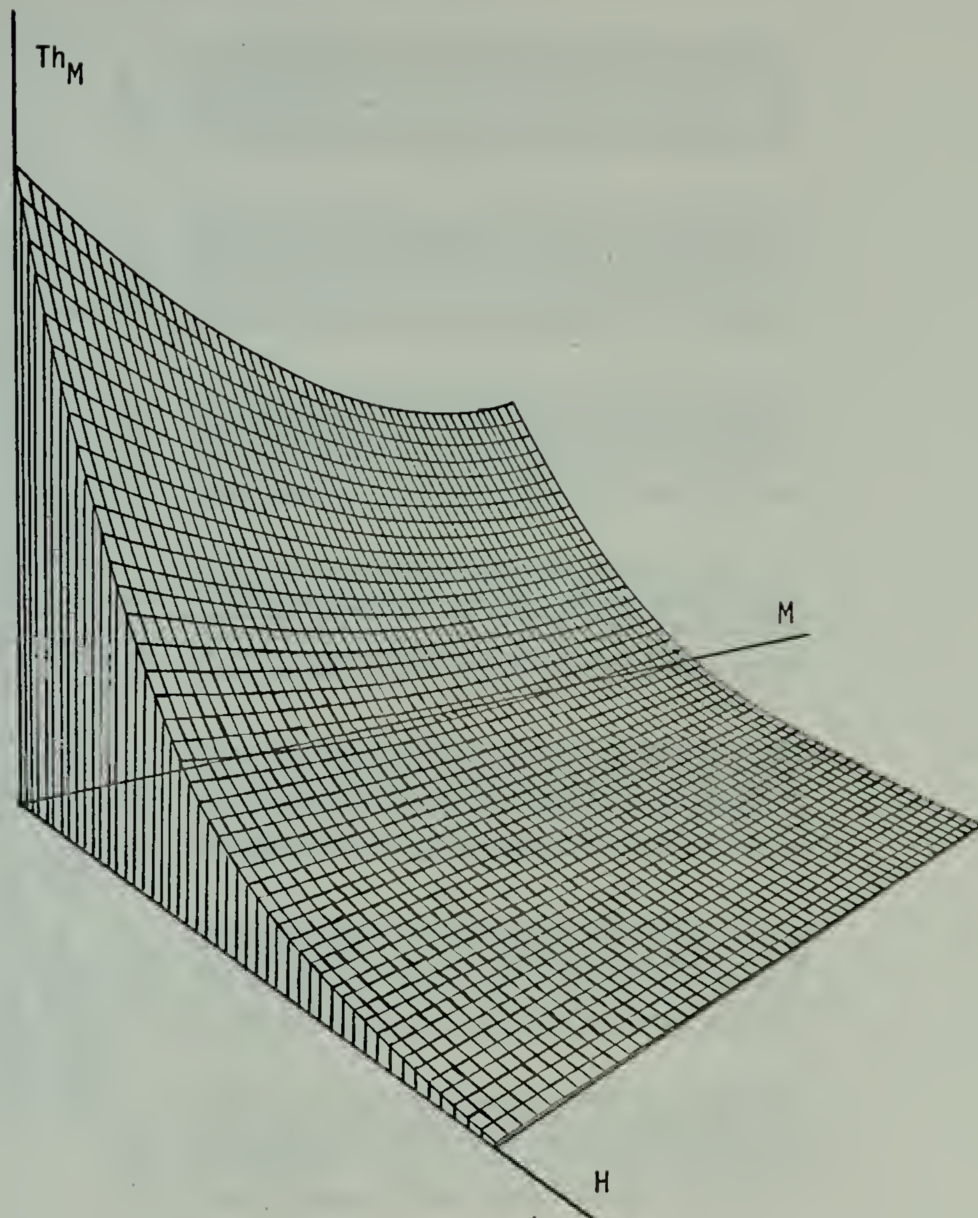

Figure 46

Th = f(M,H)

TABLE 13

MAXIMUM THRUST FOR A SUPERSONIC AIRCRAFT

HORIZONTAL PARAMETER = MACH NUMBER
VERTICAL PARAMETER = ALTITUDE

	0.0	0.100	0.200	0.300	0.400	0.500	0.600	0.700	0.800
0.0	0.8100	0.8030	0.8030	0.8100	0.8200	0.8320	0.8510	0.8720	0.8980
5000.0	0.7190	0.7128	0.7128	0.7190	0.7279	0.7386	0.7554	0.7741	0.7972
10000.0	0.6356	0.6301	0.6301	0.6356	0.6434	0.6528	0.6677	0.6842	0.7046
15000.0	0.5592	0.5543	0.5543	0.5592	0.5661	0.5743	0.5875	0.6020	0.6199
20000.0	0.4895	0.4853	0.4853	0.4895	0.4955	0.5028	0.5143	0.5270	0.5427
25000.0	0.4262	0.4225	0.4225	0.4262	0.4314	0.4378	0.4478	0.4588	0.4725
30000.0	0.3689	0.3657	0.3657	0.3689	0.3734	0.3789	0.3876	0.3971	0.4090
35000.0	0.3173	0.3145	0.3145	0.3173	0.3212	0.3259	0.3333	0.3416	0.3517
40000.0	0.2639	0.2616	0.2616	0.2639	0.2672	0.2711	0.2773	0.2841	0.2926
45000.0	0.2178	0.2159	0.2159	0.2178	0.2204	0.2237	0.2288	0.2344	0.2414
50000.0	0.1806	0.1791	0.1791	0.1806	0.1828	0.1855	0.1898	0.1944	0.2002
55000.0	0.1482	0.1470	0.1470	0.1482	0.1501	0.1523	0.1558	0.1596	0.1644
60000.0	0.1223	0.1213	0.1213	0.1223	0.1238	0.1256	0.1285	0.1317	0.1356
65000.0	0.1009	0.1001	0.1001	0.1009	0.1022	0.1037	0.1060	0.1086	0.1119
70000.0	0.0834	0.0827	0.0827	0.0834	0.0844	0.0856	0.0876	0.0898	0.0924
75000.0	0.0704	0.0698	0.0698	0.0704	0.0713	0.0723	0.0740	0.0758	0.0781
80000.0	0.0569	0.0564	0.0564	0.0569	0.0576	0.0584	0.0597	0.0612	0.0630
85000.0	0.0481	0.0477	0.0477	0.0481	0.0487	0.0494	0.0505	0.0518	0.0533
90000.0	0.0389	0.0386	0.0386	0.0389	0.0394	0.0400	0.0409	0.0419	0.0432
95000.0	0.0329	0.0326	0.0326	0.0329	0.0333	0.0338	0.0345	0.0354	0.0364
100000.0	0.0265	0.0263	0.0263	0.0265	0.0268	0.0272	0.0279	0.0285	0.0294
105000.0	0.0197	0.0196	0.0196	0.0197	0.0200	0.0203	0.0207	0.0213	0.0219
110000.0	0.0135	0.0134	0.0134	0.0135	0.0137	0.0139	0.0142	0.0146	0.0150
115000.0	0.0088	0.0087	0.0087	0.0088	0.0089	0.0090	0.0092	0.0095	0.0097
120000.0	0.0047	0.0047	0.0047	0.0047	0.0048	0.0048	0.0049	0.0051	0.0052

TABLE 13 (continued)

MAXIMUM THRUST FOR A SUPERSONIC AIRCRAFT

HORIZONTAL PARAMETER = MACH NUMBER
VERTICAL PARAMETER = ALTITUDE

	0.900	1.000	1.100	1.200	1.300	1.400	1.500	1.600	1.700
0.0	0.9240	0.9570	0.9860	1.0300	1.0700	1.1140	1.1600	1.2100	1.2600
5000.0	0.8202	0.8495	0.8753	0.9143	0.9499	0.9889	1.0297	1.0741	1.1185
10000.0	0.7250	0.7509	0.7737	0.8082	0.8396	0.8741	0.9102	0.9494	0.9886
15000.0	0.6379	0.6606	0.6807	0.7110	0.7386	0.7690	0.8008	0.8353	0.8698
20000.0	0.5584	0.5783	0.5958	0.6224	0.6466	0.6732	0.7010	0.7312	0.7614
25000.0	0.4862	0.5035	0.5188	0.5419	0.5630	0.5861	0.6103	0.6366	0.6629
30000.0	0.4208	0.4358	0.4491	0.4691	0.4873	0.5073	0.5283	0.5511	0.5738
35000.0	0.3619	0.3748	0.3862	0.4034	0.4191	0.4363	0.4544	0.4739	0.4935
40000.0	0.3011	0.3118	0.3213	0.3356	0.3486	0.3630	0.3780	0.3943	0.4105
45000.0	0.2484	0.2573	0.2651	0.2769	0.2877	0.2995	0.3119	0.3253	0.3387
50000.0	0.2060	0.2134	0.2199	0.2297	0.2386	0.2484	0.2587	0.2698	0.2810
55000.0	0.1691	0.1752	0.1805	0.1885	0.1958	0.2039	0.2123	0.2215	0.2306
60000.0	0.1395	0.1445	0.1469	0.1555	0.1616	0.1682	0.1752	0.1827	0.1903
65000.0	0.1151	0.1192	0.1229	0.1283	0.1333	0.1388	0.1445	0.1508	0.1570
70000.0	0.0951	0.0985	0.1015	0.1060	0.1101	0.1147	0.1194	0.1245	0.1297
75000.0	0.0803	0.0832	0.0857	0.0896	0.0930	0.0969	0.1009	0.1052	0.1096
80000.0	0.0649	0.0672	0.0692	0.0723	0.0751	0.0782	0.0814	0.0849	0.0884
85000.0	0.0549	0.0568	0.0585	0.0612	0.0635	0.0661	0.0689	0.0718	0.0748
90000.0	0.0444	0.0460	0.0474	0.0495	0.0514	0.0535	0.0557	0.0581	0.0606
95000.0	0.0375	0.0388	0.0400	0.0418	0.0434	0.0452	0.0471	0.0491	0.0511
100000.0	0.0302	0.0313	0.0323	0.0337	0.0350	0.0365	0.0380	0.0396	0.0412
105000.0	0.0225	0.0233	0.0240	0.0251	0.0261	0.0272	0.0283	0.0295	0.0307
110000.0	0.0154	0.0160	0.0165	0.0172	0.0179	0.0186	0.0194	0.0202	0.0210
115000.0	0.0100	0.0104	0.0107	0.0112	0.0116	0.0121	0.0126	0.0131	0.0137
120000.0	0.0054	0.0055	0.0057	0.0060	0.0062	0.0065	0.0067	0.0070	0.0073

TABLE 13 (continued)

MAXIMUM THRUST FOR A SUPERSONIC AIRCRAFT

HORIZONTAL PARAMETER = MACH NUMBER
VERTICAL PARAMETER = ALTITUDE

	1.800	1.900	2.000	2.100	2.200	2.300	2.400
0.0	1.3170	1.3750	1.4350	1.5000	1.5700	1.6380	1.7100
5000.0	1.1691	1.2206	1.2739	1.3316	1.3937	1.4541	1.5180
10000.0	1.0334	1.0789	1.1260	1.1770	1.2319	1.2852	1.3417
15000.0	0.9091	0.9492	0.9906	1.0355	1.0838	1.1307	1.1804
20000.0	0.7959	0.8309	0.8672	0.9065	0.9488	0.9899	1.0354
25000.0	0.6929	0.7235	0.7550	0.7892	0.8261	0.8618	0.8997
30000.0	0.5998	0.6262	0.6535	0.6831	0.7150	0.7460	0.7788
35000.0	0.5159	0.5386	0.5621	0.5875	0.6150	0.6416	0.6698
40000.0	0.4291	0.4480	0.4676	0.4887	0.5115	0.5337	0.5572
45000.0	0.3541	0.3697	0.3858	0.4033	0.4221	0.4404	0.4597
50000.0	0.2937	0.3066	0.3200	0.3345	0.3501	0.3652	0.3813
55000.0	0.2410	0.2517	0.2626	0.2745	0.2873	0.2998	0.3130
60000.0	0.1989	0.2076	0.2167	0.2265	0.2371	0.2474	0.2582
65000.0	0.1641	0.1713	0.1788	0.1869	0.1956	0.2041	0.2131
70000.0	0.1356	0.1415	0.1477	0.1544	0.1616	0.1686	0.1760
75000.0	0.1145	0.1196	0.1248	0.1304	0.1365	0.1424	0.1487
80000.0	0.0924	0.0965	0.1007	0.1053	0.1102	0.1150	0.1200
85000.0	0.0782	0.0816	0.0852	0.0891	0.0932	0.0973	0.1015
90000.0	0.0633	0.0661	0.0690	0.0721	0.0754	0.0787	0.0822
95000.0	0.0534	0.0558	0.0582	0.0609	0.0637	0.0665	0.0694
100000.0	0.0431	0.0450	0.0470	0.0491	0.0514	0.0536	0.0560
105000.0	0.0321	0.0335	0.0350	0.0366	0.0383	0.0399	0.0417
110000.0	0.0220	0.0230	0.0240	0.0250	0.0262	0.0273	0.0285
115000.0	0.0143	0.0149	0.0156	0.0163	0.0170	0.0178	0.0185
120000.0	0.0076	0.0080	0.0083	0.0087	0.0091	0.0095	0.0099

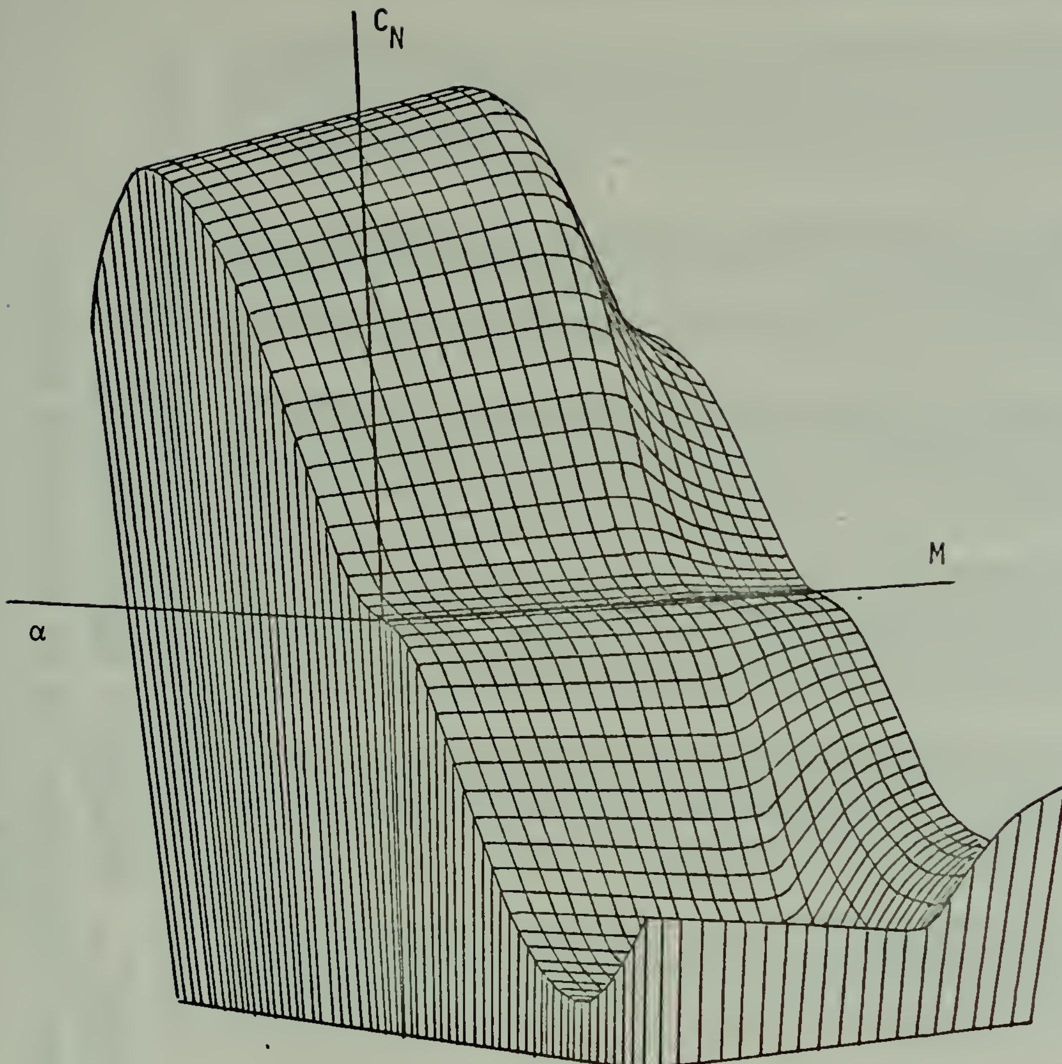

Figure 47

$C_N = f(M,\alpha)$

TABLE 14

NORMAL COEFFICIENT FOR AN AIR-TO-AIR MISSILE

HORIZONTAL PARAMETER = ANGLE OF ATTACK
VERTICAL PARAMETER = MACH NUMBER

	-120.000	-110.000	-100.000	-90.000	-80.000	-70.000	-60.000	-50.000	-40.000
0.0	-8.1000	-9.7277	-10.8563	-11.2711	-10.9920	-10.2596	-9.2265	-7.7135	-5.7900
0.1	-8.2013	-9.8493	-10.9920	-11.4120	-11.1294	-10.3878	-9.3418	-7.8099	-5.8624
0.2	-8.3700	-10.0520	-11.2181	-11.6468	-11.3584	-10.6016	-9.5340	-7.9706	-5.9830
0.3	-8.6063	-10.3357	-11.5348	-11.9756	-11.6790	-10.9008	-9.8032	-8.1956	-6.1519
0.4	-8.9100	-10.7005	-11.9419	-12.3983	-12.0912	-11.2855	-10.1492	-8.4849	-6.3690
0.5	-9.2549	-11.1147	-12.4041	-12.8782	-12.5592	-11.7224	-10.5420	-8.8133	-6.6155
0.6	-9.6778	-11.6226	-12.9710	-13.4667	-13.1332	-12.2581	-11.0237	-9.2160	-6.9178
0.7	-10.1893	-12.2369	-13.6565	-14.1784	-13.8273	-12.9060	-11.6064	-9.7032	-7.2835
0.8	-10.8000	-12.9703	-14.4750	-15.0282	-14.6560	-13.6794	-12.3020	-10.2847	-7.7200
0.9	-11.7418	-14.1014	-15.7373	-16.3388	-15.9341	-14.8724	-13.3748	-11.1816	-8.3932
1.0	-12.7153	-15.2705	-17.0421	-17.6933	-17.2551	-16.1054	-14.4837	-12.1086	-9.0891
1.1	-13.6424	-16.3839	-18.2846	-18.9834	-18.5132	-17.2796	-15.5397	-12.9914	-9.7518
1.2	-14.4450	-17.3478	-19.3603	-20.1002	-19.6024	-18.2962	-16.4539	-13.7558	-10.3255
1.3	-14.7551	-17.7202	-19.7759	-20.5317	-20.0232	-18.6890	-16.8071	-14.0511	-10.5471
1.4	-14.9006	-17.8950	-19.9710	-20.7342	-20.2207	-18.8733	-16.9729	-14.1897	-10.6512
1.5	-14.9196	-17.9178	-19.9964	-20.7606	-20.2465	-18.8974	-16.9945	-14.2077	-10.6648
1.6	-14.8500	-17.8342	-19.9031	-20.6638	-20.1520	-18.8092	-16.9152	-14.1414	-10.6150
1.7	-14.7930	-17.7658	-19.8268	-20.5845	-20.0747	-18.7371	-16.8504	-14.0872	-10.5743
1.8	-14.6981	-17.6518	-19.6996	-20.4524	-19.9459	-18.6169	-16.7423	-13.9968	-10.5064
1.9	-14.5779	-17.5074	-19.5384	-20.2851	-19.7827	-18.4646	-16.6053	-13.8823	-10.4205
2.0	-14.4450	-17.3478	-19.3603	-20.1002	-19.6024	-18.2962	-16.4539	-13.7558	-10.3255
2.1	-14.3385	-17.2199	-19.2175	-19.9520	-19.4578	-18.1613	-16.3326	-13.6543	-10.2494
2.2	-14.2341	-17.0945	-19.0776	-19.8067	-19.3161	-18.0291	-16.2137	-13.5549	-10.1747
2.3	-14.1339	-16.9741	-18.9433	-19.6673	-19.1802	-17.9022	-16.0995	-13.4595	-10.1031
2.4	-14.0400	-16.8614	-18.8175	-19.5366	-19.0528	-17.7833	-15.9926	-13.3701	-10.0360
2.5	-13.9704	-16.7778	-18.7242	-19.4398	-18.9583	-17.6951	-15.9133	-13.3038	-9.9862
2.6	-13.9050	-16.6993	-18.6366	-19.3488	-18.8696	-17.6123	-15.8388	-13.2415	-9.9395
2.7	-13.8396	-16.6207	-18.5489	-19.2578	-18.7809	-17.5295	-15.7643	-13.1793	-9.8928
2.8	-13.7700	-16.5371	-18.4556	-19.1609	-18.6864	-17.4413	-15.6850	-13.1130	-9.8430
2.9	-13.6761	-16.4244	-18.3298	-19.0303	-18.5590	-17.3224	-15.5781	-13.0236	-9.7759
3.0	-13.5759	-16.3041	-18.1955	-18.8909	-18.4230	-17.1955	-15.4640	-12.9282	-9.7043
3.1	-13.4715	-16.1787	-18.0556	-18.7456	-18.2814	-17.0632	-15.3451	-12.8287	-9.6296
3.2	-13.3650	-16.0508	-17.9128	-18.5974	-18.1368	-16.9283	-15.2237	-12.7273	-9.5535
3.3	-13.2585	-15.9228	-17.7700	-18.4492	-17.9922	-16.7934	-15.1024	-12.6259	-9.4774
3.4	-13.1541	-15.7974	-17.6301	-18.3039	-17.8505	-16.6611	-14.9835	-12.5264	-9.4027
3.5	-13.0539	-15.6771	-17.4958	-18.1644	-17.7146	-16.5342	-14.8693	-12.4310	-9.3311
3.6	-12.9600	-15.5644	-17.3700	-18.0338	-17.5872	-16.4153	-14.7624	-12.3416	-9.2640
3.7	-12.8798	-15.4681	-17.2626	-17.9223	-17.4784	-16.3138	-14.6711	-12.2653	-9.2067
3.8	-12.8081	-15.3820	-17.1664	-17.8225	-17.3811	-16.2230	-14.5894	-12.1970	-9.1554
3.9	-12.7448	-15.3060	-17.0816	-17.7344	-17.2952	-16.1428	-14.5173	-12.1367	-9.1102
4.0	-12.6900	-15.2401	-17.0081	-17.6581	-17.2208	-16.0733	-14.4549	-12.0845	-9.0710

TABLE 14 (continued)

NORMAL COEFFICIENT FOR AN AIR-TC-AIR MISSILE

HORIZONTAL PARAMETER = ANGLE OF ATTACK
VERTICAL PARAMETER = MACH NUMBER

	-30.000	-20.000	-10.000	0.0	10.000	20.000	30.000	40.000	50.000
0.0	-3.8154	-1.9706	-0.6246	0.0	0.6246	1.9706	3.8154	5.7900	7.7135
0.1	-3.8631	-1.9953	-0.6324	0.0	0.6324	1.9953	3.8631	5.8624	7.8099
0.2	-3.9426	-2.0363	-0.6454	0.0	0.6454	2.0363	3.9426	5.9830	7.9706
0.3	-4.0539	-2.0938	-0.6636	0.0	0.6636	2.0938	4.0539	6.1519	8.1956
0.4	-4.1969	-2.1677	-0.6871	0.0	0.6871	2.1677	4.1969	6.3690	8.4849
0.5	-4.3594	-2.2516	-0.7137	0.0	0.7137	2.2516	4.3594	6.6155	8.8133
0.6	-4.5586	-2.3545	-0.7463	0.0	0.7463	2.3545	4.5586	6.9178	9.2160
0.7	-4.7995	-2.4789	-0.7857	0.0	0.7857	2.4789	4.7995	7.2835	9.7032
0.8	-5.0872	-2.6275	-0.8328	0.0	0.8328	2.6275	5.0872	7.7200	10.2847
0.9	-5.5308	-2.8566	-0.9054	0.0	0.9054	2.8566	5.5308	8.3932	11.1816
1.0	-5.9894	-3.0935	-0.9805	0.0	0.9805	3.0935	5.9894	9.0891	12.1086
1.1	-6.4261	-3.3190	-1.0520	0.0	1.0520	3.3190	6.4261	9.7518	12.9914
1.2	-6.8041	-3.5143	-1.1139	0.0	1.1139	3.5143	6.8041	10.3255	13.7558
1.3	-6.9502	-3.5897	-1.1378	0.0	1.1378	3.5897	6.9502	10.5471	14.0511
1.4	-7.0187	-3.6251	-1.1490	0.0	1.1490	3.6251	7.0187	10.6512	14.1897
1.5	-7.0277	-3.6297	-1.1505	0.0	1.1505	3.6297	7.0277	10.6648	14.2077
1.6	-6.9949	-3.6128	-1.1451	0.0	1.1451	3.6128	6.9949	10.6150	14.1414
1.7	-6.9681	-3.5990	-1.1407	0.0	1.1407	3.5990	6.9681	10.5743	14.0872
1.8	-6.9233	-3.5759	-1.1334	0.0	1.1334	3.5759	6.9233	10.5064	13.9968
1.9	-6.8667	-3.5466	-1.1241	0.0	1.1241	3.5466	6.8667	10.4205	13.8823
2.0	-6.8041	-3.5143	-1.1139	0.0	1.1139	3.5143	6.8041	10.3255	13.7558
2.1	-6.7539	-3.4884	-1.1057	0.0	1.1057	3.4884	6.7539	10.2494	13.6543
2.2	-6.7048	-3.4630	-1.0976	0.0	1.0976	3.4630	6.7048	10.1747	13.5549
2.3	-6.6576	-3.4386	-1.0899	0.0	1.0899	3.4386	6.6576	10.1031	13.4595
2.4	-6.6133	-3.4157	-1.0827	0.0	1.0827	3.4157	6.6133	10.0360	13.3701
2.5	-6.5806	-3.3988	-1.0773	0.0	1.0773	3.3988	6.5806	9.9862	13.3038
2.6	-6.5498	-3.3829	-1.0722	0.0	1.0722	3.3829	6.5498	9.9395	13.2415
2.7	-6.5190	-3.3670	-1.0672	0.0	1.0672	3.3670	6.5190	9.8928	13.1793
2.8	-6.4862	-3.3501	-1.0618	0.0	1.0618	3.3501	6.4862	9.8430	13.1130
2.9	-6.4419	-3.3272	-1.0546	0.0	1.0546	3.3272	6.4419	9.7759	13.0236
3.0	-6.3948	-3.3028	-1.0469	0.0	1.0469	3.3028	6.3948	9.7043	12.9282
3.1	-6.3456	-3.2774	-1.0388	0.0	1.0388	3.2774	6.3456	9.6296	12.8287
3.2	-6.2954	-3.2515	-1.0306	0.0	1.0306	3.2515	6.2954	9.5535	12.7273
3.3	-6.2452	-3.2256	-1.0224	0.0	1.0224	3.2256	6.2452	9.4774	12.6259
3.4	-6.1960	-3.2002	-1.0143	0.0	1.0143	3.2002	6.1960	9.4027	12.5264
3.5	-6.1488	-3.1758	-1.0066	0.0	1.0066	3.1758	6.1488	9.3311	12.4310
3.6	-6.1046	-3.1530	-0.9994	0.0	0.9994	3.1530	6.1046	9.2640	12.3416
3.7	-6.0669	-3.1335	-0.9932	0.0	0.9932	3.1335	6.0669	9.2067	12.2653
3.8	-6.0331	-3.1161	-0.9877	0.0	0.9877	3.1161	6.0331	9.1554	12.1970
3.9	-6.0033	-3.1007	-0.9828	0.0	0.9828	3.1007	6.0033	9.1102	12.1367
4.0	-5.9774	-3.0873	-0.9786	0.0	0.9786	3.0873	5.9774	9.0710	12.0845

TABLE 14 (continued)

NORMAL COEFFICIENT FOR AN AIR-TO-AIR MISSILE

HORIZONTAL PARAMETER = ANGLE OF ATTACK
VERTICAL PARAMETER = MACH NUMBER

	60.000	70.000	80.000	90.000	100.000	110.000	120.000
0.0	9.2265	10.2596	10.9920	11.2711	10.8563	9.7277	8.1000
0.1	9.3418	10.3878	11.1294	11.4120	10.9920	9.8493	8.2013
0.2	9.5340	10.6016	11.3584	11.6468	11.2181	10.0520	8.3700
0.3	9.8032	10.9008	11.6790	11.9756	11.5348	10.3357	8.6063
0.4	10.1492	11.2855	12.0912	12.3983	11.9419	10.7005	8.9100
0.5	10.5420	11.7224	12.5592	12.8782	12.4041	11.1147	9.2549
0.6	11.0237	12.2581	13.1332	13.4667	12.9710	11.6226	9.6778
0.7	11.6064	12.9060	13.8273	14.1784	13.6565	12.2369	10.1893
0.8	12.3020	13.6794	14.6560	15.0282	14.4750	12.9703	10.8000
0.9	13.3748	14.8724	15.9341	16.3388	15.7373	14.1014	11.7418
1.0	14.4837	16.1054	17.2551	17.6933	17.0421	15.2705	12.7153
1.1	15.5297	17.2796	18.5132	18.9334	18.2846	16.3839	13.6424
1.2	16.4539	18.2962	19.6024	20.1002	19.3603	17.3478	14.4450
1.3	16.8071	18.6890	20.0232	20.5317	19.7759	17.7202	14.7551
1.4	16.9729	18.8733	20.2207	20.7342	19.9710	17.8950	14.9006
1.5	16.9945	18.8974	20.2465	20.7606	19.9964	17.9178	14.9196
1.6	16.9152	18.8092	20.1520	20.6638	19.9031	17.8342	14.8500
1.7	16.8504	18.7371	20.0747	20.5845	19.8268	17.7658	14.7930
1.8	16.7423	18.6169	19.9459	20.4524	19.6996	17.6518	14.6981
1.9	16.6053	18.4646	19.7827	20.2851	19.5384	17.5074	14.5779
2.0	16.4539	18.2962	19.6024	20.1002	19.3603	17.3478	14.4450
2.1	16.3326	18.1613	19.4578	19.9520	19.2175	17.2199	14.3385
2.2	16.2137	18.0291	19.3161	19.8067	19.0776	17.0945	14.2341
2.3	16.0995	17.9022	19.1802	19.6673	18.9433	16.9741	14.1339
2.4	15.9926	17.7833	19.0528	19.5366	18.8175	16.8614	14.0400
2.5	15.9133	17.6951	18.9583	19.4398	18.7242	16.7778	13.9704
2.6	15.8388	17.6123	18.8696	19.3488	18.6366	16.6993	13.9050
2.7	15.7643	17.5295	18.7809	19.2578	18.5489	16.6207	13.8396
2.8	15.6850	17.4413	18.6864	19.1609	18.4556	16.5371	13.7700
2.9	15.5781	17.3224	18.5590	19.0303	18.3298	16.4244	13.6761
3.0	15.4640	17.1955	18.4230	18.8909	18.1955	16.3041	13.5759
3.1	15.3451	17.0632	18.2814	18.7456	18.0556	16.1787	13.4715
3.2	15.2237	16.9283	18.1368	18.5974	17.9128	16.0508	13.3650
3.3	15.1024	16.7934	17.9922	18.4492	17.7700	15.9228	13.2585
3.4	14.9835	16.6611	17.8505	18.3039	17.6301	15.7974	13.1541
3.5	14.8693	16.5342	17.7146	18.1644	17.4958	15.6771	13.0539
3.6	14.7624	16.4153	17.5872	18.0338	17.3700	15.5644	12.9600
3.7	14.6711	16.3138	17.4784	17.9223	17.2626	15.4681	12.8798
3.8	14.5894	16.2230	17.3811	17.8225	17.1664	15.3820	12.8081
3.9	14.5173	16.1428	17.2952	17.7344	17.0816	15.3060	12.7448
4.0	14.4549	16.0733	17.2208	17.6581	17.0081	15.2401	12.6900

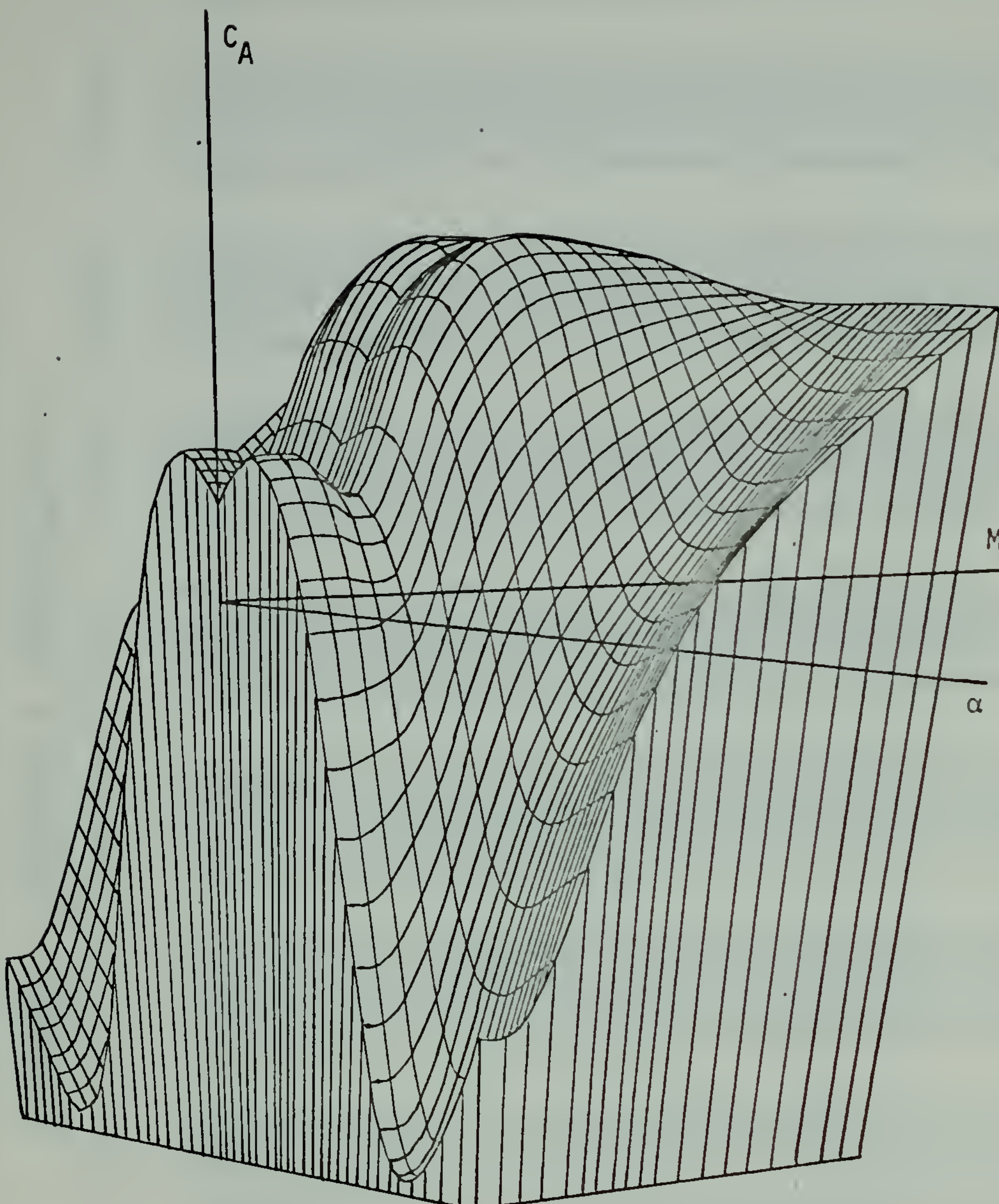

Figure 48

$C_A = f(M,\alpha)$

TABLE 15

AXIAL COEFFICIENT FOR AN AIR-TO-AIR MISSILE

HORIZONTAL PARAMETER = ANGLE OF ATTACK
VERTICAL PARAMETER = MACH NUMBER

	-120.000	-110.000	-100.000	-90.000	-80.000	-70.000	-60.000	-50.000	-40.000
0.0	-1.0584	-1.2658	-1.4288	-1.5332	-1.5270	-1.3421	-0.9512	-0.5217	-0.0932
0.1	-1.0751	-1.2863	-1.4524	-1.5587	-1.5523	-1.3641	-0.9660	-0.5287	-0.0925
0.2	-1.0735	-1.2849	-1.4512	-1.5576	-1.5513	-1.3628	-0.9642	-0.5264	-0.0897
0.3	-1.0535	-1.2616	-1.4253	-1.5301	-1.5238	-1.3383	-0.9459	-0.5148	-0.0848
0.4	-1.0150	-1.2164	-1.3747	-1.4761	-1.4700	-1.2905	-0.9109	-0.4940	-0.0780
0.5	-0.9504	-1.1375	-1.2845	-1.3787	-1.3731	-1.2063	-0.8538	-0.4665	-0.0801
0.6	-0.8705	-1.0413	-1.1756	-1.2616	-1.2564	-1.1042	-0.7823	-0.4296	-0.0758
0.7	-0.7784	-0.9326	-1.0539	-1.1315	-1.1269	-0.9894	-0.6987	-0.3794	-0.0608
0.8	-0.6771	-0.8160	-0.9252	-0.9952	-0.9910	-0.8672	-0.6052	-0.3175	-0.0305
0.9	-0.5663	-0.6985	-0.8024	-0.8689	-0.8649	-0.7471	-0.4980	-0.2244	0.0486
1.0	-0.4539	-0.5815	-0.6818	-0.7461	-0.7422	-0.6285	-0.3379	-0.1237	0.1399
1.1	-0.3441	-0.4689	-0.5669	-0.6297	-0.6260	-0.5148	-0.2797	-0.0214	0.2362
1.2	-0.2415	-0.3643	-0.4609	-0.5227	-0.5190	-0.4095	-0.1780	0.0764	0.3301
1.3	-0.1657	-0.2861	-0.3807	-0.4413	-0.4377	-0.3304	-0.1035	0.1458	0.3944
1.4	-0.0996	-0.2177	-0.3105	-0.3699	-0.3664	-0.2611	-0.0386	0.2058	0.4497
1.5	-0.0414	-0.1570	-0.2479	-0.3061	-0.3026	-0.1996	0.0183	0.2577	0.4965
1.6	0.0108	-0.1020	-0.1906	-0.2474	-0.2440	-0.1435	0.0691	0.3026	0.5355
1.7	0.0631	-0.0451	-0.1301	-0.1846	-0.1813	-0.0849	0.1191	0.3431	0.5666
1.8	0.1113	0.0081	-0.0730	-0.1250	-0.1219	-0.0299	0.1646	0.3783	0.5915
1.9	0.1553	0.0574	-0.0196	-0.0689	-0.0660	0.0213	0.2060	0.4088	0.6111
2.0	0.1953	0.1027	0.0298	-0.0168	-0.0140	0.0686	0.2432	0.4350	0.6263
2.1	0.2292	0.1412	0.0721	0.0278	0.0304	0.1088	0.2747	0.4569	0.6387
2.2	0.2600	0.1765	0.1109	0.0689	0.0714	0.1458	0.3031	0.4759	0.6482
2.3	0.2884	0.2094	0.1474	0.1076	0.1100	0.1804	0.3292	0.4927	0.6558
2.4	0.3154	0.2408	0.1823	0.1448	0.1470	0.2134	0.3539	0.5081	0.6620
2.5	0.3438	0.2738	0.2188	0.1836	0.1857	0.2481	0.3800	0.5249	0.6694
2.6	0.3716	0.3062	0.2547	0.2218	0.2238	0.2821	0.4054	0.5410	0.6761
2.7	0.3988	0.3379	0.2900	0.2594	0.2612	0.3155	0.4303	0.5564	0.6823
2.8	0.4254	0.3690	0.3247	0.2963	0.2980	0.3483	0.4545	0.5713	0.6878
2.9	0.4512	0.3992	0.3584	0.3323	0.3338	0.3801	0.4780	0.5855	0.6928
3.0	0.4764	0.4289	0.3916	0.3678	0.3692	0.4115	0.5009	0.5992	0.6972
3.1	0.5011	0.4582	0.4245	0.4029	0.4042	0.4424	0.5233	0.6121	0.7008
3.2	0.5255	0.4872	0.4571	0.4378	0.4390	0.4731	0.5452	0.6244	0.7035
3.3	0.5499	0.5167	0.4905	0.4738	0.4748	0.5044	0.5671	0.6360	0.7047
3.4	0.5740	0.5458	0.5236	0.5094	0.5103	0.5354	0.5885	0.6469	0.7051
3.5	0.5973	0.5742	0.5560	0.5444	0.5451	0.5657	0.6093	0.6572	0.7049
3.6	0.6200	0.6018	0.5876	0.5785	0.5790	0.5952	0.6293	0.6668	0.7043
3.7	0.6413	0.6279	0.6174	0.6106	0.6110	0.6230	0.6482	0.6760	0.7037
3.8	0.6618	0.6530	0.6460	0.6416	0.6419	0.6497	0.6663	0.6846	0.7028
3.9	0.6813	0.6770	0.6736	0.6714	0.6715	0.6754	0.6836	0.6926	0.7015
4.0	0.7000	0.7000	0.7000	0.7000	0.7000	0.7000	0.7000	0.7000	0.7000

TABLE 15 (continued)

AXIAL COEFFICIENT FOR AN AIR-TO-AIR MISSILE

HORIZONTAL PARAMETER = ANGLE OF ATTACK
VERTICAL PARAMETER = MACH NUMBER

	-30.000	-20.000	-10.000	0.0	10.000	20.000	30.000	40.000	50.000
0.0	0.1792	0.3169	0.3223	0.2240	0.3223	0.3169	0.1792	-0.0932	-0.5217
0.1	0.1849	0.3251	0.3306	0.2306	0.3306	0.3251	0.1849	-0.0925	-0.5287
0.2	0.1881	0.3284	0.3339	0.2337	0.3339	0.3284	0.1861	-0.0897	-0.5264
0.3	0.1886	0.3268	0.3322	0.2336	0.3322	0.3268	0.1886	-0.0848	-0.5148
0.4	0.1865	0.3202	0.3254	0.2300	0.3254	0.3202	0.1865	-0.0780	-0.4940
0.5	0.1655	0.2897	0.2946	0.2060	0.2946	0.2897	0.1655	-0.0801	-0.4665
0.6	0.1485	0.2619	0.2663	0.1854	0.2663	0.2619	0.1485	-0.0758	-0.4286
0.7	0.1418	0.2442	0.2482	0.1751	0.2482	0.2442	0.1418	-0.0608	-0.3794
0.8	0.1520	0.2442	0.2478	0.1820	0.2478	0.2442	0.1520	-0.0305	-0.3175
0.9	0.2222	0.3099	0.3133	0.2507	0.3133	0.3099	0.2222	0.0486	-0.2244
1.0	0.3076	0.3923	0.3956	0.3351	0.3956	0.3923	0.3076	0.1399	-0.1237
1.1	0.4000	0.4828	0.4861	0.4270	0.4861	0.4828	0.4000	0.2362	-0.0214
1.2	0.4915	0.5730	0.5762	0.5180	0.5762	0.5730	0.4915	0.3301	0.0764
1.3	0.5526	0.6325	0.6356	0.5786	0.6356	0.6325	0.5526	0.3944	0.1458
1.4	0.6047	0.6831	0.6862	0.6302	0.6862	0.6831	0.6047	0.4497	0.2058
1.5	0.6483	0.7251	0.7281	0.6733	0.7281	0.7251	0.6483	0.4965	0.2577
1.6	0.6836	0.7585	0.7614	0.7080	0.7614	0.7585	0.6836	0.5355	0.3026
1.7	0.7088	0.7806	0.7834	0.7321	0.7834	0.7806	0.7088	0.5666	0.3431
1.8	0.7271	0.7956	0.7983	0.7494	0.7983	0.7956	0.7271	0.5915	0.3783
1.9	0.7398	0.8048	0.8073	0.7609	0.8073	0.8048	0.7398	0.6111	0.4088
2.0	0.7480	0.8095	0.8119	0.7680	0.8119	0.8095	0.7480	0.6263	0.4350
2.1	0.7542	0.8126	0.8149	0.7732	0.8149	0.8126	0.7542	0.6387	0.4569
2.2	0.7578	0.8132	0.8154	0.7759	0.8154	0.8132	0.7578	0.6482	0.4759
2.3	0.7595	0.8119	0.8140	0.7766	0.8140	0.8119	0.7595	0.6558	0.4927
2.4	0.7599	0.8094	0.8113	0.7760	0.8113	0.8094	0.7599	0.6620	0.5081
2.5	0.7613	0.8078	0.8096	0.7764	0.8096	0.8078	0.7613	0.6694	0.5249
2.6	0.7621	0.8056	0.8073	0.7762	0.8073	0.8056	0.7621	0.6761	0.5410
2.7	0.7623	0.8027	0.8043	0.7754	0.8043	0.8027	0.7623	0.6823	0.5564
2.8	0.7618	0.7993	0.8007	0.7740	0.8007	0.7993	0.7618	0.6878	0.5713
2.9	0.7610	0.7955	0.7969	0.7722	0.7969	0.7955	0.7610	0.6928	0.5855
3.0	0.7595	0.7910	0.7922	0.7697	0.7922	0.7910	0.7595	0.6972	0.5992
3.1	0.7571	0.7856	0.7867	0.7664	0.7867	0.7856	0.7571	0.7008	0.6121
3.2	0.7537	0.7791	0.7801	0.7620	0.7801	0.7791	0.7537	0.7035	0.6244
3.3	0.7484	0.7705	0.7713	0.7556	0.7713	0.7705	0.7484	0.7047	0.6360
3.4	0.7422	0.7609	0.7616	0.7482	0.7616	0.7609	0.7422	0.7051	0.6469
3.5	0.7353	0.7507	0.7513	0.7403	0.7513	0.7507	0.7353	0.7049	0.6572
3.6	0.7281	0.7401	0.7406	0.7320	0.7406	0.7401	0.7281	0.7043	0.6668
3.7	0.7213	0.7302	0.7305	0.7242	0.7305	0.7302	0.7213	0.7037	0.6760
3.8	0.7143	0.7202	0.7204	0.7163	0.7204	0.7202	0.7143	0.7028	0.6846
3.9	0.7072	0.7101	0.7102	0.7082	0.7102	0.7101	0.7072	0.7015	0.6926
4.0	0.7000	0.7000	0.7000	0.7000	0.7000	0.7000	0.7000	0.7000	0.7000

TABLE 15 (continued)

AXIAL COEFFICIENT FOR AN AIR-TO-AIR MISSILE

HORIZONTAL PARAMETER = ANGLE OF ATTACK
VERTICAL PARAMETER = MACH NUMBER

	60.000	70.000	80.000	90.000	100.000	110.000	120.000
0.0	-0.9512	-1.3421	-1.5270	-1.5332	-1.4288	-1.2658	-1.0584
0.1	-0.9660	-1.3641	-1.5523	-1.5587	-1.4524	-1.2863	-1.0751
0.2	-0.9642	-1.3628	-1.5513	-1.5576	-1.4512	-1.2849	-1.0735
0.3	-0.9459	-1.3383	-1.5238	-1.5301	-1.4253	-1.2616	-1.0535
0.4	-0.9109	-1.2905	-1.4700	-1.4761	-1.3747	-1.2164	-1.0150
0.5	-0.8538	-1.2063	-1.3731	-1.3787	-1.2845	-1.1375	-0.9504
0.6	-0.7823	-1.1042	-1.2564	-1.2616	-1.1756	-1.0413	-0.8705
0.7	-0.6987	-0.9894	-1.1269	-1.1315	-1.0539	-0.9326	-0.7784
0.8	-0.6052	-0.8672	-0.9910	-0.9952	-0.9252	-0.8160	-0.6771
0.9	-0.4980	-0.7471	-0.8649	-0.8689	-0.8024	-0.6985	-0.5663
1.0	-0.3879	-0.6285	-0.7422	-0.7461	-0.6818	-0.5815	-0.4539
1.1	-0.2797	-0.5148	-0.6260	-0.6297	-0.5669	-0.4689	-0.3441
1.2	-0.1780	-0.4095	-0.5190	-0.5227	-0.4609	-0.3643	-0.2415
1.3	-0.1035	-0.3304	-0.4377	-0.4413	-0.3807	-0.2861	-0.1657
1.4	-0.0386	-0.2611	-0.3664	-0.3699	-0.3105	-0.2177	-0.0996
1.5	0.0183	-0.1996	-0.3026	-0.3061	-0.2479	-0.1570	-0.0414
1.6	0.0691	-0.1435	-0.2440	-0.2474	-0.1906	-0.1020	0.0108
1.7	0.1191	-0.0849	-0.1813	-0.1846	-0.1301	-0.0451	0.0631
1.8	0.1646	-0.0299	-0.1219	-0.1250	-0.0730	0.0081	0.1113
1.9	0.2060	0.0213	-0.0660	-0.0689	-0.0196	0.0574	0.1553
2.0	0.2432	0.0686	-0.0140	-0.0168	0.0298	0.1027	0.1953
2.1	0.2747	0.1083	0.0304	0.0278	0.0721	0.1412	0.2292
2.2	0.3031	0.1458	0.0714	0.0689	0.1109	0.1765	0.2600
2.3	0.3292	0.1804	0.1100	0.1076	0.1474	0.2094	0.2884
2.4	0.3539	0.2134	0.1470	0.1448	0.1823	0.2408	0.3154
2.5	0.3800	0.2481	0.1857	0.1836	0.2188	0.2738	0.3438
2.6	0.4054	0.2821	0.2238	0.2218	0.2547	0.3062	0.3716
2.7	0.4303	0.3155	0.2612	0.2594	0.2900	0.3379	0.3988
2.8	0.4545	0.3483	0.2980	0.2963	0.3247	0.3690	0.4254
2.9	0.4780	0.3801	0.3338	0.3323	0.3584	0.3992	0.4512
3.0	0.5009	0.4115	0.3692	0.3678	0.3916	0.4289	0.4764
3.1	0.5233	0.4424	0.4042	0.4029	0.4245	0.4582	0.5011
3.2	0.5452	0.4731	0.4390	0.4378	0.4571	0.4872	0.5255
3.3	0.5671	0.5044	0.4748	0.4738	0.4905	0.5167	0.5499
3.4	0.5885	0.5354	0.5103	0.5094	0.5236	0.5458	0.5740
3.5	0.6093	0.5657	0.5451	0.5444	0.5560	0.5742	0.5973
3.6	0.6293	0.5952	0.5790	0.5785	0.5876	0.6018	0.6200
3.7	0.6482	0.6230	0.6110	0.6106	0.6174	0.6279	0.6413
3.8	0.6663	0.6497	0.6419	0.6416	0.6460	0.6530	0.6618
3.9	0.6836	0.6754	0.6715	0.6714	0.6736	0.6770	0.6813
4.0	0.7000	0.7000	0.7000	0.7000	0.7000	0.7000	0.7000

APPENDIX C

INTERPOLATION

In the optimization problems solved herein the aerodynamic data is given in tabular form. The dependent variable D is given as a function of two independent variables M and α in all cases. Excerpts from the tables used in computation are presented in Appendix B.

For a given M and α quantities D, $\frac{\partial D}{\partial M}$, $\frac{\partial D}{\partial \alpha}$, $\frac{\partial^2 D}{\partial M^2}$, $\frac{\partial^2 D}{\partial \alpha^2}$, and $\frac{\partial^2 D}{\partial M \partial \alpha}$ are required by the optimization algorithm. Parabolic interpolation is used to obtain these quantities. In this Appendix parabolic interpolation for two independent variables is derived.

1. Parabolic Interpolation in the Plane

To apply parabolic interpolation to a tabular function of two independent variables the nearest point in the tables to the given point (M,α) must first be found. It is assumed that the tabular data is given at constant intervals ΔM and $\Delta\alpha$ in the independent variables. The nearest point given in the tables and the surrounding eight points are required in the interpolation and are shown in Figure 49. The parameters θ and ϕ locate the point (M,α) from the nearest tabular point (M_s,α_s). If (M_s,α_s) is the nearest point then

$$-\frac{1}{2} \leq \phi \leq \frac{1}{2} \tag{C.1}$$

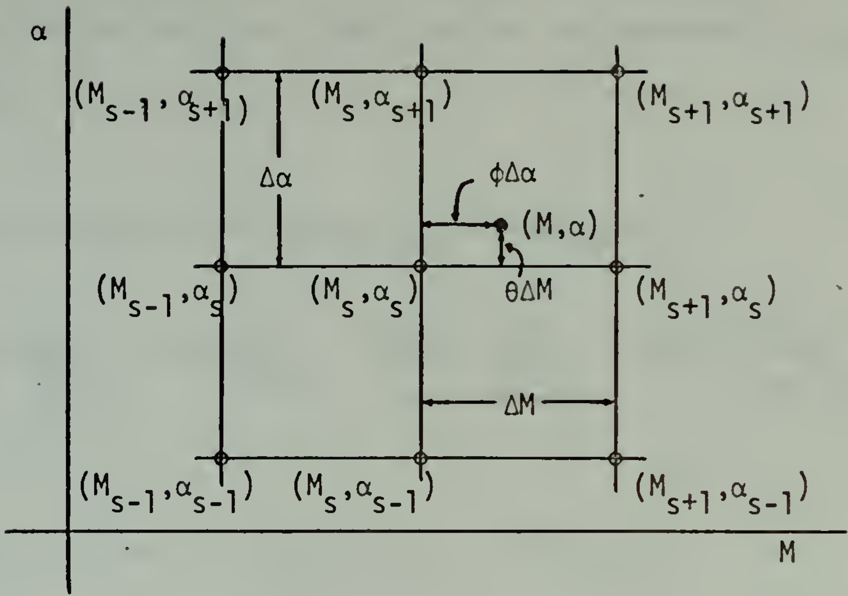

Figure 49

and

$$-\frac{1}{2} \leq \theta \leq \frac{1}{2} \tag{C.2}$$

The inequalities (C.1) and (C.2) hold unless the nearest point (M_s,α_s) is on a border of the table. In this case (M_s,α_s) is chosen one point in from the border. The parameters θ and ϕ then satisfy

$$-1 \leq \phi \leq 1 \tag{C.3}$$

and

$$-1 \leq \theta \leq 1 \tag{C.4}$$

Writing Taylor series expansions including up to second order terms for the eight points surrounding (M_s,α_s), we obtain

$$D(M_s+\Delta M,\alpha_s+\Delta\alpha) = D(M_{s+1},\alpha_{s+1}) \approx D(M_s,\alpha_s) \tag{C.5}$$

$$+ \Delta M \left.\frac{\partial D}{\partial M}\right|_s + \Delta\alpha \left.\frac{\partial D}{\partial \alpha}\right|_s + \frac{(\Delta M)^2}{2} \left.\frac{\partial^2 D}{\partial M^2}\right|_s + \frac{(\Delta\alpha)^2}{2} \left.\frac{\partial^2 D}{\partial \alpha^2}\right|_s + \Delta M\Delta\alpha \left.\frac{\partial^2 D}{\partial M\partial\alpha}\right|_s$$

$$D(M_s-\Delta M,\alpha_s-\Delta\alpha) = D(M_{s-1},\alpha_{s-1}) \approx D(M_s,\alpha_s) \tag{C.6}$$

$$- \Delta M \left.\frac{\partial D}{\partial M}\right|_s - \Delta\alpha \left.\frac{\partial D}{\partial \alpha}\right|_s + \frac{(\Delta M)^2}{2} \left.\frac{\partial^2 D}{\partial M^2}\right|_s + \frac{(\Delta\alpha)^2}{2} \left.\frac{\partial^2 D}{\partial \alpha^2}\right|_s + \Delta M\Delta\alpha \left.\frac{\partial^2 D}{\partial M\partial\alpha}\right|_s$$

$$D(M_s-\Delta M,\alpha_s+\Delta\alpha) = D(M_{s-1},\alpha_{s+1}) \approx D(M_s,\alpha_s) \tag{C.7}$$

$$- \Delta M \left.\frac{\partial D}{\partial M}\right|_s + \Delta\alpha \left.\frac{\partial D}{\partial \alpha}\right|_s + \frac{(\Delta M)^2}{2} \left.\frac{\partial^2 D}{\partial M^2}\right|_s + \frac{(\Delta\alpha)^2}{2} \left.\frac{\partial^2 D}{\partial \alpha^2}\right|_s - \Delta M\Delta\alpha \left.\frac{\partial^2 D}{\partial M\partial\alpha}\right|_s$$

$$D(M_s+\Delta M,\alpha_s-\Delta\alpha) = D(M_{s+1},\alpha_{s-1}) \approx D(M_s,\alpha_s) \tag{C.8}$$

$$+ \Delta M \left.\frac{\partial D}{\partial M}\right|_s - \Delta\alpha \left.\frac{\partial D}{\partial \alpha}\right|_s + \frac{(\Delta M)^2}{2} \left.\frac{\partial^2 D}{\partial M^2}\right|_s + \frac{(\Delta\alpha)^2}{2} \left.\frac{\partial^2 D}{\partial \alpha^2}\right|_s - \Delta M\Delta\alpha \left.\frac{\partial^2 D}{\partial M\partial\alpha}\right|_s$$

$$D(M_s+\Delta M,\alpha_s) = D(M_{s+1},\alpha_s) \approx D(M_s,\alpha_s) + \Delta M \left.\frac{\partial D}{\partial M}\right|_s + \frac{(\Delta M)^2}{2} \left.\frac{\partial^2 D}{\partial M^2}\right|_s \tag{C.9}$$

$$D(M_s-\Delta M,\alpha_s) = D(M_{s-1},\alpha_s) \approx D(M_s,\alpha_s) - \Delta M \left.\frac{\partial D}{\partial M}\right|_s + \frac{(\Delta M)^2}{2} \left.\frac{\partial^2 D}{\partial M^2}\right|_s \tag{C.10}$$

$$D(M_s,\alpha_s+\Delta\alpha) = D(M_s,\alpha_{s+1}) \approx D(M_s,\alpha_s) + \Delta\alpha \left.\frac{\partial D}{\partial \alpha}\right|_s + \frac{(\Delta\alpha)^2}{2} \left.\frac{\partial^2 D}{\partial \alpha^2}\right|_s \tag{C.11}$$

$$D(M_s,\alpha_s-\Delta\alpha) = D(M_s,\alpha_{s-1}) \approx D(M_s,\alpha_s) - \Delta\alpha \left.\frac{\partial D}{\partial \alpha}\right|_s + \frac{(\Delta\alpha)^2}{2} \left.\frac{\partial^2 D}{\partial \alpha^2}\right|_s \tag{C.12}$$

Subtracting equation (C.10) from equation (C.9), we obtain

$$D(M_{s+1},\alpha_s) - D(M_{s-1},\alpha_s) \approx 2\Delta M \left.\frac{\partial D}{\partial M}\right|_s$$

or

$$\left.\frac{\partial D}{\partial M}\right|_s \approx \frac{D(M_{s+1},\alpha_s) - D(M_{s-1},\alpha_s)}{2\Delta M} \quad . \tag{C.13}$$

Subtracting equation (C.12) from équation (C.11), we obtain

$$D(M_s,\alpha_{s+1}) - D(M_s,\alpha_{s-1}) \approx 2\Delta\alpha \left.\frac{\partial D}{\partial \alpha}\right|_s$$

or

$$\left.\frac{\partial D}{\partial \alpha}\right|_s \quad \frac{D(M_s,\alpha_{s+1}) - D(M_s,\alpha_{s-1})}{2\Delta\alpha} \quad . \tag{C.14}$$

Adding equation (C.10) to equation (C.9), we obtain

$$D(M_{s+1},\alpha_s) + D(M_{s-1},\alpha_s) \approx 2D(M_s,\alpha_s) + (\Delta M)^2 \left.\frac{\partial^2 D}{\partial M^2}\right|_s$$

or

$$\left.\frac{\partial^2 D}{\partial M^2}\right|_s \approx \frac{D(M_{s+1},\alpha_s) - 2D(M_s,\alpha_s) + D(M_{s-1},\alpha_s)}{(\Delta M)^2} \qquad (C.15)$$

Adding equation (C.12) to equation (C.11), we obtain

$$D(M_s,\alpha_{s+1}) + D(M_s,\alpha_{s-1}) \approx 2D(M_s,\alpha_s) + (\Delta\alpha)^2 \left.\frac{\partial^2 D}{\partial \alpha^2}\right|_s$$

or

$$\left.\frac{\partial^2 D}{\partial \alpha^2}\right|_s \approx \frac{D(M_s,\alpha_{s+1}) - 2D(M_s,\alpha_s) + D(M_s,\alpha_{s-1})}{(\Delta\alpha)^2} \qquad (C.16)$$

Subtracting equation (C.7) plus equation (C.8) from equation (C.5) plus equation (C.6), we obtain

$$D(M_{s+1},\alpha_{s+1}) + D(M_{s-1},\alpha_{s-1}) - D(M_{s-1},\alpha_{s+1}) - D(M_{s+1},\alpha_{s-1}) \approx 4\Delta M\Delta\alpha \left.\frac{\partial^2 D}{\partial M\partial\alpha}\right|_s \qquad (C.17)$$

or

$$\left.\frac{\partial^2 D}{\partial M\partial\alpha}\right|_s \approx \frac{D(M_{s+1},\alpha_{s+1}) + D(M_{s-1},\alpha_{s-1}) - D(M_{s-1},\alpha_{s+1}) - D(M_{s+1},\alpha_{s-1})}{4\Delta M\Delta\alpha}$$

A Taylor series is written for the point (M,α). Using equations (C.13), C.14), (C.15), (C.16), and (C.17), we may reduce this series to

$$D(M_s+\theta\Delta M,\alpha_s+\phi\Delta\alpha) = D(M,\alpha) \approx D(M_s,\alpha_s) + \frac{\theta}{2}[D(M_{s+1},\alpha_s) - D(M_{s-1},\alpha_s)]$$

$$+ \frac{\phi}{2}[D(M_s,\alpha_{s+1})-D(M_s,\alpha_{s-1})] + \frac{\theta^2}{2}[D(M_{s+1},\alpha_s)-2D(M_s,\alpha_s)+D(M_{s-1},\alpha_s)]$$

$$+ \frac{\phi^2}{2}[D(M_s,\alpha_{s+1})+D(M_s,\alpha_{s-1})-2D(M_s,\alpha_s)] \tag{C.18}$$

$$+ \frac{\theta\phi}{4}[D(M_{s+1},\alpha_{s+1})+D(M_{s-1},\alpha_{s-1})-D(M_{s-1},\alpha_{s+1})-D(M_{s+1},\alpha_{s-1})] \; .$$

Rearranging, we have

$$D(M,\alpha) \approx \frac{\theta\phi}{4} D(M_{s-1},\alpha_{s-1}) + \frac{\phi(\phi-1)}{2} D(M_s,\alpha_{s-1})$$

$$- \frac{\theta\phi}{4} D(M_{s+1},\alpha_{s-1}) + \frac{\theta(\theta+1)}{2} D(M_{s+1},\alpha_s)$$

$$+ \frac{\theta\phi}{4} D(M_{s+1},\alpha_{s+1}) + \frac{\phi(\phi+1)}{2} D(M_s,\alpha_{s+1}) \tag{C.19}$$

$$- \frac{\theta\phi}{4} D(M_{s-1},\alpha_{s+1}) + \frac{\theta(\theta-1)}{2} D(M_{s-1},\alpha_s)$$

$$+ (1-\theta^2-\phi^2) D(M_s,\alpha_s) \; .$$

Equation (C.19) is the expression used to interpolate for the value of D in terms of the surrounding none tabular points. To obtain expressions for the required partial derivatives, observe that

$$M = M_s + \theta \Delta M \tag{C.20}$$

and

$$\alpha = \alpha_s + \phi \Delta\alpha \quad . \tag{C.21}$$

Therefore,

$$\frac{d\theta}{dM} = \frac{1}{\Delta M} \tag{C.22}$$

and

$$\frac{d\phi}{d\alpha} = \frac{1}{\Delta\alpha} \quad . \tag{C.23}$$

The chain rule for partial derivatives yields

$$\frac{\partial D}{\partial M}\,(M_s+\theta\Delta M,\alpha_s+\phi\Delta\alpha) = \frac{\partial D}{\partial M}\,(M,\alpha) = \frac{\partial D(M,\alpha)}{\partial\theta}\,\frac{\partial\theta}{\partial M} \quad . \tag{C.24}$$

Taking the partial derivative of equation (C.19) with respect to θ, we obtain

$$\frac{\partial D}{\partial M}(M,\alpha) = \frac{1}{\Delta M}\Big[\frac{\phi}{4} D(M_{s-1},\alpha_{s-1}) - \frac{\phi}{4} D(M_{s+1},\alpha_{s-1}) + \frac{2\theta+1}{2} D(M_{s+1},\alpha_s)$$

$$+ \frac{\phi}{4} D(M_{s+1},\alpha_{s+1}) - \frac{\phi}{4} D(M_{s-1},\alpha_{s+1}) + \frac{2\theta-1}{2} D(M_{s-1},\alpha_s) \qquad (C.25)$$

$$- 2\theta\, D(M_s,\alpha_s)\Big] \quad .$$

Using similar procedures, we may derive the remaining expressions,

$$\frac{\partial D}{\partial \alpha}(M,\alpha) = \frac{1}{\Delta \alpha}\Big[\frac{\theta}{4} D(M_{s-1},\alpha_{s-1}) + \frac{2\phi-1}{2} D(M_s,\alpha_{s-1}) - \frac{\theta}{4} D(M_{s+1},\alpha_{s-1})$$

$$+ \frac{\theta}{4} D(M_{s+1},\alpha_{s+1}) + \frac{2\phi+1}{2} D(M_s,\alpha_{s+1}) - \frac{\theta}{4} D(M_{s-1},\alpha_{s+1}) \qquad (C.26)$$

$$- 2\phi\, D(M_s,\alpha_s)\Big]$$

$$\frac{\partial^2 D}{\partial M^2}(M,\alpha) = \frac{1}{(\Delta M)^2}\left[D(M_{s+1},\alpha_s) - 2D(M_s,\alpha_s) + D(M_{s-1},\alpha_s)\right] \qquad (C.27)$$

$$\frac{\partial^2 D}{\partial \alpha^2}(M,\alpha) = \frac{1}{(\Delta \alpha)^2}\left[D(M_s,\alpha_{s-1}) - 2D(M_s,\alpha_s) + D(M_s,\alpha_{s+1})\right] \qquad (C.28)$$

$$\frac{\partial^2 D}{\partial M \partial \alpha}(M,\alpha) = \frac{1}{4\Delta M \Delta \alpha}\Big[D(M_{s-1},\alpha_{s-1}) - D(M_{s+1},\alpha_{s-1}) + D(M_{s+1},\alpha_{s+1})$$

$$- D(M_{s-1},\alpha_{s+1})\Big] \qquad (C.29)$$

APPENDIX D

EMPIRICAL RELATIONS

In the problem treated in Section VI empirical relations are used for

$$\sigma = f(H), \tag{D.1}$$

$$a = f(H), \tag{D.2}$$

and

$$M_M = f(H) \tag{D.3}$$

where the parameters are air density ratio (σ), speed of sound (a), maximum Mach number (M_M), and altitude (H). The air density ratio is defined as

$$\sigma \overset{\Delta}{=} \frac{\rho}{\rho_o} \tag{D.4}$$

where σ is sea level standard day density. This Appendix presents these empirical relations and compares the values obtained from these relations with standard atmospheric conditions.

1. Air Density Ratio

The empirical relation used for air density ratio is

$$\sigma = e^{-c_1 h} + c_3 h^{-c_2 h} \tag{D.5}$$

where

$$h = \frac{H}{H_L} \tag{D.6}$$

and

$$H_L = 36{,}089 \text{ ft.} \tag{D.7}$$

$$c_1 = 1.54100 \tag{D.8}$$

$$c_2 = 1.80445 \tag{D.9}$$

$$c_3 = 0.4130 \tag{D.10}$$

Figure 50 is a plot of the values of σ obtained from equation (D.5) compared to those obtained from standard atmospheric tables.

2. Speed of Sound

The empirical relation used for the speed of sound is

$$a = a_o(1-c_7h) \quad , \quad h < 1 \tag{D.11}$$

$$= 971 \text{ ft./sec.} \quad , \quad h \geq 1 \tag{D.12}$$

where the parameter a_o is the speed of sound at sea level on a standard day; that is

$$a_o = 1116.89 \text{ ft./sec.} \tag{D.13}$$

and

$$c_7 = 0.1331 \tag{D.14}$$

Figure 51 is a plot of a vs. H. The expressions (D.11) and (D.12) duplicate exactly the values obtained from standard atmospheric tables.

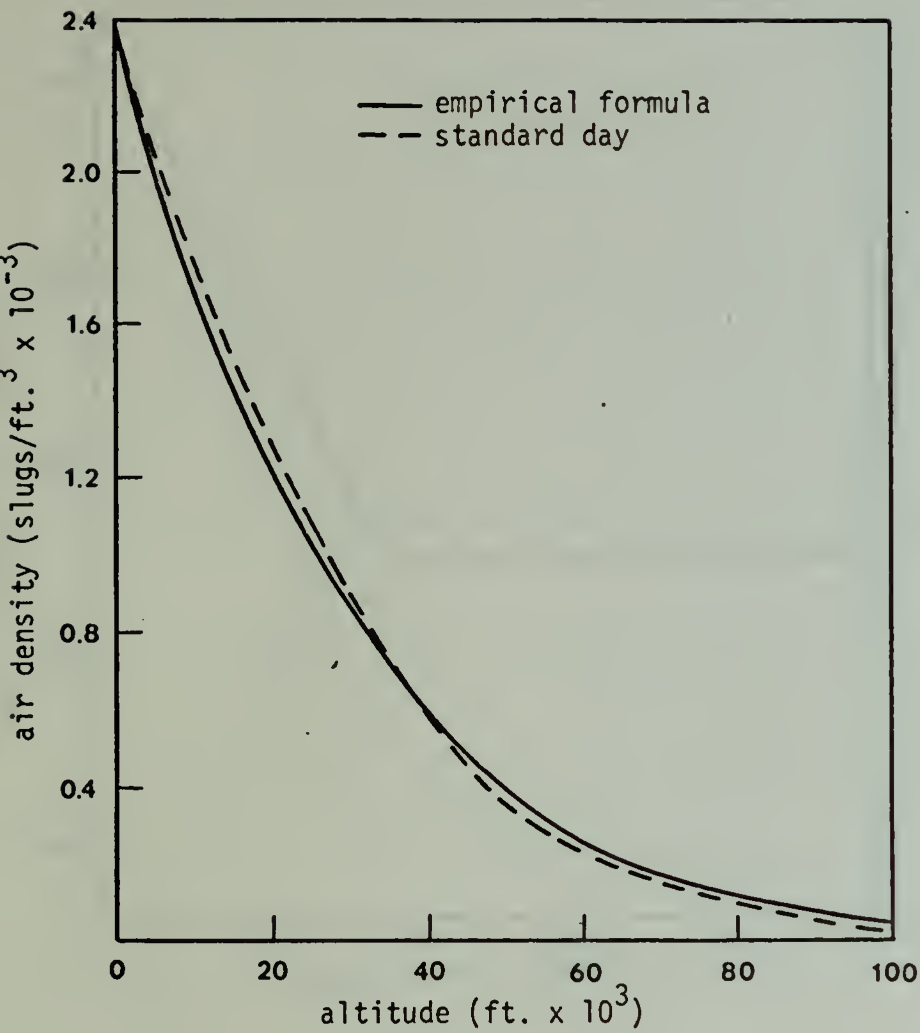

Figure 50

Air density vs. altitude

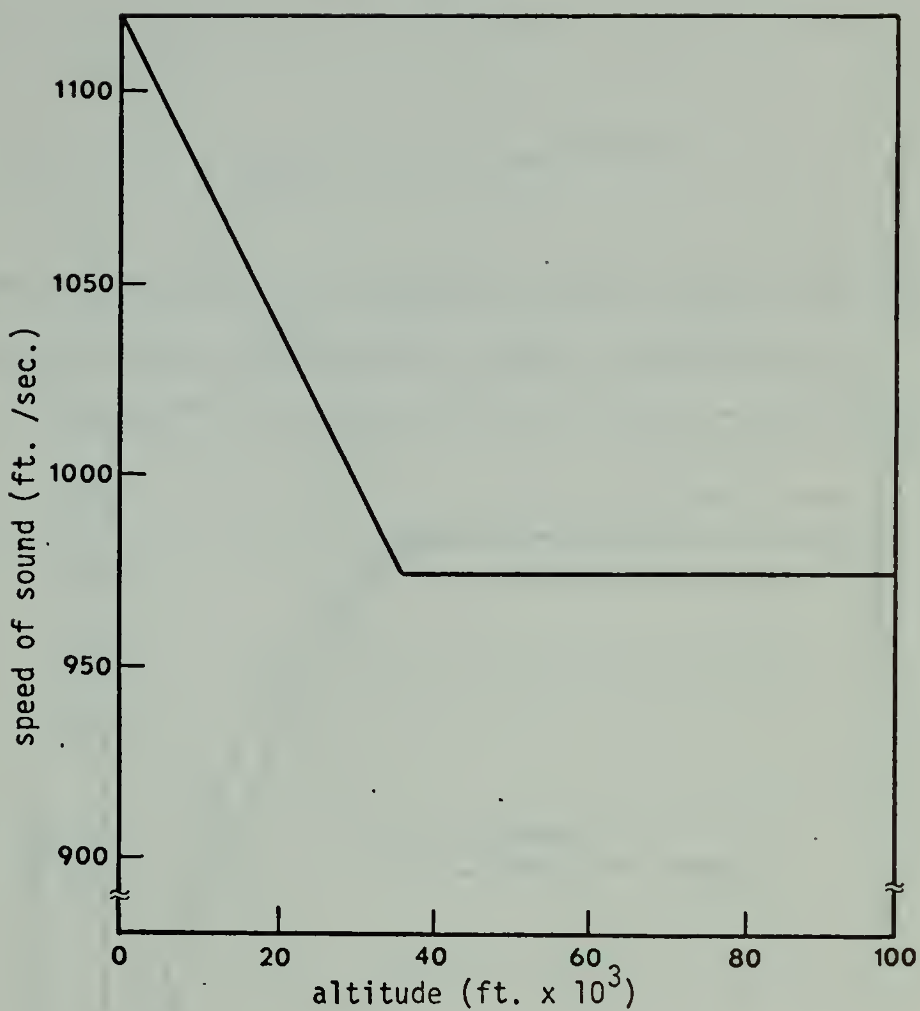

Figure 51

Speed of sound vs. altitude

3. Maximum Mach Number

The empirical relation used for the maximum Mach number of the aircraft for the problem solved in Section VI is

$$M_M = 2.1 - 1.1e^{-2.4h} \qquad \text{(D.15)}$$

Figure 52 is a plot of equation (E.9) along with the actual restrictions of the aircraft under consideration.

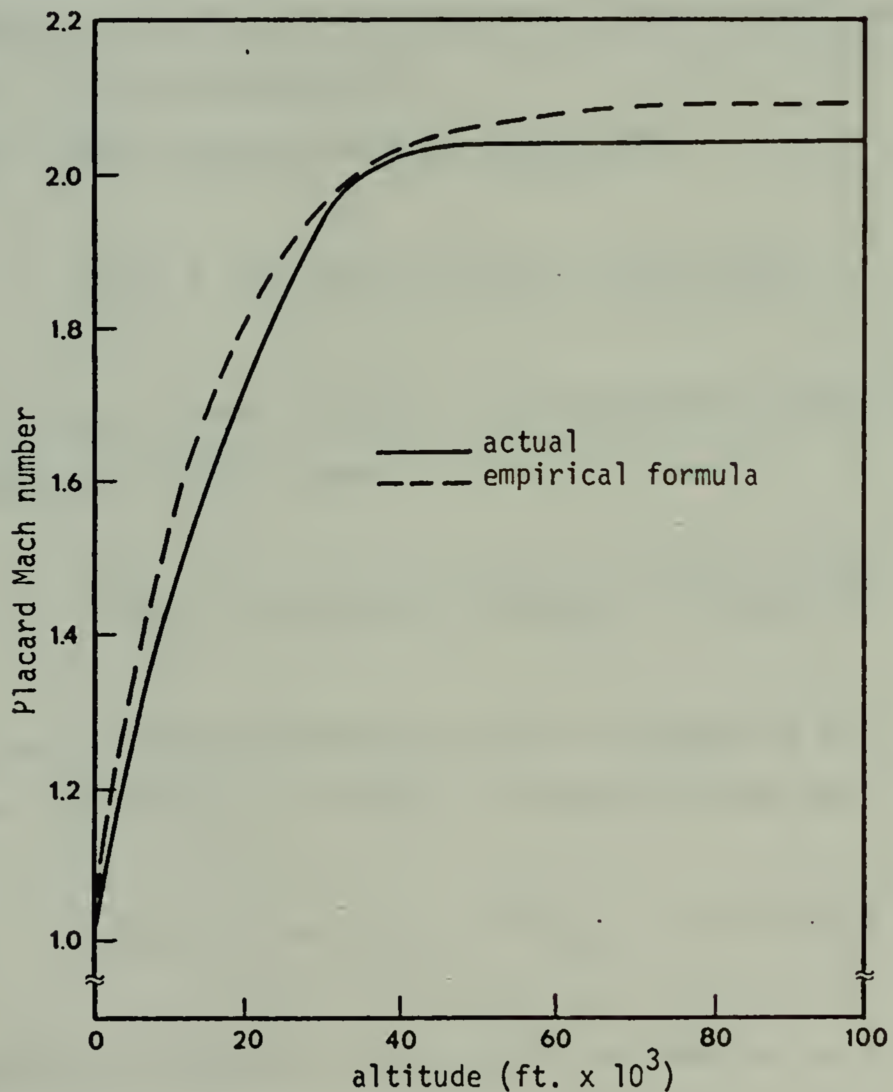

Figure 52
Placard Mach number vs. altitude

APPENDIX E

A CONVEXITY THEOREM

In this Appendix the following theorem on convexity is proved.

Theorem 1: If $f(\underset{\sim}{x})$ is convex on R^n where $\underset{\sim}{x} \varepsilon R^n$, and $f \geq 0$, then $f^K(\underset{\sim}{x})$ is convex on R^n where K is any positive integer.

This theorem is proved by mathematical induction. First, the following theorem is proved.

Theorem 2: If $f(\underset{\sim}{x})$ is convex on R^n where $\underset{\sim}{x} \varepsilon R^n$, and $f \geq 0$, then $f^2(\underset{\sim}{x})$ is convex on R^n.

Proof: The function $f(\underset{\sim}{x})$ is convex if

$$f[\lambda \underset{\sim}{x}_2 + (1-\lambda)\underset{\sim}{x}_1] \leq \lambda f(\underset{\sim}{x}_2) + (1-\lambda)f(\underset{\sim}{x}_1) \qquad \text{(E.1)}$$

for all $\underset{\sim}{x}_1$, $\underset{\sim}{x}_2$ and $\lambda \varepsilon [0,1]$. Squaring both sides of inequality (E.1) we have

$$f^2[\lambda \underset{\sim}{x}_2 + (1-\lambda)\underset{\sim}{x}_1] \leq [\lambda f(\underset{\sim}{x}_2) + (1-\lambda)f(\underset{\sim}{x}_1)]^2 \ . \qquad \text{(E.2)}$$

The sense of the inequality (E.2) is retained as $f \geq 0$. To prove that $f^2(\underset{\sim}{x})$ is convex, it must be shown that

$$f^2[\lambda \underset{\sim}{x}_2 + (1-\lambda)\underset{\sim}{x}_1] \leq \lambda f^2(\underset{\sim}{x}_2) + (1-\lambda)f^2(\underset{\sim}{x}_1) \ . \qquad \text{(E.3)}$$

Observing inequality (E.2), (E.3) is seen to be a true inequality if it can be shown that

$$[\lambda f(\underset{\sim}{x}_2) + (1-\lambda)f(\underset{\sim}{x}_1)]^2 \leq \lambda f^2(\underset{\sim}{x}_2) + (1-\lambda)f^2(\underset{\sim}{x}_1) \ . \qquad (E.4)$$

To show that inequality (E.4) is true, we proceed as follows. Since $\lambda \varepsilon [0,1]$, it is true that

$$\lambda[f(\underset{\sim}{x}_2) - f(\underset{\sim}{x}_1)]^2 \leq [f(\underset{\sim}{x}_2) - f(\underset{\sim}{x}_1)]^2 \ . \qquad (E.5)$$

Expanding inequality (E.5), we have

$$\lambda[f(\underset{\sim}{x}_2 - f(\underset{\sim}{x}_1)]^2 \leq f^2(\underset{\sim}{x}_2) - 2f(\underset{\sim}{x}_2)f(\underset{\sim}{x}_1) + f^2(\underset{\sim}{x}_1) \ . \qquad (E.6)$$

Rearranging inequality (E.6), we have

$$\lambda[f(\underset{\sim}{x}_2) - f(\underset{\sim}{x}_1)]^2 + 2f(\underset{\sim}{x}_2)f(\underset{\sim}{x}_1) - f^2(\underset{\sim}{x}_1) \leq f^2(\underset{\sim}{x}_2) . \qquad (E.7)$$

Subtracting $f^2(\underset{\sim}{x}_1)$ from both sides, we obtain

$$\lambda[f(\underset{\sim}{x}_2) - f(\underset{\sim}{x}_1)]^2 + 2f(\underset{\sim}{x}_1)[f(\underset{\sim}{x}_2) - f(\underset{\sim}{x}_1)] \leq f^2(\underset{\sim}{x}_2) - f^2(\underset{\sim}{x}_1) \ . \qquad (E.8)$$

Multiplying inequality (E.8) by λ , we have

$$\lambda^2 f^2(\underset{\sim}{x}_2) - 2\lambda^2 f(\underset{\sim}{x}_2)f(\underset{\sim}{x}_1) + \lambda^2 f^2(\underset{\sim}{x}_1) + 2\lambda f(\underset{\sim}{x}_1)f(\underset{\sim}{x}_2) \qquad (E.9)$$
$$- 2\lambda f^2(\underset{\sim}{x}_1) \leq \lambda f^2(\underset{\sim}{x}_2) - \lambda f^2(\underset{\sim}{x}_1) \ .$$

Adding $f^2(\underset{\sim}{x}_1)$ to both sides of inequality (E.9), we obtain

$$\lambda^2 f^2(\underset{\sim}{x}_2) - 2\lambda^2 f(\underset{\sim}{x}_2) f(\underset{\sim}{x}_1) + 2\lambda f(\underset{\sim}{x}_1) f(\underset{\sim}{x}_2) + f^2(\underset{\sim}{x}_1)$$
$$-2\lambda f^2(\underset{\sim}{x}_1) + \lambda^2 f^2(\underset{\sim}{x}_1) \leq \lambda f^2(\underset{\sim}{x}_2) - \lambda f^2(\underset{\sim}{x}_1) + f^2(\underset{\sim}{x}_1) \ . \tag{E.10}$$

Simplifying inequality (E.10), we obtain

$$[\lambda f(\underset{\sim}{x}_2) + (1-\lambda) f(\underset{\sim}{x}_1)]^2 \leq \lambda f^2(\underset{\sim}{x}_2) + (1-\lambda) f^2(\underset{\sim}{x}_1) \ . \tag{E.11}$$

This is the inequality we set out to show. The theorem is proved.

Second, the following theorem is proved.

<u>Theorem 3:</u> If $f^K(\underset{\sim}{x})$ is convex on R^n where $\underset{\sim}{x} \varepsilon R^n$, and $f \geq 0$, then $f^{K+1}(\underset{\sim}{x})$ is convex on R^n.

<u>Proof:</u> It has already been shown that if $f(\underset{\sim}{x})$ is convex and $f \geq 0$, then $f^2(\underset{\sim}{x})$ is convex. It is now assumed that

$$f^K[\lambda \underset{\sim}{x}_2 + (1-\lambda)\underset{\sim}{x}_1] \leq \lambda f^K(\underset{\sim}{x}_2) + (1-\lambda) f^K(\underset{\sim}{x}_1) \quad . \tag{E.12}$$

Multiplying both sides of inequality (E.12) by $f[\lambda \underset{\sim}{x}_2 + (1-\lambda)\underset{\sim}{x}_1]$ a positive quantity, we obtain

$$f^{K+1}[\lambda \underset{\sim}{x}_2 + (1-\lambda)\underset{\sim}{x}_1] \leq [\lambda f^K(\underset{\sim}{x}_2) + (1-\lambda) f^K(\underset{\sim}{x}_1)]\{f[\lambda \underset{\sim}{x}_2 + (1-\lambda)\underset{\sim}{x}_1]\} \ . \tag{E.13}$$

Substituting the expression (E.1) into inequality (E.13), we have

$$f^{K+1}[\lambda \underset{\sim}{x}_2+(1-\lambda)\underset{\sim}{x}_1] \le [\lambda f^K(\underset{\sim}{x}_2)+(1-\lambda)f^K(\underset{\sim}{x}_1)][\lambda f(\underset{\sim}{x}_2)+(1-\lambda)f(\underset{\sim}{x}_1)]. \tag{E.14}$$

To prove that $f^{K+1}(\underset{\sim}{x})$ is convex it must be shown that

$$f^{K+1}[\lambda \underset{\sim}{x}_2+(1-\lambda)\underset{\sim}{x}_1] \le \lambda f^{K+1}(\underset{\sim}{x}_2) + (1-\lambda)f^{K+1}(\underset{\sim}{x}_1) . \tag{E.15}$$

Observing inequality (E.14), (E.15) is seen to be a true inequality if it can be shown that

$$[\lambda f^K(\underset{\sim}{x}_2)+(1-\lambda)f^K(\underset{\sim}{x}_1)][\lambda f(\underset{\sim}{x}_2)+(1-\lambda)f(\underset{\sim}{x}_1)] \le \lambda f^{K+1}(\underset{\sim}{x}_2) + (1-\lambda)f^{K+1}(\underset{\sim}{x}_1) . \tag{E.16}$$

To show that inequality (E.16) is true we proceed as follows. The expression

$$[f^K(\underset{\sim}{x}_2) - f^K(\underset{\sim}{x}_1)][f(\underset{\sim}{x}_2) - f(\underset{\sim}{x}_1)] \tag{E.17}$$

is always a positive number because the signs of the expressions in parentheses in expression (E.17) must be the same. The following inequality holds

$$\lambda[f^K(\underset{\sim}{x}_2)-f^K(\underset{\sim}{x}_1)][f(\underset{\sim}{x}_2)-f(\underset{\sim}{x}_1)] \le [f^K(\underset{\sim}{x}_2)-f^K(\underset{\sim}{x}_1)][f(\underset{\sim}{x}_2)-f(\underset{\sim}{x}_1)]. \tag{E.18}$$

Expanding and multiplying by λ, we obtain

$$\lambda^2[f^{K+1}(\underset{\sim}{x}_2)-f^K(\underset{\sim}{x}_1)f(\underset{\sim}{x}_2)-f(\underset{\sim}{x}_1)f^K(\underset{\sim}{x}_2)+f^{K+1}(\underset{\sim}{x}_1)] \leq \lambda[f^{K+1}(\underset{\sim}{x}_2)-f^K(\underset{\sim}{x}_1)f(\underset{\sim}{x}_2)-f(\underset{\sim}{x}_1)f^K(\underset{\sim}{x}_2)+f^{K+1}(\underset{\sim}{x}_1)] \; . \tag{E.19}$$

Rearranging inequality (E.19) and subtracting $2\lambda f^{K+1}(\underset{\sim}{x}_1)$ from both sides, we obtain

$$\lambda^2[f^{K+1}(\underset{\sim}{x}_2)-f^K(\underset{\sim}{x}_1)f(\underset{\sim}{x}_2)-f(\underset{\sim}{x}_1)f^K(\underset{\sim}{x}_2)+f^{K+1}(\underset{\sim}{x}_1)] + \lambda[f^K(\underset{\sim}{x}_1)f(\underset{\sim}{x}_2)+f(\underset{\sim}{x}_1)f^K(\underset{\sim}{x}_2)-2f^{K+1}(\underset{\sim}{x}_1)] \leq \lambda[f^{K+1}(\underset{\sim}{x}_2)-f^{K+1}(\underset{\sim}{x}_1)]. \tag{E.20}$$

Further expansion and rearranging yields

$$\lambda^2 f^{K+1}(\underset{\sim}{x}_2)+\lambda f^K(\underset{\sim}{x}_1)f(\underset{\sim}{x}_2)-\lambda^2 f^K(\underset{\sim}{x}_1)f(\underset{\sim}{x}_2)+\lambda f(\underset{\sim}{x}_1)f^K(\underset{\sim}{x}_2)-\lambda^2 f(\underset{\sim}{x}_1)f^K(\underset{\sim}{x}_2) - 2\lambda f^{K+1}(\underset{\sim}{x}_1)+\lambda^2 f^{K+1}(\underset{\sim}{x}_1) \leq \lambda f^{K+1}(\underset{\sim}{x}_2)-\lambda f^{K+1}(\underset{\sim}{x}_1) \; . \tag{E.21}$$

Adding $f^{K+1}(x_1)$ to both sides and rearranging further, we have

$$\lambda^2 f^{K+1}(\underset{\sim}{x}_2)+ \lambda(1-\lambda)f^K(\underset{\sim}{x}_1)f(\underset{\sim}{x}_2)+ \lambda(1-\lambda)f(\underset{\sim}{x}_1)f^K(\underset{\sim}{x}_2)+(1-\lambda)^2 f^{K+1}(\underset{\sim}{x}_1) \leq \lambda f^{K+1}(\underset{\sim}{x}_2)+(1-\lambda)f^{K+1}(\underset{\sim}{x}_1) \tag{E.22}$$

or

$$[\lambda f^K(\underset{\sim}{x}_2)+(1-\lambda)f^K(\underset{\sim}{x}_1)][\lambda f(\underset{\sim}{x}_2)+(1-\lambda)f(\underset{\sim}{x}_1)] \leq \lambda f^{K+1}(\underset{\sim}{x}_2)+(1-\lambda)f^{K+1}(\underset{\sim}{x}_1) \; . \tag{E.23}$$

This is the inequality we set out to show in (E.16). The theorem is proved.

It has been shown that if $f(\underset{\sim}{x})$ is convex and $f \leq 0$ then $f^2(\underset{\sim}{x})$ is convex. By Theorem 3, $f^3(\underset{\sim}{x})$ is convex. By Theorem 3 again, $f^4(\underset{\sim}{x})$ is convex. This reasoning can be followed for all powers K where K is a positive integer. The basic theorem is established.

LIST OF REFERENCES

1. Bryson, A. E., "Applications of Optimal Control Theory in Aerospace Engineering," Journal of Spacecraft and Rockets, v. 4, no. 5, p. 545-553, May 1967.

2. Bryson, A. E. and Denham, W. F., "A Steepest-Ascent Method for Solving Optimum Programming Problems," Journal of Applied Mechanics, p. 247-257, June 1962.

3. Bryson, A. E. and Hedrick, J. K., "Minimum Time Turns for a Supersonic Airplane at Constant Altitude," Journal of Aircraft, v. 8, no. 3, p. 182-187, March 1971.

4. Bryson, A. E., Hoffman, W. C., and Desai, M. N., The Energy-State Approximation in Performance Optimization of Supersonic Aircraft, AIAA Paper 68-877, Pasadena, California, August 1968.

5. Kelley, H. J. and Edelbaum, T. N., "Energy Climbs, Energy Turns, and Asymptotic Expansions," Journal of Aircraft, v. 7, no. 1, p. 93-95, January-February 1970.

6. Kelley, H. J. and Lefton, L., Differential Turns, paper presented at AIAA Atmospheric Flight Mechanics Specialists Conference, Palo Alto, California, 11-13 September 1972.

7. Landgraf, S. K., "Some Applications of Performance Optimization Techniques to Aircraft," Journal of Aircraft, v. 2, no. 2, p. 153-154, March-April 1965.

8. Taylor, L. W., Smith, H. J., and Iliff, K. W., "Experience Using Balakrishnan's Epsilon Technique to Compute Optimum Flight Profiles," Journal of Aircraft, v. 7, no. 2, p. 182-197, March-April 1970.

9. Fiacco, A. V. and McCormick, G. P., Nonlinear Programming: Sequential Unconstrained Minimization Techniques, Wiley, 1968.

10. Jones, A. P. and McCormick, G. P., "A Generalization of the Method of Balakrishnan: Inequality Constraints and Initial Conditions," SIAM Journal on Control, p. 218-225, May 1970.

11. Taylor, J. M., Optimization: Application of the Epsilon Method, Ph.D. Thesis, Dept. of Electrical Engineering, University of Wyoming, Laramie, 1970.

12. Taylor, J. M. and Constantinides, C. T., "Optimization: Application of the Epsilon Method," IEEE Transactions on Automatic Control, p. 128-131, February 1972.

13. Department of Engineering, University of California Los Angeles Report 67-61, On a New Computing Technique in Optimal Control, by A. V. Balakrishnan, December 1967.

14. Balakrishnan, A. V., On a New Computing Technique in Optimal Control and Its Application to Minimal Time Flight Profile Optimization, paper presented at International Colloquium on Methods of Optimization, 2nd, Novosibirsk, USSR, June 1968.

15. Athans, M. and Falb, P. L., Optimal Control: An Introduction to the Theory and Its Applications, McGraw-Hill, 1966.

16. Kirk, D. E., Optimal Control Theory: an Introduction, Prentice-Hall, 1970.

17. Rockafellar, R. T., Convex Analysis, Princeton, 1970.

18. Rockafellar, R. T., "Integrals Which are Convex Functionals," Pacific Journal of Mathematics, v. 24, no. 3, p. 525-539, 1968.

19. Miele, A., Flight Mechanics: Theory of Flight Paths, Addison-Wesley, 1962.

INITIAL DISTRIBUTION LIST

		No. Copies
1.	Defense Documentation Center Cameron Station Alexandria, Virginia 22314	2
2.	Library, Code 0212 Naval Postgraduate School Monterey, California 93940	2
3.	Chairman, Department of Aeronautics Naval Postgraduate School Monterey, California 93940	1
4.	Chairman, Department of Electrical Engineering Naval Postgraduate School Monterey, California 93940	1
5.	Professor D. E. Kirk, Code 52Ki Department of Electrical Engineering Naval Postgraduate School Monterey, California 93940	3
6.	Professor F. D. Faulkner, Code 53Fa Department of Mathematics Naval Postgraduate School Monterey, California 93940	1
7.	Professor H. A. Titus, Code 52Ts Department of Electrical Engineering Naval Postgraduate School Monterey, California 93940	1
8.	Professor R. A. Hess, Code 57He Department of Aeronautics Naval Postgraduate School Monterey, California 93940	1
9.	Professor A. E. Fuhs, Code 57Fu Department of Aeronautics Naval Postgraduate School Monterey, California 93940	1
10.	Professor A. Gerba, Code 52Gz Department of Electrical Engineering Naval Postgraduate School Monterey, California 93940	1

		No. Copies
11.	Dr. D. E. Zilmer, Code 607 Naval Weapons Center China Lake, California 93555	1
12.	CDR. W. J. H. Smithey Department of Aeronautics Naval Postgraduate School Monterey, California 93940	1
13.	CDR. Marle D. Hewett Naval Air Test Center Patuxent River, Maryland	3

SECURITY CLASSIFICATION OF THIS PAGE (When Data Entered)

REPORT DOCUMENTATION PAGE		READ INSTRUCTIONS BEFORE COMPLETING FORM
1. REPORT NUMBER	2. GOVT ACCESSION NO.	3. RECIPIENT'S CATALOG NUMBER
4. TITLE (and Subtitle) A Second-Order Epsilon Method for Constrained Trajectory Optimization		5. TYPE OF REPORT & PERIOD COVERED Ph.D. Thesis; June, 1974
		6. PERFORMING ORG. REPORT NUMBER
7. AUTHOR(s) Marle David Hewett		8. CONTRACT OR GRANT NUMBER(s)
9. PERFORMING ORGANIZATION NAME AND ADDRESS Naval Postgraduate School Monterey, California 93940		10. PROGRAM ELEMENT, PROJECT, TASK AREA & WORK UNIT NUMBERS
11. CONTROLLING OFFICE NAME AND ADDRESS Naval Postgraduate School Monterey, California 93940		12. REPORT DATE June 1974
		13. NUMBER OF PAGES 213
14. MONITORING AGENCY NAME & ADDRESS(if different from Controlling Office) Naval Postgraduate School Monterey, California 93940		15. SECURITY CLASS. (of this report) Unclassified
		15a. DECLASSIFICATION/DOWNGRADING SCHEDULE

16. DISTRIBUTION STATEMENT (of this Report)

Approved for public release; distribution unlimited.

17. DISTRIBUTION STATEMENT (of the abstract entered in Block 20, if different from Report)

18. SUPPLEMENTARY NOTES

19. KEY WORDS (Continue on reverse side if necessary and identify by block number)

optimization	aircraft	state
trajectory	limitation	control
inequality	penalty	missile
performance	convexity	

20. ABSTRACT (Continue on reverse side if necessary and identify by block number)

A second-order epsilon method is developed for trajectory optimization problems. The method is applied to several aircraft and missile performance and air combat maneuvering problems. Heavy emphasis is placed on the realistic modeling of the flight vehicle's motion and maneuvering limitations.

The proposed optimization technique, which is an extension of Balakrishnan's epsilon method, uses either the full

DD FORM 1 JAN 73 1473 EDITION OF 1 NOV 65 IS OBSOLETE
(Page 1) S/N 0102-014-6601 |

SECURITY CLASSIFICATION OF THIS PAGE (When Data Entered)

(20. continued)

second-order Newton-Raphson method or the "modified" Newton-Raphson method to minimize the epsilon functional. The full Newton-Raphson method exhibits terminal convergence characteristics superior to the "modified" method, whereas the "modified" method is generally superior in the initial stages of a problem. An algorithm is developed which uses both techniques in a complementary way.

A new penalty functional which has desirable theoretical properties and exhibits excellent computational behavior is introduced to treat state and control inequality constraints.

Thesis 151205
H52624 Hewett
c.1
A second-order epsilon method for constrained trajectory optimization.